NEUROCHEMICAL CHARACTERIZATION OF THE RODENT PRIMARY SENSORY SYSTEM

BY

EMILY G. TILLMAAND

DISSERTATION

Submitted in partial fulfillment of the requirements
for the degree of Doctor of Philosophy in Neuroscience
in the Graduate College of the
University of Illinois at Urbana-Champaign, 2018

Urbana, Illinois

Doctoral Committee:

Professor Jonathan V. Sweedler, Chair
Professor Martha U. Gillette
Assistant Professor Catherine A. Christian
Assistant Professor Qin Liu

ABSTRACT

Primary sensory neurons and their associated tissues are important targets for neurochemical study. Disorders of the sensory system, including chronic pain and itch, can be extremely devastating and, in many cases, difficult to treat. Part of the difficulty of treating such disorders is the limited understanding that we have for the multitude of chemical players involved in the communication of sensation within the nervous system. One particular set of intercellular signaling molecules, neuropeptides, are known to play an important role in the transmission of pain and itch signals from the peripheral system to the spinal cord. While we have a basic understanding of how many of these molecules are involved in sensory transmission, further knowledge would be benefited by more accurate and spatially relevant sampling and characterization. However, due to their low concentration and dynamic presence, the detection of these molecules in a non-targeted manner poses a unique challenge.

This dissertation focuses on characterizing the peptides found in the tissues of the sensory system and released from primary sensory neurons in culture as well as improving culturing and stimulation paradigms for future research. We have worked to characterize the full content of peptides within the dorsal root ganglia, which houses the cell bodies of the primary sensory neurons, as well as other related tissues of rat and to detect changes in the peptide content of the dorsal root ganglia and dorsal horn upon generation of an itch model in mice. We have also designed a physiologically relevant sensory neuron culturing system and made strides toward spatially relevant release sampling and neuropeptide detection.

To my family and friends, who remind me who I am.

“A friend is someone who knows the song in your heart and can sing it back to you when you have forgotten the words.” -- Unknown

ACKNOWLEDGEMENTS

It takes a large number of people to bring a PhD to fruition and, in my case at least, to sustain one as she is growing. To all the people who have been involved in this process in one way or another, I thank you.

Special acknowledgement goes to my advisor, Professor Jonathan Sweedler, for the opportunity to be a member of this wonderful lab and to grow into my own as a scientist. Additionally, my committee members, both present and past, have devoted time and energy to the cause, and cheered me along every step of the way. Professors Martha Gillette, Qin Liu, Catherine Christian, Taher Saif, and Catherine Best, as well as subgroup members Professor Ralph Nuzzo and Drs. Stanislav Rubakhin, Joselle McCracken, and Adina Badea, I will forever be thankful for your help and wisdom.

To all of my lab-mates, many whom are named within these pages, thank you so much for making my work days wonderful. It takes a special group of people to dedicate our lives to this work, and I am beyond proud to have spent countless hours in the office and lab with each of you.

To my dedicated, enthusiastic, ever-present undergraduate students, Ashley Lenhart and Yujin Lee, I could not have done this work without you. I enjoyed working with you and watching you grow. You greatly added to my graduate school experience.

To the staff of the Neuroscience and Medical Scholars Programs, you have been an ever-present help for a wide range of graduate-school related issues. Thank you especially to Sam Beshers, Stephanie Pregent, Jenni Crum, and Heather Wright for your help and guidance along the way.

Finally, any success of mine needs to be shared with my support crew, who has held me up throughout this process. To Itamar, my partner in work and life; my parents and grandmother, Conley, Patricia, and Dolores, who instilled in me the importance of education, a hard work ethic, a steady faith, and both a love of science and the ability to write about it; my siblings, Saretta, Lydia, and Arden, who have been my life-long friends; my graduate school squad, Ritu, Alex, Kelsey, Joey, Amogh, Jari, Hua-Chia, Amit, and Thanh who always know what I'm going through and have provided countless hours of fun and encouragement; Kenny, Ian, and Penelope, with whom I shared a home for many years; and my cheerleaders from afar, Jen, Abby, Stefanie, Lauren, and Stephanie, I cannot thank you enough. You are the real winners in my book.

TABLE OF CONTENTS

Chapter 1
Introduction and Document Overview

1.1 Introduction

The primary sensory system is an important target for neurochemical study. Mainly composed of primary sensory neurons, their support cells, and the nerves and ganglia in which they reside, the system also interfaces with skin, viscera, and the spinal cord. Disorders of the sensory system, including chronic pain and chronic itch, can be extremely devastating and, in many cases, difficult to treat. Part of the difficulty of treating such disorders is the limit of understanding that we have for the multitude of chemical players involved in such disorders. Although there is much knowledge about chemical and molecular players involved in pain and itch sensation, most studies focus on one or a few molecular players rather than take a global approach. As a lab with expertise in untargeted mass spectrometric techniques and a focus on neurochemistry, we have the unique opportunity to add more comprehensive information about the chemical players involved in the primary sensory system to the knowledge pool. While there are various molecules we could study using mass spectrometry, we decided to focus on neuropeptides.

1.2 Neuropeptides and the Primary Sensory System

Neuropeptides are short chains of amino acids processed from protein precursors which are synthesized in, stored by and released from neurons in order to influence a wide range of physiological systems through neurotransmission, neuromodulation, and hormonal affects [1, 2]. How the neuropeptide affects the function of the cell upon which

it is acting depends largely on the pattern of receptors for that peptide, their distance from the releasing neurons, and the various other signaling molecules involved. In relation to pain and itch (considered noxious stimuli), there are a variety of neuropeptides that are released in response to many distinct stimuli types, locations, and intensities while acting to either attenuate or facilitate the perception of pain or itch.

Not surprisingly, the sensation and transmission of noxious stimuli within the body is quite complex [3]. Very basically, sensory information about the state of the periphery is brought in to the central nervous system (CNS) through the dorsal root and trigeminal ganglia. These ganglia are made up of sensory neurons categorized by what type of stimuli they are receiving. Of the four types of sensation, mechanosensation, proprioception, thermosensation, and nociception, it is the neurons that respond to noxious stimuli (including temperature, pH, and concentration of circulating factors that signal tissue damage) with which we are interested. Particularly, the Aδ and C nociceptive neurons are those carrying such information [3].

The primary afferents of these sensory neurons terminate on second order neurons in the dorsal horn of the spinal cord, either superficially in laminae I and II or deeper in laminae IV and V. The axons of the second order neurons then move through the lateral spinothalamic tract to innervate the medial and posterolateral thalamus or the anterior spinothalamic tract to innervate the lateral thalamus, respectively [3]. From the thalamus, signals are sent to both the primary and secondary somatosensory cortex as well as emotional processing centers [3]. The nervous system also modulates pain perception through a descending pathway consisting of white matter tracts moving through the periaqueductal gray (PAG) to the rostro-ventral medulla (RVM) and down through the

spinal cord [3, 4]. Neuropeptides are involved at all signaling levels of perception, from sensation transmission to descending modulatory mechanisms to mediation of emotional responses.

1.2.1 Neuropeptides and Pain

The roles of various neuropeptides in pain transmission are quite complex and can depend on the location, amount, and receptor type available as well as the responses of other neuropeptides in the system. A basic overview is that there are peptides such as substance P (SP), calcitonin gene related peptide (CGRP), somatostatin (STT), and vasoactive intestinal peptide (VIP) which facilitate hyperalgesia and sensitization upon noxious stimuli at the primary afferent or spinal cord levels [2, 3, 5, 6]. Then, there are peptides such as the opioids (enkephalins, endorphins, dynorphin), galanin, and neuropeptide Y (NPY), which induce analgesia by blocking the mechanisms of pain response induced by SP and CGRP [2, 5, 7, 8]. Further, there are peptides such as cholecystokinin (CCK), which reduce opioid action and, therefore, increase hypersensitivity, as well as those like neurotensin (NT), which act on various peptidergic systems and induce seemingly contradictory results [4, 5].

The major hyperalgesic peptide is SP. A member of the tachykinin family, along with neuropeptides neurokinin A and neurokinin B, SP was first isolated in 1931, although its sensory transmission properties were not discovered until the 1950s and it was not sequenced until 1971. The tachykinins have multiple functions, with pain being one. SP and neurokinin A are the two tachykinins that are mostly expressed in sensory neurons [2]. SP is found in many primary sensory neurons, in both their peripheral and central terminals. It is also found throughout the CNS, including the superficial lamina (I and II)

of the spinal cord [5]. It is believed that the excitatory effects of tachykinins can be assumed by VIP in the spinal cord, especially following axotomy [2, 5].

SP and another sensitizing peptide, CGRP, are colocalized in C-fiber primary sensory neurons and are released upon sensation of noxious stimuli, both centrally and peripherally. Both peptides induce slow, long-lasting depolarizations of the neurons on which they act, as well as inflammatory responses from blood vessels and immune cells in the vicinity of the injury [2, 3, 5]. Taken together, these changes induce hyperalgesia and sensitization of the affected neurons. The edema and inflammation caused by the release of SP and GCRP into the tissue may spread to the innervated areas of nearby nociceptors, acting as noxious stimuli, causing further release of SP and CGRP and continuing the cycle [2, 3]. In addition to the sensitizing effects of SP, CGRP, and VIP, STT is also included in the group of hyperalgesia inducing peptides. This peptide responds to noxious stimuli of a thermal nature and is not found to coexist with SP, although it can coexist with CGRP [6].

Opioid peptides, or endogenous opiates, were discovered in the mid-1970s in a search for morphine analogs [2]. Since then, much work has been done to understand their function in the hope to find a good alternative to morphine for the treatment of pain. Opioids are located both peripherally and centrally and influence both ascending and descending pain pathways through three main receptor types: μ (MOPR), δ (DOPR), and κ (KOPR), [2, 8]. Centrally, the opioids act either by hyperpolarizing their target cells via increased potassium ion currents or through neuromodulation and inhibition of neurotransmitter release [2, 8]. However, peripherally, they have been shown to inhibit calcium ion currents, blocking the excitability of peripheral neurons, induction of action

potentials, and release of neuropeptides like SP and CGRP [8]. To further confirm this action, *Beaudry et al*. have found that both MOPR and DOPRs are located on peptidergic primary neurons and that their agonists block SP release [7]. This inhibition of afferent neuron excitation upon injury reduces the inflammatory effects of SP and CGRP release mentioned previously. During chronic pain, opioid peptide receptors are upregulated in the spinal cord and periphery [7] and β-endorphin, met-enkephalin and dynorphin-A are upregulated in immune cells [8], indicating an effort by the body to control or alleviate the pain.

1.2.2 Neuropeptides and Itch

Chronic itch (pruritis) occurs in 25.5% of the population, with incidence increasing with age [9]. Associated with various medical conditions such as liver disease, asthma, eczema, elevated body mass index, and increased anxiety, pruritis can be quite debilitating [9, 10]. The neural processing pathways and the molecules involved in itch sensation are still being elucidated. Recent studies have shown that Mas-related G-protein coupled receptors (Mrgprs) [11], specifically MrgprA3, MrgprC11, and MrgprD, are important players in the itch pathway [12, 13]. Although immunohistochemical, morphological, and functional characterizations of these neurons provide useful information, the in-depth characterization of the cell signaling molecules found within and released from these cells would improve our understanding of itch sensation. Performing peptidomics to determine their chemical content provides critical details on the contribution of these cells to itch. These studies can also provide clues into the functional relationship between individual molecules and the cells in which they are found.

The involvement of neuropeptides in pain response is extensive and we expect to find similar complexity in the neuropeptides involved in itch sensation. Already, SP [14], endothelin-1 [15, 16], neuromedin B (NMB) [17], CGRP [18], natriuretic peptide B and the kappa-opioid dynorphin [19] are implicated in the itch response. The transcriptomic data shows that natriuretic polypeptide b, agouti-related peptide, neurotensin, and adenylate cyclase activating polypeptide 1 are upregulated in itch sensing neurons [20]. However, we know that increased expression does not always translate to increased peptide content [21, 22]; therefore, it is important to characterize the changes in peptide content in the itch sensing neurons in the peripheral nervous system.

1.3 Modeling Physiological Systems

1.3.1 Primary Cell Culture

One basic way to model a physiological system is through cell culture. Culturing cells taken directly from an organism, or primary cells, is an important tool for studying the chemical content of a cell type. Primary sensory neuron cell culture has provided important information about the growth conditions, chemical needs and susceptibilities, and expression changes within these cells under certain perturbations. In fact, much of the information already discussed about the neurochemical content of sensory neurons was elucidated using cell culture systems.

While less reproducible than cell culture lines, primary cell culture is more relevant to the model organism from which the cells are obtained, and is therefore considered more physiologically relevant, especially when characterizing the behavior and chemical content of the cells. Additionally, while there is a cell line created out of a rat pheochromocytoma, PC12, that can be induced to differentiate into a neuron-like cells

[23, 24] and hybrid cell lines have been created for neuronal study [25, 26], neurons are inherently a non-dividing and non-passageable cell type. Therefore, we used primary cells isolated from the DRG of adult and neonatal rats as well as mice for our studies. Additionally, we did not purify the cultures to maintain only neuronal cells but instead included glial and support cells isolated from the ganglion within our culture system.

1.3.2 Microfluidic Devices

Microfluidic devices, as they are used in biology, are devices that rely on the physics of small-volume fluidics to create controlled microenvironments for cell growth [27, 28]. Generally created out of poly-dimethylsiloxane (PDMS), which is a breathable, non-toxic, optically clear material, microfluidic devices have been particularly useful in the study of neurobiology and neurochemistry [28, 29]. The use of microfluidic devices for compartmentalized growth [30], spatially controlled experiments [30, 31], specific chemical damage [31], chemical gradient generation [32, 33], controlled sampling [27], and even peptide quantitation [34] has been demonstrated by our group and others.

For this project, the rationale for using microfluidic devices is three-fold. First, by using a device with cell culture compartments separated by microchannels, a more physiologically relevant structural growth scheme was provided for the sensory neurons. Second, by decreasing the amount of media used within the culture system, the relative concentration of the analytes was increased. Third, the structural specificity provided by the microfluidic device allows for the collection of sample in a spatially relevant manner, important for analysis of neuropeptide release from both the “skin” the “spinal cord” side of the device simultaneously.

1.3.3 Other Systems

There are other types of systems that can be used to create physiologically relevant *ex vivo* or *in vitro* models, upon which this document will touch briefly. Generally, the systems include tools that can be used for creating viable three-dimensional cultures such as scaffolds [35, 36], fibers [37], hydrogels [36, 38], spheroid cultures [39-41] and more. This area of research is exciting and innovative and would be a good direction to take this project in the future.

1.4 Detection and Characterization of Neuropeptide Content and Release using Mass Spectrometry

Often, information about the expected neuropeptide content of a cell type or tissue is provided using transcriptomics and/or immunological techniques, such as radioimmunoassay [42, 43], enzyme-linked immunosorbent assay (ELISA) [44], or immunohistochemistry [45]. While transcriptomic information about the expected peptide content of a sample can be helpful, the genetic expression profile does not always translate to actual peptide content as there are various regulated processing, transportation, storage, and release steps involved in the peptide response to perturbations [2, 21, 22]. On the other hand, immune-based assays are targeted to one or a few pre-selected analytes and, therefore, miss much of the chemically complex information that can be gained from an untargeted detection approach. Also, chemical identification of a molecule cannot be performed using immune-based assays. Therefore, untargeted mass spectrometric analysis is an important tool for studying the complex peptide dynamics within a system.

Peptidomics, or the characterization of the peptides within a system with the goal of creating a list of peptide players, is an important first step toward understanding the multitude of peptide players within a sample and how they might change upon specific perturbations. Performing peptidomics on a whole tissue, such as the DRG, both allows us to gain insight into chemical content changes within the system and provides a comprehensive list of peptide masses to which we can match the masses from our released peptide samples.

Peptide release studies, on the other hand, provide details on the release of certain peptides from individual cell types or locations. For example, CGRP and/or SP release from sensory neurons [42-44] and intact dorsal root and trigeminal ganglia [45] has been demonstrated, whereas ghrelin is released from gastrointestinal tract cells [46] and insulin and insulin-like peptides are released from cells of the liver, pancreas, and brain [47]. For full characterization of the peptide content, however, mass spectrometry (MS) is most helpful due to its ability to detect low amounts of analyte without pre-selection and has been used to characterize peptide release [27, 34].

For the purposes of this project, two types of MS are particularly useful, especially when used together. Whole tissue measurements are performed using a liquid chromatography electrospray ionization (LC-ESI) MS and the cell release measurements as well as some single cell peptide measurements are performed using matrix-assisted laser desorption/ionization time-of-flight (MALDI-TOF) MS. Combining these two methods is particularly effective in allowing us to assign identifications to signals detected in the release samples by MALDI-TOF through matching the masses with those of peptides characterized by LC-ESI MS, which is more efficient at identification but needs larger

amounts of sample [48-50]. More information about MS and its uses can be found in Chapters 2 and 3.

1.5 Overview of Document

Within this dissertation document, you will find the descriptions and results of my projects, as well as ideas for additional work. The document begins with two reviews followed by my co-first authored research publication, outlining the peptidomics and secretomics of the primary sensory system. The rest of the dissertation follows with the work resulting from that project.

Chapter 2 consists of a published review (EG Tillmaand and JV Sweedler *Microphysiological Systems* June 2018, Volume 2, Issue 4, doi: 10.21037/mps.2018.05.01) outlining the importance of using microphysiological systems in neurochemistry and ways that mass spectrometric analysis can be applied to such systems.

Chapter 3 consists of an excerpt from a published review (Ong TH, Tillmaand EG, Makurath M, Rubakhin SS, Sweedler JV. *Biochim Biophys Acta*. 2015 Jul;1854(7):732-40. doi: 10.1016/j.bbapap.2015.01.008). This chapter discusses methods for sampling from the extracellular environment for components of cellular release.

Chapter 4 consists of published work outlining the peptidomics of the DRG and how it compares to the peptidomics of the dorsal and ventral root spinal nerves, as well as measurements of peptide release from all aspects of the intact sensory system, DRG explants, and cultured DRG cells (Tillmaand EG, Yang N, Croushore-Kindt C, Rubakhin

SS, Sweedler JV. *JASMS*. December 2015, Volume 26, Issue 12, pp 2051–2061, doi: 10.1007/S13361-015-1256-1).

Chapter 5 consists of work performed toward understanding the peptide changes that occur in sensory system related tissues within models of itch-producing disorders.

Chapter 6 outlines the work performed in the search for SP released from primary sensory neurons in our culture system.

Chapter 7 is an investigation into a more physiologically relevant cell culture system and includes forays into extracellular matrix protein stamping, explant cultures, co-cultures, and the use of microfluidic devices. This chapter also includes a new primary sensory microphysiological system design that could be useful for future studies of the primary sensory system and which utilizes a cell culture material built off of work published with the Nuzzo group (Badea A, McCracken JM, Tillmaand EG, Kandel ME, Oraham AW, Mevis MB, Rubakhin SS, Popescu G, Sweedler JV, Nuzzo RG. *ACS Appl Mater Interfaces*. 2017 Sep 13;9(36):30318-30328. doi: 10.1021/acsami.7b06742).

Chapter 8 consists of work toward characterizing primary sensory neuron subtypes. This project was born out of the complexity of the subtypes of neurons located in the DRG and an improved methodology for single cell peptide profiling developed in the lab.

In summary, my dissertation research has focused on characterizing neuropeptides found in and released from primary sensory neurons. After characterizing the peptides found within both cultured DRG cells and intact DRG tissue (Chapter 4), I worked to 1) apply our current knowledge of the sensory system and ability to characterize peptides to explore the peptide changes in itch models (Chapter 5); 2) verify the validity of our cell

culture and stimulation paradigm (Chapter 6), and 3) develop a physiologically relevant system in which to culture the cells and perform more specific stimulations (Chapter 7).

1.6 Conclusions

Neuropeptides can be found in all aspects of sensory transmission, from sensation to facilitation to inhibition. They dynamically respond to injury and inflammation through a complex set of interactions to help central processing centers gain information about and respond to possible harm. However, sometimes this intricate system gets disrupted and chronic pain and itch symptoms prevail, even without obvious injury or after healing from injury appears to have occurred. Elucidating how the sensory system is affected on a molecular level and what the overall neuropeptide profiles of the system look like both in healthy and diseased states is an important area of study for gaining a better understanding of these chronic disorders. This document discusses the work performed toward accomplishing this goal.

1.7 Work Cited

1. Merighi, A., ed. *Neuropeptides: Methods and Protocols, Methods in Molecular Biology*. Vol. 789. 2011, Springer Science+Business Media, LLC.
2. Strand, F.L., ed. *Neuropeptides: Regulators of Physiological Processes*. 1998, The MIT Press: Cambridge.
3. Squire, L., et al., eds. *Fundamental Neuroscience*. Third ed. 2008, Elsevier.
4. Kleczkowska, P. and A.W. Lipkowski, *Neurotensin and neurotensin receptors: Characteristic, structure–activity relationship and pain modulation—A review.* European Journal of Pharmacology, 2013. **716**(1–3): p. 54-60.
5. Xu, X.-J. and Z. Wiesenfeld-Hallin, *Neuropeptides: Pain*, in *Encyclopedia of Neuroscience*, L.R. Squire, Editor. 2009, Academic Press: Oxford.
6. Kuraishi, Y., et al., *Evidence that substance P and somatostatin transmit separate information related to pain in the spinal dorsal horn.* Brain Research, 1985. **325**(1–2): p. 294-298.
7. Beaudry, H., D. Dubois, and L. Gendron, *Activation of Spinal μ- and δ-Opioid Receptors Potently Inhibits Substance P Release Induced by Peripheral Noxious Stimuli.* The Journal of Neuroscience, 2011. **31**(37): p. 13068-13077.
8. Stein, C., M. Schafer, and H. Machelska, *Attacking pain at its source: new perspectives on opioids.* Nat Med, 2003. **9**(8): p. 1003-1008.
9. Matterne, U., et al., *Incidence and determinants of chronic pruritus: a population-based cohort study.* Acta Derm Venereol, 2013. **93**(5): p. 532-7.
10. Akiyama, T. and E. Carstens, *Neural processing of itch.* Neuroscience, 2013. **250**: p. 697-714.
11. Dong, X., et al., *A diverse family of GPCRs expressed in specific subsets of nociceptive sensory neurons.* Cell, 2001. **106**(5): p. 619-32.
12. Liu, Q., et al., *Sensory neuron-specific GPCRs Mrgprs are itch receptors mediating chloroquine-induced pruritus.* Cell, 2009. **139**(7): p. 1353-1365.
13. Liu, Q., et al., *The distinct roles of two GPCRs, MrgprC11 and PAR2, in itch and hyperalgesia.* Sci Signal, 2011. **4**(181): p. ra45.
14. Andoh, T., et al., *Substance P induction of itch-associated response mediated by cutaneous NK 1 tachykinin receptors in mice.* Journal of Pharmacology and Experimental Therapeutics, 1998. **286**(3): p. 1140-1145.

15. Katugampola, R., M.K. Church, and G.F. Clough, *The neurogenic vasodilator response to endothelin-1: a study in human skin in vivo.* Experimental Physiology, 2000. **85**(06): p. 839-846.
16. Trentin, P.G., et al., *Endothelin-1 causes pruritus in mice.* Exp Biol Med (Maywood), 2006. **231**(6): p. 1146-51.
17. Sukhtankar, D.D. and M.-C. Ko, *Physiological Function of Gastrin-Releasing Peptide and Neuromedin B Receptors in Regulating Itch Scratching Behavior in the Spinal Cord of Mice.* PLoS One, 2013. **8**(6): p. e67422.
18. Rogoz, K., et al., *Multimodal use of calcitonin gene-related peptide and substance P in itch and acute pain uncovered by the elimination of vesicular glutamate transporter 2 from transient receptor potential cation channel subfamily V member 1 neurons.* J Neurosci, 2014. **34**(42): p. 14055-68.
19. Kardon, Adam P., et al., *Dynorphin Acts as a Neuromodulator to Inhibit Itch in the Dorsal Horn of the Spinal Cord.* Neuron, 2014. **82**(3): p. 573-586.
20. Usoskin, D., et al., *Unbiased classification of sensory neuron types by large-scale single-cell RNA sequencing.* Nat Neurosci, 2015. **18**(1): p. 145-153.
21. Maier, T., M. Güell, and L. Serrano, *Correlation of mRNA and protein in complex biological samples.* FEBS Letters, 2009. **583**(24): p. 3966-3973.
22. Wilhelm, M., et al., *Mass-spectrometry-based draft of the human proteome.* Nature, 2014. **509**(7502): p. 582-7.
23. Vaudry, D., et al., *Signaling Pathways for PC12 Cell Differentiation: Making the Right Connections.* Science, 2002. **296**(5573): p. 1648-1649.
24. Satoh, T., et al., *Induction of neural differentiation in PCR cells B-cell stimulatory factor 2/interleukin-6*. Vol. 8. 1988. 3546-9.
25. Hikawa, N. and T. Takenaka, *Mature sensory neuron-derived hybrid cell line expressing NGF-dependent neurite extension.* Brain Research, 1997. **774**(1): p. 225-228.
26. Francel, P.C., R.J. Miller, and G. Dawson, *Modulation of Bradykinin-Induced Inositol Trisphosphate Release in a Novel Neuroblastoma X Dorsal Root Ganglion Sensory Neuron Cell Line (F-11).* Journal of Neurochemistry, 1987. **48**(5): p. 1632-1639.
27. Croushore, C.A., et al., *Microfluidic Device for the Selective Chemical Stimulation of Neurons and Characterization of Peptide Release with Mass Spectrometry.* Analytical Chemistry, 2012. **84**(21): p. 9446-9452.
28. Wang, J., et al., *Microfluidics: A new cosset for neurobiology.* Lab on a Chip, 2009. **9**(5): p. 644-652.

29. Pearce, T.M. and J.C. Williams, *Microtechnology: Meet neurobiology.* Lab on a Chip, 2007. **7**(1): p. 30-40.
30. Jokinen, V., et al., *A microfluidic chip for axonal isolation and electrophysiological measurements.* Journal of Neuroscience Methods, 2013. **212**(2): p. 276-282.
31. Young Lee, C., E. Romanova, and J. Sweedler, *Laminar stream of detergents for subcellular neurite damage in a microfluidic device: A simple tool for the study of neuroregeneration*. Vol. 10. 2013. 036020.
32. Xiao, R.-R., et al., *Simultaneous Generation of Gradients with Gradually Changed Slope in a Microfluidic Device for Quantifying Axon Response*. Vol. 85. 2013.
33. Liu, W., et al., *Change of laminin density stimulates axon branching via growth cone myosin II-mediated adhesion.* Integrative Biology, 2013. **5**(10): p. 1244-1252.
34. Zhong, M., et al., *Label-free quantitation of peptide release from neurons in a microfluidic device with mass spectrometry imaging.* Lab on a Chip, 2012. **12**(11): p. 2037-2045.
35. Rowe, L., et al., *Active 3-D microscaffold system with fluid perfusion for culturing in vitro neuronal networks.* Lab on a Chip, 2007. **7**(4): p. 475-482.
36. Kunze, A., et al., *Micropatterning neural cell cultures in 3D with a multi-layered scaffold.* Biomaterials, 2011. **32**(8): p. 2088-2098.
37. Daud, M.F.B., et al., *An aligned 3D neuronal-glial co-culture model for peripheral nerve studies.* Biomaterials, 2012. **33**(25): p. 5901-5913.
38. Lozano, R., et al., *3D printing of layered brain-like structures using peptide modified gellan gum substrates.* Biomaterials, 2015. **67**: p. 264-273.
39. Kato-Negishi, M., et al., *A neurospheroid network-stamping method for neural transplantation to the brain.* Biomaterials, 2010. **31**(34): p. 8939-8945.
40. Choi, Y.J., J. Park, and S.-H. Lee, *Size-controllable networked neurospheres as a 3D neuronal tissue model for Alzheimer's disease studies.* Biomaterials, 2013. **34**(12): p. 2938-2946.
41. Fennema, E., et al., *Spheroid culture as a tool for creating 3D complex tissues.* Trends in Biotechnology, 2013. **31**(2): p. 108-115.
42. Qin, N., et al., *TRPV2 Is Activated by Cannabidiol and Mediates CGRP Release in Cultured Rat Dorsal Root Ganglion Neurons.* The Journal of Neuroscience, 2008. **28**(24): p. 6231-6238.
43. Vasko, M., W. Campbell, and K. Waite, *Prostaglandin E2 enhances bradykinin-stimulated release of neuropeptides from rat sensory neurons in culture.* The Journal of Neuroscience, 1994. **14**(8): p. 4987-4997.

44. Ahluwalia, J., et al., *Anandamide regulates neuropeptide release from capsaicin-sensitive primary sensory neurons by activating both the cannabinoid 1 receptor and the vanilloid receptor 1 in vitro.* European Journal of Neuroscience, 2003. **17**(12): p. 2611-2618.
45. Eberhardt, M., et al., *Calcitonin gene-related peptide release from intact isolated dorsal root and trigeminal ganglia.* Neuropeptides, 2008. **42**(3): p. 311-317.
46. Sakata, I. and T. Sakai, *Ghrelin Cells in the Gastrointestinal Tract.* International Journal of Peptides, 2010. **2010**: p. 945056.
47. Fernandez, A.M. and I. Torres-Alemán, *The many faces of insulin-like peptide signalling in the brain.* Nat Rev Neurosci, 2012. **13**(4): p. 225-239.
48. Lee, J.E., et al., *Endogenous peptide discovery of the rat circadian clock: a focused study of the suprachiasmatic nucleus by ultrahigh performance tandem mass spectrometry.* Molecular & Cellular Proteomics, 2010. **9**(2): p. 285-297.
49. Hatcher, N.G., et al., *Mass spectrometry-based discovery of circadian peptides.* Proceedings of the National Academy of Sciences of the United States of America, 2008. **105**(34): p. 12527-12532.
50. Tillmaand, E.G., et al., *Peptidomics and Secretomics of the Mammalian Peripheral Sensory-Motor System.* J Am Soc Mass Spectrom, 2015.

Chapter 2

Integrating Mass Spectrometry with Microphysiological Systems for Improved Neurochemical Studies

2.1 Notes

This chapter is an invited review co-authored by Emily Tillmaand and Jonathan Sweedler published in *Microphysiological Systems* (June 2018, Volume 2, Issue 4, doi: 10.21037/mps.2018.05.01) and reproduced with permission. This work was supported by the National Institute on Drug Abuse under Award No. P30 DA018310, and the National Science Foundation under Award Nos. CHE-16-06791 and DGE- 17-35252. The content is solely the responsibility of the authors and does not necessarily represent the official views of the funding agencies.

2.2 Abstract

Microphysiological systems, often referred to as "organs-on-chips", are in vitro platforms designed to model the spatial, chemical, structural, and physiological elements of in vivo cellular environments. They enhance the evaluation of complex engineered biological systems and are a step between traditional cell culture and in vivo experimentation. As neurochemists and measurement scientists studying the molecules involved in intercellular communication in the nervous system, we focus here on recent advances in neuroscience using microneurological systems and their potential to interface with mass spectrometry. We discuss a number of examples – microfluidic devices, spheroid cultures, hydrogels, scaffolds, and fibers – highlighting those that would benefit from mass spectrometric technologies to obtain improved chemical information.

2.3 Introduction

Until recently, scientists interested in examining cellular-level physiological responses to perturbations have used cultures of cells grown on dishes within a supportive medium. These cell cultures reduce the complexity of the living system to a level at which we can reasonably begin to understand the chemical, physical, and spatial influences affecting cellular behavior. Over the years, reductionist research strategies have advanced a broad range of scientific fields. However, it has become obvious that cells behave differently in cell culture than they do within the body. These differences may lead researchers to incorrect conclusions, with potentially detrimental effects on health-related research and scientific advancement. To solve this issue, and to gain more accurate insight into the physiologically based relationships among cells within the body, there has been a push to develop relevant microsystems in which cells are arranged in layers, cultured with other cells, or seeded onto various structures and geometries or within materials that more closely mimic those found in the body [1-3]. The goals are twofold: to improve the relevance of the cell culturing environment through the introduction of chemicals, gradients, cell types, and three-dimensional (3D) structures, and to create platforms that allow spatial and temporal specificity during sampling.

While there are many benefits to using reductionist techniques, they tend to limit the amount of information that can be gained from cells removed from the context in which they develop, especially when investigating dynamic cellular processes. The actual chemical messengers, such as proteins, peptides, and metabolites, rather than genetic differences, are often the markers for change within a biological system. Traditional cell culture systems cannot reproduce the variety of chemical, structural, and mechanical

interactions that influence cellular growth, development, communication, and susceptibility to disorders and pathologies [3,4]. In fact, cells cultured in three-dimensional (3D) systems have been shown to have different morphologies [2,5], biochemical gradients and content [2,5-11], electrophysiological profiles (12), and responses to chemotherapeutics and irradiation [7,8,13], as compared to two- dimensional (2D) cell cultures.

The relevance of the cell culture environment to the physiological system being investigated is particularly important in the study of neurochemistry. The nervous system uses a variety of intercellular messengers, including classical neurotransmitters, neuropeptides, metabolites, lipids, and even gases, to communicate important information throughout the body [14]. These intercellular signaling molecules and the information conveyed through them vary depending on their locations, amounts, and degradation pathways within the nervous system [15-17]. Additionally, the presence of these molecules and the responses of the target cells also depend on the surrounding environment, changing along with external perturbations [18,19], the presence or absence of other chemical or spatial signals [20,21], and the structural or geometric patterns in a growth system [22]. The goal of some neurochemical research is to gain a more complete understanding of the molecules involved in both healthy and diseased neurological systems in order to create better therapeutics for neurological disorders. This is a tall order that involves dynamic monitoring of intracellular, extracellular, signaling, and non-signaling molecules. We need to be able to understand specific relationships between perturbations in the nervous system and the resulting information flow via chemical messengers in both a temporal and spatial manner. While this is a daunting

task, the development of in vitro environments that mimic in vivo environments can bring us a step closer to realizing this goal.

In addition to creating physiologically relevant environments through the introduction of chemicals, gradients, and 3D structures or geometries within a system, microphysiological devices also improve the ability to spatially and temporally define physical sampling steps within an experiment [23-28]. This is vital to neurochemical investigation in which the specific spatial localization of perturbations allows the study of neural damage and repair, release of cell signaling molecules, and even the specific cells involved in the response. Similarly, temporal relationships between cellular insults and signal transmission are central to gaining an improved understanding of the influence these molecules have on information transfer.

As with advancements in any field, moving toward the development of more physiologically relevant microsystems comes with a need to apply emerging analytical toolsets to the new cell culture platforms and importantly, improve the chemical characterization of microneurological systems. Often, characterization of microphysiological systems is performed using morphological or physiological methods that provide little chemical information. In some cases, immunological techniques are used to target a few preselected molecules for analysis, and/or gene expression profiles are determined. However, to be confident that a newly developed system appropriately represents the chemical make-up of the tissue being mimicked, in-depth chemical characterization should be employed. After all, while transcriptomics provides information on the potential of a system, it is the molecules present that dictate its actual physiological state. The improved physiological relevance of microphysiological systems should lead

to important new discoveries, particularly in the neurochemical or cell signaling realm; therefore, we should be focusing on ways to better interrogate the systems for unique chemical information. Mass spectrometry (MS) is the single most information-rich chemical characterization technique available, allowing the detection and identification of a wide range of molecules in both a targeted and an untargeted manner. We expect that through the coupling of MS to these microsystems, we will be able to better characterize the dynamic chemical make-up of the cells involved, as well as the molecular messengers used in the information flow between cellular groups, both under physiological conditions and as a result of external perturbations.

For those of us who are more accustomed to thinking about reductionist approaches, there are multiple examples of biologists and engineers working together to create innovative platforms for the development of relevant microsystems. In this review, we broadly outline MS approaches of relevance to these systems, discuss the use of microfluidic devices, spheroids, hydrogels, and scaffolds to create appropriate microsystems, and lastly, highlight the exciting progress and future potential of interfacing these approaches to obtain improved chemical information for advancing neurochemical research.

2.4 MS as a chemical characterization approach

2.4.1 Introduction to MS

While the goal of many microsystem designs is to create an improved cell culturing environment and enhanced sampling system defined by the spatial and temporal aspects of the device, eventually the samples need to be characterized. If a preselected set of molecules are of interest, specific molecular or affinity probes can be used. However, for

more untargeted or less well-characterized analytes, MS remains the most chemically information-rich approach because it allows the characterization and quantitation of thousands of molecular species, usually without analyte preselection. There are a multitude of modern mass spectrometric techniques to choose from. The method selected depends on several factors, including sample properties and instrumental parameters, which together determine the compounds detected. Although detailed descriptions of all of the available hardware and operating procedures for MS are not within the scope of this review, a brief overview is provided to aid in the selection of the appropriate MS-based characterization approach. Critical considerations include choosing the appropriate sample conditioning method (including a separation step), vaporization and ionization approaches, and mass analyzer. Readers interested in learning more about MS are referred to several recent reviews [29-31].

2.4.2 Analysis of Small Sample Volumes via MS

Researchers interested in characterizing a wide range of molecules using a microphysiological system, either present in the environment surrounding the system or found within the system, can efficiently couple the device to a mass spectrometer for the collection of small-volume samples. The most straightforward microphysiological systems for this type of sampling are those with direct inlet and outlet ports and/or direct access to the material that will be collected. The next steps depend on the desired information and the MS instrumentation available. The two most commonly employed MS characterization approaches are matrix-assisted laser desorption/ionization (MALDI) and electrospray ionization (ESI), as they are both well suited for small-volume samples [32-36].

For a dried sample, MALDI MS is a fast method that involves incorporating the analyte with an organic matrix, which when irradiated with a laser, vaporizes and ionizes the sample [34,37]. MALDI measurements have been performed from cellular releasates, individual cells, and even directly from tissue slices [38]. Basically, if a small-volume (picoliter to microliter) sample is dried and the appropriate chemical matrix added, efficient detection of a broad range of molecules becomes possible. MALDI has a high salt tolerance and requires nanoliter-volume samples [27,32,39], making it useful for the analysis of small-volume biological samples, and even individual cells [40-42]. Additionally, for precious samples, the recovery of leftover analytes is possible [43]. Sample conditioning can enhance MALDI analysis, for example, by desalting and concentration via solid phase extraction (SPE) [44,45]. After extraction, analytes of interest can be eluted onto a target plate (by SPE) or dried down, reconstituted in an appropriate amount of solvent, and then placed on the plate (by SPE or liquid extraction). In both situations, the sample is plated, mixed with a matrix, and dried in preparation for mass spectrometric analysis.

While MALDI has a number of advantages, an issue with MALDI is that interfacing it to separations, such as liquid chromatography (LC) or capillary electrophoresis (CE), adds complexity as compared to ionization techniques that use samples in solution. Without a preseparation with MALDI, ion suppression can occur; thus, there are applications that are better suited to LC-ESI-MS. In ESI-MS, a liquid sample is sprayed from a capillary via the application of an electrical potential to the end of the capillary [35,46]. The electrosprayed droplets are desolvated and vaporized, resulting in multiply charged ions, which are introduced into the mass analyzer [35]. ESI works well as a characterization

approach after a liquid phase separation, and so often follows CE [44,47] or LC [48]. The figures of merit of ESI make it particularly useful for the identification and quantitation of a wide range of analytes within complex samples [35]. Researchers interested in evaluating the analytes within a microphysiological system would benefit from using these techniques, although other MS ionization approaches are available [49].

2.4.3 Analysis of Large, Complex Samples via MS

At the other end of the volume scale, a number of metabolomics or proteomics approaches have evolved that take larger-volume samples, condition them, and then perform an LC separation followed by high performance MS, including tandem MS (MS/MS) [48]. As mentioned in the previous section, LC separation is important for the reduction of the chemical complexity and dynamic range inherent to biological samples, with the goal of separating the samples into chemically simpler fractions. LC-MS/MS generally requires larger amounts of sample than direct MALDI MS profiling, but is useful for peptidomic, metabolomic, or proteomic studies, as well as for quantitation.

2.4.4 Direct Imaging of Samples using MS

MALDI MS is increasingly being employed for spatially resolved tissue characterization in an approach termed mass spectrometry imaging (MSI). In a common embodiment of MSI, a laser samples the surface in a raster pattern, and at each point, a mass spectrum is acquired. The resulting spectra are then used to create images of ion intensity at specific locations within the sample [50]. Instead of interrogating a tissue with MS, one can use MSI to spatially measure the compounds within a microfabricated device [51,52]. Additionally, because microphysiological systems can contain complex 3D structures, these structures can be removed from the systems and processed as though they are

tissue through a series of stabilization and sectioning steps prior to analysis [38,53]. MSI can be performed using MALDI MS, secondary ion MS (SIMS), or desorption electrospray ionization MS [54]. Each ionization method has distinct figures of merit as well as different sample preparation requirements [50,54]. No matter which detection modality is used, MSI is useful for researchers who want to obtain spatial information on the molecular content of their samples, both for basic study and to determine how well the model systems compare to the in vivo systems they are mimicking.

2.4.5 Single Cell Measurements via MS

Understanding the chemical differences between cells is an important objective for neurochemical studies. Various MS methods can be employed for single cell measurements, including the aforementioned MALDI, ESI, and SIMS [38]. Single cells contain femtoliters to picoliters of liquid and, therefore, measurements require high sensitivity and low limits of detection. Additionally, cells contain a complex mixture of molecules, requiring wide analyte coverage and ionization of intact biomolecules. Direct sampling from specific cells using liquid microjunction extraction for CE-ESI MS [55], and direct MALDI profiling of individual cells sorted into microarrays [42] or dissociated onto slides [56], are methods that are currently employed to interrogate the chemical content of single cells, offering great potential for integration with microphysiological systems.

2.4.6 Sample Preparation Considerations for MS

We outline the factors that impact the selection of the sampling and measurement protocols. For sampling from a microphysiological system, we expect that cells, tissues, and extracellular fluid would be the most common types of samples obtained. The sample preparation method selected for an MS analysis depends on a variety of factors, including

the tissue or model the sample came from, the chemical information the researcher is trying to obtain, the instrument that will be used for the analysis, and how much time will elapse between sample preparation and analysis. In addition, a decision has to be made about whether it is important to the experimental objective to maintain structural, temporal, or location information, a choice that impacts how samples are collected and prepared.

For example, if chemical characterization of different cellular populations is the goal, cells could be detached (or “dissected”) from the device, suspended in a liquid media, stabilized with glycerol or a similar substance so that they remain intact during a drying step, washed to remove the excess glycerol, dried under a nitrogen stream, and coated with a matrix in preparation for MALDI. Alternatively, the cells could be individually prepared for intracellular media sampling by CE. These sampling approaches would allow for intracellular chemical characterization of different cell types, but would not maintain the spatial relationships of the cells. In studies where retaining spatially relevant chemical information is more important, the system could instead be frozen, cryogenically sliced, and then the slices deposited onto MALDI target plates, stabilized, and covered in a matrix for MS analysis. This type of sample preparation maintains intra- and extracellular areas as well as spatial relationships between cells. On the other hand, if analysis of cell signaling molecules is the goal, extracellular fluid can be collected from the device in a temporal or spatially relevant manner, subjected to sample clean-up via SPE to remove the salts from the extracellular media, and then either mixed with a MALDI matrix or prepared with an appropriate solvent for LC-MS analysis. Finally, if the goal is to understand as much chemical information as possible about a certain system (at the

expense of spatial detail), the cells or tissues can be homogenized, the proteins, peptides, small molecules, or metabolites extracted, and the sample subjected to an SPE step and then prepared for LC prior to MS analysis. These are just a few examples of sample preparation methods that can be employed prior to MS analysis.

2.5 Microphysiological Systems for Neurobiological Studies

2.5.1 Microfluidic Systems

Microfluidic systems for biological applications rely on the physics and chemistry of small-volume materials and fluidic interactions to create intricate platforms for the growth, analysis, and manipulation of cells on a micrometer scale [57]. When applied to biological systems, they have historically been used as a reductionist approach for single cell analyses, cell sorting, and compartmentalization; however, microfluidic devices are also used to create microphysiological systems [28,58-63]. The small-volume fluidic interactions allow for the formation of specially controlled microenvironments that can mimic the physiological milieu and structural relationships, while also providing opportunities for sampling, observation, and introduction of specific perturbations [64,65]. These attributes allow for the design of studies to provide a more accurate picture of cellular responses. Our research group has had success using microfluidic devices to sample from cells for mass spectrometric analysis [27,51,52,66], and we look forward to performing similar experiments utilizing microphysiological systems.

The move away from traditional cell culture, and toward constructing a microphysiological system, can be facilitated by co-culturing different cell types in a microfluidic device. While many fields use the technology, the intricate relationships between neurons and their surrounding cells make co-culture for neurochemical investigation particularly relevant.

First and foremost, neurons and glia are interdependent, and studies have shown that neurons behave differently with and without glia in their cultures [28,58,61]. Therefore, both types of cells need to be incorporated into the microfluidic device. For example, Majumdar et al. [58] demonstrated a microfluidic device for the co-culture of primary hippocampal neurons and glial cells in which both types of cells were not physically in contact, but glial-conditioned media flowed directly from glia to the neurons. They found that the neurons co-cultured with glia had greater transfection efficiency than traditional cell cultures, demonstrating the influence of glial presence in the culture system. Li and Ren et al. [28] developed a microfluidic device in which axonal injury can be studied within a system that includes both neurons and glia. They showed that their system allowed re-growth of axons when glial cells were introduced to the culture system. With the understanding that neuronal/glial interactions are important to study, Park et al. [59] kept the neuronal cell bodies physically separated but allowed interaction between oligodendrocytes and the neuronal axons for the study of myelination (Figure 2.1a).

With microphysiological systems, it is important that target tissues are incorporated within the model system. Neurons develop, regenerate, and function based on their surroundings [14,28,67], supporting the need for functional neuromuscular junctions, sensory systems, and brain structures that can be studied. The neuromuscular junction consists of the spinal motor neurons, the cell bodies of which can be found in the ventral horn of the spinal cord, and their target organ, muscle. Recently, Kim et al. [60] demonstrated a microsystem in which spinal cord and muscle tissues were placed within channels located on opposing sides of the device, connected with microchannels. Axons from the spinal cord grew across the microchannels and innervated the muscle tissue.

Southam et al. [61] described the use of a commercial dual-chamber microfluidic device to culture motor neurons and glia on one side of the device and myocytes on the other. They demonstrated the growth of motor neuron axons through the microchannels and into the myotube side (Figure 2.1b) and discussed the importance of glial cells and target muscle tissue for the health of the motor neuron in culture.

Perhaps more exciting is a system reported by the Perlson group [20,62], created using a slice of an embryonic spinal cord explant co-cultured with myotubes. In this microfluidic device, the axons from the motor neurons grew through grooves to innervate the myotubes. One of their studies revealed not only that the axons grew more quickly through the grooves when the myoblasts were present than when they are not, but also that the growth factor glial cell line-derived neurotrophic factor only promoted axonal growth and innervation when applied to the axons of the motor neurons, and not when applied to the cell body [20]. This outcome is a demonstration of the important new biochemical insights that can be gained from using microphysiological systems.

For the peripheral sensory nervous system, there is one more “side” to account for within the microsystem. The cell body of the sensory neuron resides in the sensory ganglia located near the spinal cord [68,69]. Sensory neurons only have one outgrowth, an axon, which bifurcates, extending one branch to the skin or viscera and the other into the dorsal horn of the spinal cord. Using a popular microfluidic device design [70], Tsantoulas and colleagues [71] created the sensory ending side of this system by culturing primary sensory neurons from the dorsal root ganglion on one side of a two-chamber device and keratinocytes on the other, to resemble the skin (Figure 2.1c). They demonstrated the

successful innervation of the keratinocytes by the sensory neurons, as have other groups using separate two-compartment co-culture models [21,72,73].

As for the side of the sensory neuron axon that extends to the spinal cord, a few groups have demonstrated functional cultures between neurons of the dorsal horn of the spinal cord and those of the dorsal root ganglia [74-77]. Additionally, Johnson et al. [26] demonstrated a 3D printed tri-chamber device within which they successfully cultured peripheral sensory neurons, Schwann cells and epithelial cells or hippocampal neurons, and peripheral sensory neurons and Schwann cells, in chambers 1, 2, and 3, respectively. While hippocampal neurons are not secondary sensory neurons, this is one of the only successful central nervous system (CNS) to peripheral nervous system micro-cultures. Unfortunately, there are not yet any microsystems that can mimic the peripheral sensory system from skin to spinal cord; however, work is being done in this area.

Another important area of research for the design of microfluidic systems includes the re-creation of the blood-brain barrier (BBB). Understanding the BBB is important to the study of neurochemistry because it is the gatekeeper of the brain, regulating which molecules are allowed to enter the CNS from the blood. Various groups have designed devices that mimic certain aspects of the BBB [78]. Two similar device designs, one created by the Sundaram group [63] and another by the Wikswo group [79], successfully modeled the neurovascular unit by using multiple layers, including a neural chamber, and a vascular chamber, and a microporous membrane separating the two (Figure 2.1d) [79]. The neural chamber consisted of a physiologically relevant mix of neurons and support cells such as astrocytes and microglia (for the Sundaram group) or pericytes (for the Wikswo group), and the vascular chamber contained microvascular endothelial cells. Both groups

reported the ability to include flow within their design, which is imperative for the appropriate function of endothelial cells and for mimicking vasculature. Importantly, the Wikswo group seeded the neurons and astrocytes within a collagen gel in the “brain” chamber to even better model brain structure, and also used human-derived cells within their system. Another noteworthy BBB device design is the Ingber group’s [80] use of a microfluidic system to create a cylindrical lumen inside a microchannel within which astrocytes, pericytes, and endothelial cells were seeded. This work is important because it incorporates the appropriate shape of the blood vessels (cylinder), unlike the rectangular channels used by other groups, and also removes the membrane barrier between cell types, allowing them to be in physical contact with each other, as they are in the body.

2.5.2 Spheroids

Another way to create physiologically relevant nervous system models is to place neurons and their support cells together and let them assemble or aggregate on their own. The creation of spheroid cultures relies on the cells’ natural proclivity to aggregate, rather than on the strict design of structural, chemical, and physical relationships used by microfluidic devices. A spheroid culture is both a way to create a more natural state for the cells under investigation, and a means to study the natural formation of cellular aggregates. Spheroid culturing technique is based on keeping cells in suspension so that they will join together, rather than settle on and form attachments to a particular cell-culturing surface. Aggregation can be encouraged through stirring, suspending cells in drops from a surface, and plating in non-adhesive microarray wells. Once aggregated, the spheroids tend to demonstrate behavior similar to that found in vivo, such as exhibiting the proper

intercellular relationships or secreting their own extracellular matrix (ECM) [81]. The creation of spheroids and spheroid networks can be useful in the study of intercellular interactions and cell-ECM interactions [81], toxicity studies [82], and even neural tissue transplantation [83].

As an example of spheroid neural cultures being used to study disease, the Lee lab [82] built an in vitro model of Alzheimer's disease using a network of neurospheres to model the layered cellular architecture of the brain's cortex for the study of beta amyloid exposure. Building on this model, Park et. al. [84] incorporated the constant fluid flow that is found in physiological systems. The potential implications for their model in the study of Alzheimer's disease is important to note, particularly for understanding the response of the tissue to beta amyloid exposure as well as for toxicity studies for potential therapeutics.

Another group, led by Kato-Negishi [83], created a network of neurospheres that could then be used as a stamp and placed directly onto cortical tissue. While it is unclear how this type of brain tissue would actually function once incorporated into a living system, the researchers did show integration between the stamped neurosphere network and the whole brain tissue; which is a promising step forward for future cognitive interface work.

Recently, Pamies et al. [85] demonstrated the creation of a reproducible, size-controlled spheroid culture using induced pluripotent stem cells differentiated into a structure containing appropriately localized neurons, oligodendrocytes, and astrocytes as well as neural sub- populations, such as those expressing dopamine, glutamine, or GABA. Since they are derived from human cells and are uniformly made, these brain microphysiological

systems, as they are called, could be particularly useful for pharmaceutical or neurotoxicity studies.

Spheroids can also be used within microfluidic devices. For example, the Kamm group [65] described an enhanced co-culture microfluidic device in which a 3D system was created that allows for the culture of both a neurosphere on one side of the device and a muscle strip on the other, with axonal outgrowth from the neurosphere connecting to the muscle strip (Figure 2.2a).

2.5.3 Hydrogels, Fibers, and Other Soft Materials

The incorporation of various soft materials into cell culture is another way that physiological relevance can be enhanced in an engineered system. Hydrogels are highly absorbent cross-linked polymers that can be used in a variety of ways. They are particularly useful in the creation of microphysiological systems because they are mechanically and structurally similar to tissue and extracellular matrix [86]. This similarity to natural tissue, along with a level of porosity that allows for cell migration and nutrient and waste exchange, combine to make hydrogels prime materials for creating 3D cell cultures [86,87].

Lozano et al. [87] designed a system in which a peptide-modified polymer, gellan gum-RGD, was mixed with cortical cells and printed using a 3D printing system into a layered structure similar to that of the cortex (Figure 2.2b). The authors found that the neurons and glia were functional, and that synapses formed between printed layers. Therefore, they succeeded in creating a 3D cortex-like structure with viable neurons encapsulated inside, demonstrating appropriate growth and neurite extension. Similarly, Kunze et al. [88] used microfluidic devices to create alginate-enriched agarose hydrogel layers that

model the structure of the cortex (Figure 2.2c). The layers can also be perfused with nutrients and/or stimulated with chemicals in a gradient and are oriented in the x-y plane for facile microscope imaging. While their system used only one type of cell, the importance of their device in correctly simulating the external environment for the neurons of the cortex cannot be dismissed.

Huval et al. [89] created a 3D system in which a dorsal root ganglion explant was placed within a dual hydrogel encasement system that had been treated with both growth-permissive and growth-inhibiting molecules so that the axonal outgrowth followed a discrete nerve-like path. This “microscale organotypic model of peripheral nerve tissue,” as they described it, has a similar structure and electrophysiological function as nerve tissue, making it a potential model for use in pharmaceutical and clinical testing. It would also be an interesting model for injury, regeneration, and neurochemical studies.

A multi-layered microfluidic device to fabricate hydrogel constructs that mimic the structure of a nerve bundle, with its complex cross-sectional morphology, was designed by Kitagawa et al. [90]. They used sodium alginate to create stiff microfibers that were encapsulated by a softer hydrogel, which included sodium alginate mixed with propylene glycol alginate. The PC12 neuron-like cells grew along the stiff microfibers, creating an analogous structure to an axon surrounded by Schwann cells.

Hydrogels influence cellular responses based on the stiffness, charge, and other properties of the gel [91]. While the ability to tune a hydrogel creates unlimited opportunities for creating various environments within which cells can grow, the sensitivity of the cells to the hydrogel environment may not make them optimal for the study of in

vivo responses, unless a hydrogel that has the exact same parameters as the cell's environment is used.

Daud et al. [92] created nerve-like structures via electrospun polycaprolactone fiber scaffolds. These fibers, aligned in groups and created with uniform diameters of 1, 5, or 8 μm, allowed for the alignment of neurons, axons, and Schwann cells as they grew in culture. They used primary cell cultures and dorsal root ganglion explants, observing that neuronal and Schwann cell co-localization occurred for the dorsal root ganglion cultures, but not as extensively for the neuronal and primary Schwann cell cultures. The authors also studied primary neuron cell culture versus neuron/Schwann cell co-culture and concluded that axons extended further in the presence of Schwann cells than without. Both results add evidence to the importance of using an in vitro system that is the most closely related to the in vivo system.

A microscaffold system made from an array of microfabricated towers is the solution that Rowe et al. [93] designed to overcome the lack of appropriate circulation to 3D cell cultures. They used hollow microtowers that contained multiple fluid ports, which allowed for media and nutrient perfusion throughout the device. This group also included electrodes on the towers for ease of future electrophysiological stimulation or recording.

As a final example, Zou et al. [94] used self-assembly of the peptide IKVAV to create a scaffold of nanofibers, which were useful for guiding the outgrowth of axons from a dorsal root ganglion explant.

2.6 Applying MS to Microphysiological Systems for Chemical Analyses

The microsystems highlighted in this review were initially developed to improve scientists' ability to model in vivo physiology with many used to perform morphological, immunofluorescent, and even some biochemical analyses. Each of the microfluidic systems discussed are also well suited for chemical integration with mass spectrometric analysis and can be used to collect cellular releasates, or would only need small adjustments in the form of stimulation and sampling ports for coupling with off-chip analysis by MS.

Microfluidic devices have a history of being coupled with mass spectrometric analysis [27,52,95-98], and we expect this will continue. Perfusion of media through input and output ports for stimulations and sample collection is the simplest approach, while others might opt for employing microdialysis-like methods or adding more intricate on-chip processing steps to the sample collection [96,98]. Although these adjustments could require changes to the design and fabrication of a microfluidic device, existing media perfusion ports can also be used for perturbations or sampling. For designs that do not have direct access, holes of varying diameters can be punched into the devices using biopsy punches or via less invasive sampling methods, such as a syringe and needle. Finally, researchers may opt to revise their designs and fabrication methods to create an optimized interface between their devices and the mass spectrometer.

Neurospheres can be incorporated into MS in two ways. First, they can be cultured within a microfluidic framework, as described by Uzel et al. [65]. Within a microfluidic device, neurospheres would provide a physiologically relevant cell culture construct and sampling would occur through perfusion, similarly to how it is outlined above. Additionally, the

cellular and chemical composition of a neurosphere, as well as its ability to create its own extracellular matrix, would be interesting to study using MSI. The neurospheres can be sectioned and then subjected to MSI to examine their chemical make-up, as described by the Hummon group [53,54] in their study of spherical cultures (Figure 2.3) [54]. Impressively, they were able to identify proteins and their distributions within colon carcinoma spheroids. Additionally, the surroundings of the neurospheres could be directly imaged using SIMS or MALDI without sectioning, helping to better understand the development of the extracellular matrix and surrounding environment, similar to how our group images biofilms [99].

Systems created out of hydrogels, scaffolds, and fibers can be sectioned and imaged similarly to neurospheres, or can be perfused and have analytes collected via sampling from device output ports, similar to sampling from microfluidic devices. Additionally, procedures such as microdialysis may be successful for sampling from within a hydrogel or scaffolded “tissue”. Specifically for polymer-based systems, one issue that may occur is that even if sampling is successful, the polymer content may suppress or overwhelm the signal from the sample. However, the current success in coupling MS with microfluidic devices that employ polymer materials, as described above, the use of hydrogels for localized protein extraction prior to MS analysis [100], and the compatibility of MS with microsystems using poly(dimethylsiloxane) [101], polycarbonate [102], and poly(methyl methacrylate) [103], demonstrate that polymer contamination from devices may not be as large an issue as some have assumed. Should concerns arise when using specific polymer-based devices, these issues could be potentially resolved through data analysis techniques, such as subtraction of the peaks associated with the intervening polymers.

Further, the development of non-polymer-based materials, improved sample clean-up techniques., and increased instrumental resolution and sensitivity could be future solutions to potential polymer contamination issues.

Additionally, single cell measurements for the detection of rare cells or the measurement of appropriate cell ratios/types within the system can be performed through direct sampling from the microphysiological device or by harvesting the cells through enzymatic digestion and dissociation and measuring their cell profiles using microarrays [42] or microscopy-guided MS analysis after dispersion [56].

We acknowledge that a limitation of using MS to chemically characterize microphysiological systems is the potentially low amount of analyte present in such small systems, particularly when performing non-targeted analyses. However, recent improvements to mass analyzers and sample introduction systems have led to large decreases in the sample amounts required, with work using zeptomole amounts of metabolites and proteins now being reported. However, when using MS for these small-volume studies, researchers are cautioned that although the chemical information obtained by MS analysis does not require analyte preselection, the resulting data is often not comprehensive.

Finally, when working with human tissue samples, there are often time delays, and issues with sampling variability and non-uniform storage conditions, all of which can greatly impact the chemical information obtained from the tissues. When robust microphysiological systems become available, they will be an excellent source of samples from which we could gain a multitude of chemical details about normal human growth,

development, and aging, as well as disease progression. It is important to develop the analytical techniques now for when that time comes.

2.7 Conclusions

For years, the study of neurochemistry has relied on both in vivo systems, which can be difficult to control, and a range of in vitro 2D cell cultures and organotypic slices, which offer improved control and access to the cells but are not ideal models for living systems. Now, thanks to both improved microtechnologies and a better understanding of the nervous system, we have the tools at hand to build in vitro systems that behave more closely to in vivo systems.

A range of MS measurement approaches offer the most information-rich, non-targeted chemical characterization options available for characterizing metabolites, peptides, and proteins within a living system. Coupling microphysiological systems to mass spectrometers requires attention to the hyphenation details in order to obtain the greatest information on a dynamic cellular environment without introducing biases. While the analytical performance for mass spectrometers is impressive, there are numerous opportunities for improved interfaces between microphysiological systems and mass spectrometric measurement technologies, and we expect systems with enhanced spatial, chemical, and temporal resolution to be introduced in the coming years. Presently there are only a few examples of microphysiological systems having been used for analytical inquiries, and even fewer in neurochemistry; nonetheless, we look forward to the neurochemical insights to be gained from continued research in this area. We envision exciting progress in the integration of microphysiological systems with mass

spectrometric analysis and expect that the high information content of MS will enable new discoveries about the molecular players in both health and disease.

2.8 Figures

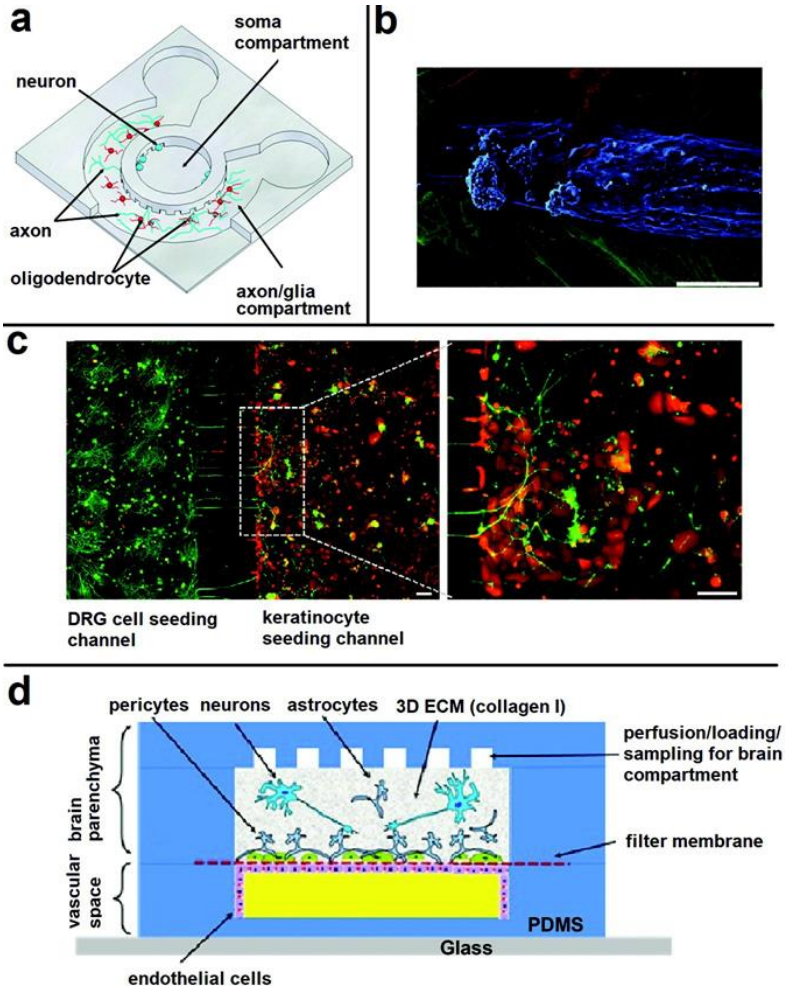

Figure 2.1: Microfluidic devices for the creation of microneurological systems. (a) Schematic illustration of the microfluidic compartmentalized CNS neuron co-culture platform. A 3D view of the circular device. Reproduced from Park J, Koito H, Li J, et al. Microfluidic Compartmentalized Co-Culture Platform for CNS Axon Myelination Research. Biomed Microdevices 2009;11:1145. Copyright (2009) with permission of Springer (59). (b) False-colored SEM image showing motor neurons (red) interacting with myotubules (blue) in the distal chamber of a microfluidic device. Scale bar: 5 µm. Reprinted from Southam KA, King AE, Blizzard CA, et al. Microfluidic Primary Culture Model of the Lower Motor Neuron–Neuromuscular Junction Circuit. J Neurosci Methods 2013;218:164-9. Copyright (2013) with permission from Elsevier (61). (c) Co-culture of rat neonatal keratinocytes (stained for cytokeratin 5, red) with rat neonatal primary sensory neurons (stained for B3 tubulin, green) in a dual chamber device. Scale bar: 100 µm. Adapted from Tsantoulas C, Farmer C, Machado P, et al. Probing Functional Properties of Nociceptive Axons Using a Microfluidic Culture System. PLoS One 2013;8:e80722. Provided under Creative Commons license 3.0 (71). (d) Schematic of a neurovascular unit created within a microfluidic device. Adapted from Brown JA, Pensabene V, Markov DA, et al. Recreating Blood-Brain Barrier Physiology and Structure on Chip: A Novel Neurovascular Microfluidic Bioreactor. Biomicrofluidics 2015;9:054124. Provided under Creative Commons license 3.0. (79).

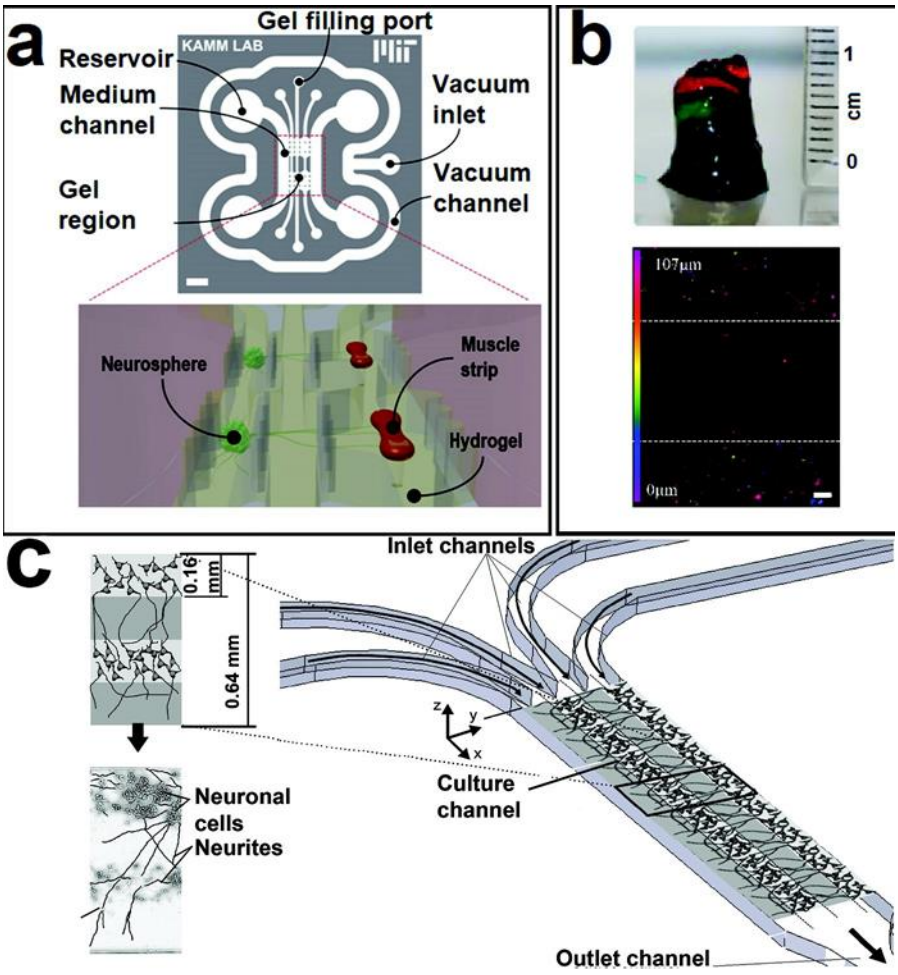

Figure 2.2: The use of neurospheres and hydrogels in microphysiological model systems. (a) Schematic of the integration of neurosphere culture within a microfluidic device. Adapted from Uzel SGM, Platt RJ, Subramanian V, et al. Microfluidic Device for the Formation of Optically Excitable, Three-Dimensional, Compartmentalized Motor Units. Science Advances 2016;2. Provided under Creative Commons Attribution-NonCommercial 4.0 International license. http://advances.sciencemag.org/content/2/8/e1501429.full (65). (b) Hydrogel layered cortex models. Top: 3D printed hydrogel layers Bottom: fluorescent images showing the layers with and without cells. The scale bar represents 100 μm. Reprinted from Lozano R, Stevens L, Thompson BC, et al. 3D Printing of Layered Brain-Like Structures Using Peptide Modified Gellan Gum Substrates. Biomaterials 2015;67:264-73, Copyright (2015) with permission from Elsevier (87). (c) Schematic of a microfluidic device used to create hydrogel layers imitating the cortex. Reprinted from Kunze A, Giugliano M, Valero A, et al. Micropatterning Neural Cell Cultures in 3D with a Multi-Layered Scaffold. Biomaterials 2011;32:2088-98. Copyright (2011) with permission from Elsevier (88).

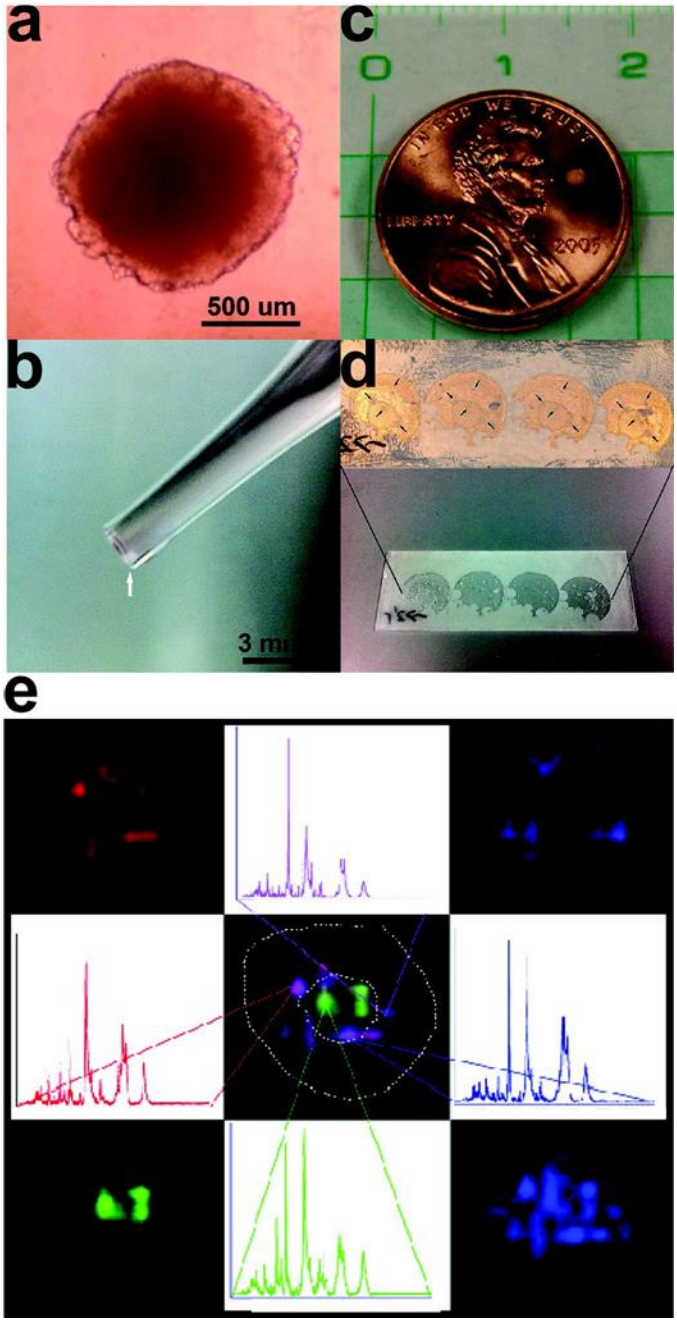

Figure 2.3: MS imaging of spherical cultures. (a) A spherical liver cell culture. (b) Arrow is pointing to the spherical culture in a pipet tip. (c) Spherical culture size compared to a penny (the white spot next to Lincoln's nose). (d) Spherical cultures imbedded in gelatin, sectioned, and placed on an indium tin oxide-coated microscope slide. The areas consisting of the cell culture slices are small and are located at the tips of the small black lines in the top image. (e) Representative mass spectra and corresponding ion intensity maps for MSI on the spherical culture. Adapted with permission from Li H, Hummon AB. Imaging Mass Spectrometry of Three- Dimensional Cell Culture Systems. Anal Chem 2011;83:8794-801, ref (54). Copyright 2011 American Chemical Society.

2.9 Work Cited

1. Wikswo JP. *The Relevance and Potential Roles of Microphysiological Systems in Biology and Medicine*. Exp Biol Med (Maywood) 2014;**239**:1061-72.
2. Baker BM, Chen CS. *Deconstructing the Third Dimension – How 3D Culture Microenvironments Alter Cellular Cues*. J Cell Sci 2012;**125**:3015-24.
3. Huang S, Wikswo J. *Dimensions of Systems Biology. Reviews of Physiology Biochemistry and Pharmacology*. Berlin, Heidelberg: Springer; 2007. p. 81-104.
4. Li X, Valadez AV, Zuo P, et al. *Microfluidic 3D Cell Culture: Potential Application for Tissue- Based Bioassays*. Bioanalysis 2012;**4**:1509-25.
5. Baharvand H, Hashemi SM, Kazemi Ashtiani S, et al. *Differentiation of Human Embryonic Stem Cells into Hepatocytes in 2D and 3D Culture Systems in Vitro*. Int J Dev Biol 2006;**50**:645- 52.
6. Yue X, Lukowski JK, Weaver EM, et al. *Quantitative Proteomic and Phosphoproteomic Comparison of 2D and 3D Colon Cancer Cell Culture Models*. J Proteome Res 2016;**15**:4265- 76.
7. Kumar HR, Zhong X, Hoelz DJ, et al. *Three-Dimensional Neuroblastoma Cell Culture: Proteomic Analysis between Monolayer and Multicellular Tumor Spheroids*. Pediatr Surg Int 2008;**24**:1229-34.
8. Desoize B, Jardillier J-C. *Multicellular Resistance: A Paradigm for Clinical Resistance?* Crit Rev Oncol/Hematol 2000;**36**:193-207.
9. Edmondson R, Broglie JJ, Adcock AF, et al. *Three-Dimensional Cell Culture Systems and Their Applications in Drug Discovery and Cell-Based Biosensors*. Assay Drug Dev Technol 2014;**12**:207-18.
10. Benya PD, Shaffer JD. *Dedifferentiated Chondrocytes Reexpress the Differentiated Collagen Phenotype When Cultured in Agarose Gels*. Cell 1982;**30**:215-24.
11. Zietarska M, Maugard CM, Filali-Mouhim A, et al. *Molecular Description of a 3D in Vitro Model for the Study of Epithelial Ovarian Cancer (Eoc)*. Mol Carcinog 2007;**46**:872-85.
12. Frega M, Tedesco M, Massobrio P, et al. *Network Dynamics of 3D Engineered Neuronal Cultures: A New Experimental Model for in-Vitro Electrophysiology*. 2014;**4**:5489.
13. Shield K, Ackland ML, Ahmed N, et al. *Multicellular Spheroids in Ovarian Cancer Metastases: Biology and Pathology*. Gynecol Oncol 2009;**113**:143-8.
14. Squire L, Berg D, Bloom F, et al., editors. Fundamental Neuroscience. Third ed.: Elsevier; 2008.

15. Strand FL, editor. Neuropeptides: Regulators of Physiological Processes. Cambridge, MA: The MIT Press; 1998.

16. Xu X-J, Wiesenfleld-Hallin Z. *Neuropeptides: Pain*. In: Squire LR, editor. Encyclopedia of Neuroscience. Oxford: Academic Press; 2009. p. 931–4.
17. Parenti C, Aricò G, Ronsisvalle G, et al. *Supraspinal Injection of Substance P Attenuates Allodynia and Hyperalgesia in a Rat Model of Inflammatory Pain*. Peptides 2012;**34**:412-8.
18. Hubbard RD, Quinn KP, Martinez JJ, et al. *The Role of Graded Nerve Root Compression on Axonal Damage, Neuropeptide Changes, and Pain-Related Behaviors*. Stapp Car Crash J 2008;**52**:33-58.
19. Lee KE, Winkelstein BA. *Joint Distraction Magnitude Is Associated with Different Behavioral Outcomes and Substance P Levels for Cervical Facet Joint Loading in the Rat*. J Pain 2009;**10**:436-45.
20. Zahavi EE, Ionescu A, Gluska S, et al. *A Compartmentalized Microfluidic Neuromuscular Co-Culture System Reveals Spatial Aspects of GDNF Functions*. J Cell Sci 2015;**128**:1241-52.
21. Roggenkamp D, Falkner S, Stäb F, et al. *Atopic Keratinocytes Induce Increased Neurite Outgrowth in a Coculture Model of Porcine Dorsal Root Ganglia Neurons and Human Skin Cells*. J Invest Dermatol 2012;**132**:1892-900.
22. Millet LJ, Gillette MU. *New Perspectives on Neuronal Development Via Microfluidic Environments*. Trends Neurosci 2012;**35**:752-61.
23. Tsamandouras N, Chen WLK, Edington CD, et al. *Integrated Gut and Liver Microphysiological Systems for Quantitative in Vitro Pharmacokinetic Studies*. AAPS J 2017;**19**:1499-512.
24. Blundell C, Tess ER, Schanzer ASR, et al. *A Microphysiological Model of the Human Placental Barrier*. Lab Chip 2016;**16**:3065-73.
25. Kilic O, Pamies D, Lavell E, et al. *Brain-on-a-Chip Model Enables Analysis of Human Neuronal Differentiation and Chemotaxis*. Lab Chip 2016;**16**:4152-62.
26. Johnson BN, Lancaster KZ, Hogue IB, et al. *3D Printed Nervous System on a Chip*. Lab Chip 2016;**16**:1393-400.
27. Croushore CA, Supharoek SA, Lee CY, et al. *Microfluidic Device for the Selective Chemical Stimulation of Neurons and Characterization of Peptide Release with Mass Spectrometry*. Anal Chem 2012.

28. Li L, Ren L, Liu W, et al. *Spatiotemporally Controlled and Multifactor Involved Assay of Neuronal Compartment Regeneration after Chemical Injury in an Integrated Microfluidics*. Anal Chem 2012;**84**:6444-53.
29. Glish GL, Vachet RW. *The Basics of Mass Spectrometry in the Twenty-First Century*. Nat Rev Drug Discov 2003;**2**:140-50.
30. Maher S, Jjunju FPM, Taylor S. *Colloquium: 100 Years of Mass Spectrometry: Perspectives and Future Trends*. Rev Mod Phys 2015;**87**:113-35.
31. Rubakhin SS, Sweedler JV. *A Mass Spectrometry Primer for Mass Spectrometry Imaging*. In: Rubakhin SS, Sweedler JV, editors. Mass Spectrometry Imaging: Principles and Protocols. Totowa, NJ: Humana Press; 2010. p. 21-49.
32. Romanova EV, Aerts JT, Croushore CA, et al. *Small-Volume Analysis of Cell–Cell Signaling Molecules in the Brain*. Neuropsychopharmacology 2014;**39**:50-64.
33. Hillenkamp F, Karas M. *The MALDI Process and Method*. MALDI MS. Wiley-VCH Verlag GmbH & Co. KGaA; 2007. p. 1-28.
34. Dreisewerd K. *Recent Methodological Advances in MALDI Mass Spectrometry*. Anal Bioanal Chem 2014;**406**:2261-78.
35. Wilm M. *Principles of Electrospray Ionization*. Mol Cell Proteomics 2011;10:M111.009407.
36. Qi M, Philip MC, Yang N, et al. *Single Cell Neurometabolomics*. ACS Chem Neurosci 2017;**9**:40-50.
37. Watson JT, Sparkman OD. *Introduction to Mass Spectrometry: Instrumentation, Applications, and Strategies for Data Interpretation*. Wiley; 2013.
38. Comi TJ, Do TD, Rubakhin SS, et al. *Categorizing Cells on the Basis of Their Chemical Profiles: Progress in Single-Cell Mass Spectrometry*. J Am Chem Soc 2017;**139**:3920-9.
39. Signor L, Boeri Erba E. *Matrix-Assisted Laser Desorption/Ionization Time of Flight (MALDI- TOF) Mass Spectrometric Analysis of Intact Proteins Larger Than 100 Kda*. J Visualized Exp 2013:50635.
40. Jansson ET, Comi TJ, Rubakhin SS, et al. *Single Cell Peptide Heterogeneity of Rat Islets of Langerhans*. ACS Chem Biol 2016;**11**:2588-95.
41. Romanova EV, Rubakhin SS, Monroe EB, et al. *Single Cell Mass Spectrometry. Single Cell Analysis*. Wiley-VCH Verlag GmbH & Co. KGaA; 2009. p. 109-33.
42. Urban PL, Jefimovs K, Amantonico A, et al. *High-Density Micro-Arrays for Mass Spectrometry*. Lab Chip 2010;**10**:3206-9.
43. Cockrill SL, Foster KL, Wildsmith J, et al. *Efficient Micro-Recovery and Guanidination of Peptides Directly from MALDI Target Spots*. BioTechniques 2005;**38**:301-4.

44. Ong T-H, Tillmaand EG, Makurath M, et al. *Mass Spectrometry-Based Characterization of Endogenous Peptides and Metabolites in Small Volume Samples*. Biochim Biophys Acta 2015;**1854**:732-40.

45. Hatcher NG, Richmond TA, Rubakhin SS, et al. *Monitoring Activity-Dependent Peptide Release from the CNS Using Single-Bead Solid-Phase Extraction and MALDI TOF MS Detection*. Anal Chem 2005;**77**:1580-7.
46. Fenn JB, Mann M, Meng CK, et al. *Electrospray Ionization–Principles and Practice*. Mass Spectrom Rev 1990;**9**:37-70.
47. Klepárník K. *Recent Advances in the Combination of Capillary Electrophoresis with Mass Spectrometry: From Element to Single-Cell Analysis*. Electrophoresis 2013;**34**:70-85.
48. Niessen WMA. *Progress in Liquid Chromatography–Mass Spectrometry Instrumentation and Its Impact on High-Throughput Screening*. J Chromatogr 2003;**1000**:413-36.
49. Wu C, Dill AL, Eberlin LS, et al. *Mass Spectrometry Imaging under Ambient Conditions*. Mass Spectrom Rev 2013;**32**:218-43.
50. Shariatgorji M, Svenningsson P, Andrén PE. *Mass Spectrometry Imaging, an Emerging Technology in Neuropsychopharmacology*. Neuropsychopharmacology 2014;**39**:34-49.
51. Jo K, Heien ML, Thompson LB, et al. *Mass Spectrometric Imaging of Peptide Release from Neuronal Cells within Microfluidic Devices*. Lab Chip 2007;**7**:1454-60.
52. Zhong M, Lee CY, Croushore CA, et al. *Label-Free Quantitation of Peptide Release from Neurons in a Microfluidic Device with Mass Spectrometry Imaging*. Lab Chip 2012;**12**:2037-45.
53. Ahlf Wheatcraft DR, Liu X, Hummon AB. *Sample Preparation Strategies for Mass Spectrometry Imaging of 3D Cell Culture Models*. J Visualized Exp 2014:52313.
54. Li H, Hummon AB. *Imaging Mass Spectrometry of Three-Dimensional Cell Culture Systems*. Anal Chem 2011;**83**:8794-801.
55. Comi TJ, Makurath MA, Philip MC, et al. *MALDI MS Guided Liquid Microjunction Extraction for Capillary Electrophoresis–Electrospray Ionization MS Analysis of Single Pancreatic Islet Cells*. Anal Chem 2017;**89**:7765-72.
56. Comi TJ, Neumann EK, Do TD, et al. *microMS: A Python Platform for Image-Guided Mass Spectrometry Profiling*. J Am Soc Mass Spectrom 2017;**28**:1919-28.
57. Wang J, Ren L, Li L, et al. *Microfluidics: A New Cosset for Neurobiology*. Lab Chip 2009;**9**:644-52.

58. Majumdar D, Gao Y, Li D, et al. *Co-Culture of Neurons and Glia in a Novel Microfluidic Platform*. J Neurosci Methods 2011;**196**:38-44.
59. Park J, Koito H, Li J, et al. *Microfluidic Compartmentalized Co-Culture Platform for CNS Axon Myelination Research*. Biomed Microdevices 2009;**11**:1145.

60. Kim Y-t, Karthikeyan K, Chirvi S, et al. *Neuro-Optical Microfluidic Platform to Study Injury and Regeneration of Single Axons*. Lab Chip 2009;**9**:2576-81.
61. Southam KA, King AE, Blizzard CA, et al. *Microfluidic Primary Culture Model of the Lower Motor Neuron–Neuromuscular Junction Circuit*. J Neurosci Methods 2013;**218**:164-9.
62. Ionescu A, Zahavi EE, Gradus T, et al. *Compartmental Microfluidic System for Studying Muscle–Neuron Communication and Neuromuscular Junction Maintenance*. Eur J Cell Biol 2016;**95**:69-88.
63. Achyuta AKH, Conway AJ, Crouse RB, et al. *A Modular Approach to Create a Neurovascular Unit-on-a-Chip*. Lab Chip 2013;**13**:542-53.
64. Croushore CA, Sweedler JV. *Microfluidic Systems for Studying Neurotransmitters and Neurotransmission*. Lab Chip 2013;**13**:1666-76.
65. Uzel SGM, Platt RJ, Subramanian V, et al. *Microfluidic Device for the Formation of Optically Excitable, Three-Dimensional, Compartmentalized Motor Units*. Sci Adv 2016;**2**:e1501429.
66. Chang Young L, Romanova EV, Sweedler JV. *Laminar Stream of Detergents for Subcellular Neurite Damage in a Microfluidic Device: A Simple Tool for the Study of Neuroregeneration*. J Neural Eng 2013;**10**:036020.
67. Bear MF, Connors BW, Paradiso MA. *Neuroscience: Exploring the Brain*. 2nd ed. Philadelphia: Lippincott Williams & Wilkins; 2001.
68. Devor M. *Unexplained Peculiarities of the Dorsal Root Ganglion*. Pain 1999;Suppl **6**:S27-35.
69. *Hogan Q. Labat Lecture: The Primary Sensory Neuron: Where It Is, What It Does, and Why It Matters*. Reg Anesth Pain Med 2010;**35**:306-11.
70. Taylor AM, Blurton-Jones M, Rhee SW, et al. *A Microfluidic Culture Platform for CNS Axonal Injury, Regeneration and Transport*. Nat Methods 2005;**2**:599-605.
71. Tsantoulas C, Farmer C, Machado P, et al. *Probing Functional Properties of Nociceptive Axons Using a Microfluidic Culture System*. PLoS One 2013;**8**:e80722.
72. Tsutsumi M, Nakatani M, Kumamoto J, et al. *In Vitro Formation of Organized Structure between Keratinocytes and Dorsal-Root-Ganglion Cells*. Exp Dermatol 2012;**21**:886-8.

73. Klusch A, Ponce L, Gorzelanny C, et al. *Coculture Model of Sensory Neurites and Keratinocytes to Investigate Functional Interaction: Chemical Stimulation and Atomic Force Microscope–Transmitted Mechanical Stimulation Combined with Live-Cell Imaging*. J Invest Dermatol 2013;**133**:1387-90.
74. Bird MM. *Establishment of Synaptic Connections between Explants of Embryonic Neural Tissue in Culture: Experimental Ultrastructural Studies*. Exp Brain Res 1985;**57**:337-47.
75. Vikman KS, Backström E, Kristensson K, et al. *A Two-Compartment in Vitro Model for Studies of Modulation of Nociceptive Transmission*. J Neurosci Methods 2001;**105**:175-84.
76. Ohshiro H, Ogawa S, Shinjo K. *Visualizing Sensory Transmission between Dorsal Root Ganglion and Dorsal Horn Neurons in Co-Culture with Calcium Imaging*. J Neurosci Methods 2007;**165**:49-54.
77. Shipshina MS, Fedulova SA, Veselovskii NS. *Induction of Long-Term Depression of Synaptic Transmission in a Co-Culture of DRG and Spinal Dorsal Horn Neurons of Rats*. Neurophysiology 2011;**43**:261-70.
78. Phan DT, Bender RHF, Andrejecsk JW, et al. *Blood–Brain Barrier-on-a-Chip: Microphysiological Systems That Capture the Complexity of the Blood–Central Nervous System Interface*. Exp Biol Med;**0**:1535370217694100.
79. Brown JA, Pensabene V, Markov DA, et al. *Recreating Blood-Brain Barrier Physiology and Structure on Chip: A Novel Neurovascular Microfluidic Bioreactor*. Biomicrofluidics 2015;**9**:054124.
80. Herland A, van der Meer AD, FitzGerald EA, et al. *Distinct Contributions of Astrocytes and Pericytes to Neuroinflammation Identified in a 3D Human Blood-Brain Barrier on a Chip*. PLoS One 2016;**11**:e0150360.
81. Fennema E, Rivron N, Rouwkema J, et al. *Spheroid Culture as a Tool for Creating 3D Complex Tissues*. Trends Biotechnol 2013;**31**:108-15.
82. Choi YJ, Park J, Lee S-H. *Size-Controllable Networked Neurospheres as a 3D Neuronal Tissue Model for Alzheimer's Disease Studies*. Biomaterials 2013;**34**:2938-46.
83. Kato-Negishi M, Tsuda Y, Onoe H, et al. *A Neurospheroid Network-Stamping Method for Neural Transplantation to the Brain*. Biomaterials 2010;**31**:8939-45.
84. Park J, Lee BK, Jeong GS, et al. *Three-Dimensional Brain-on-a-Chip with an Interstitial Level of Flow and Its Application as an in Vitro Model of Alzheimer's Disease*. Lab Chip 2015;**15**:141-50.

85. Pamies D, Barreras P, Block K, et al. *A Human Brain Microphysiological System Derived from Induced Pluripotent Stem Cells to Study Neurological Diseases and Toxicity*. ALTEX 2017;**34**:362-76.
86. Turunen S, Haaparanta A-M, Äänismaa R, et al. *Chemical and Topographical Patterning of Hydrogels for Neural Cell Guidance in Vitro*. J Tissue Eng Regen Med 2013;**7**:253-70.
87. Lozano R, Stevens L, Thompson BC, et al. *3D Printing of Layered Brain-Like Structures Using Peptide Modified Gellan Gum Substrates*. Biomaterials 2015;**67**:264-73.
88. Kunze A, Giugliano M, Valero A, et al. *Micropatterning Neural Cell Cultures in 3D with a Multi-Layered Scaffold*. Biomaterials 2011;**32**:2088-98.
89. Huval RM, Miller OH, Curley JL, et al. *Microengineered Peripheral Nerve-on-a-Chip for Preclinical Physiological Testing*. Lab Chip 2015;**15**:2221-32.
90. Yoichi K, Yoji N, Yuya Y, et al. *Patterned Hydrogel Microfibers Prepared Using Multilayered Microfluidic Devices for Guiding Network Formation of Neural Cells*. Biofabrication 2014;**6**:035011.
91. Wang TY, Forsythe JS, Parish CL, et al. *Biofunctionalisation of Polymeric Scaffolds for Neural Tissue Engineering*. J Biomater Appl 2012;**27**:369-90.
92. Daud MFB, Pawar KC, Claeyssens F, et al. *An Aligned 3D Neuronal-Glial Co-Culture Model for Peripheral Nerve Studies*. Biomaterials 2012;**33**:5901-13.
93. Rowe L, Almasri M, Lee K, et al. *Active 3-D Microscaffold System with Fluid Perfusion for Culturing in Vitro Neuronal Networks*. Lab Chip 2007;**7**:475-82.
94. Zou Z, Zheng Q, Wu Y, et al. *Growth of Rat Dorsal Root Ganglion Neurons on a Novel Self- Assembling Scaffold Containing IKVAV Sequence*. Mater Sci Eng 2009;**29**:2099-103.
95. Wei H, Li H, Gao D, et al. *Multi-Channel Microfluidic Devices Combined with Electrospray Ionization Quadrupole Time-of-Flight Mass Spectrometry Applied to the Monitoring of Glutamate Release from Neuronal Cells*. Analyst 2010;**135**:2043-50.
96. Mao S, Zhang J, Li H, et al. *Strategy for Signaling Molecule Detection by Using an Integrated Microfluidic Device Coupled with Mass Spectrometry to Study Cell-to-Cell Communication*. Anal Chem 2013;**85**:868-76.
97. Dugan CE, Kennedy RT. *Measurement of Lipolysis Products Secreted by 3T3-L1 Adipocytes Using Microfluidics*. Methods Enzymol 2014;**538**:195-209.
98. Li X, Hu H, Zhao S, et al. *Microfluidic Platform with in-Chip Electrophoresis Coupled to Mass Spectrometry for Monitoring Neurochemical Release from Nerve Cells*. Anal Chem 2016;**88**:5338-44.

99. Baig NF, Dunham SJB, Morales-Soto N, et al. *Multimodal Chemical Imaging of Molecular Messengers in Emerging Pseudomonas Aeruginosa Bacterial Communities*. Analyst 2015;**140**:6544-52.
100. Rizzo DG, Prentice BM, Moore JL, et al. *Enhanced Spatially Resolved Proteomics Using on-Tissue Hydrogel-Mediated Protein Digestion*. Anal Chem 2017;**89**:2948-55.
101. Chan JH, Timperman AT, Qin D, et al. *Microfabricated Polymer Devices for Automated Sample Delivery of Peptides for Analysis by Electrospray Ionization Tandem Mass Spectrometry*. Anal Chem 1999;**71**:4437-44.
102. Xu N, Lin Y, Hofstadler SA, et al. *A Microfabricated Dialysis Device for Sample Cleanup in Electrospray Ionization Mass Spectrometry*. Anal Chem 1998;**70**:3553-6.
103. Meng Z, Qi S, Soper SA, et al. *Interfacing a Polymer-Based Micromachined Device to a Nanoelectrospray Ionization Fourier Transform Ion Cyclotron Resonance Mass Spectrometer.* Anal Chem 2001;**73**:1286-91.

Chapter 3

Measuring Cellular Microenvironments and Release via MS

3.1 Notes

This chapter is an excerpt from a review written by Dr. Ta-Hsuan Ong, Dr. Emily Tillmaand, Monika Makurath, Dr. Stanislav Rubakhin, and Dr. Jonathan Sweedler. (*Biochim Biophys Acta*. 2015 Jul;1854(7):732-40. doi: 10.1016/j.bbapap.2015.01.008) and is reproduced with permission. The excerpt that follows is the section of the review that I wrote, reviewing improved methods for measuring chemical components of extracellular environments using mass spectrometry (MS).

3.2 Introduction

The investigation of stimulated cellular release provides an opportunity to determine a subset of cellular metabolites and peptides that are likely to be involved in cell-to-cell signaling. Secretomics, the study of the compounds released from a cell, uses a wide range of methodologies, including MS, microfluidics, Western blotting, enzyme-linked immunosorbent assays, gel electrophoresis, radioimmunoassay / labeling with radioactive isotopes, and amperometric detection [1-9]. Released compounds vary from small diatomic gases to large proteoglycans and peptides; thus, it is not surprising that a range of characterization approaches are required to assay this large variety of analyte types.

MS is an important tool for studying cellular release as it provides multiplexed information about the protein, peptide, and metabolite content of the releasate without the need for analyte pre-selection. The focus of cellular release studies range from biomarker detection and identification to the determination of protein concentrations [1]. We have

chosen to highlight work that has involved the detection and identification of cell-to-cell signaling molecules in the nervous system. Uncovering the peptide composition of cellular releasate helps to elucidate the functional roles of observed peptides by relating their release parameters to specific stimulation paradigms. For peptides with known activities and targets, it may help to define the physiological role of the studied cell. MALDI-time-of-flight (TOF) MS is often used to study peptide secretion due to its salt tolerance, low detection limits, and ability to be hyphenated with a variety of sample conditioning approaches [10]. As with all single cell studies, secretomics is complicated by the chemical complexity of extracellular environments, low analyte amounts, and the need to remove unwanted chemical components from the sample prior to MS analysis. Microfluidic technologies enable efficient single cell culture, direct cell stimulation, and more specific temporal and spatial capture of released analytes.

3.3 Using Microfluidics for Sampling

Many microfluidic systems have been designed for the capture, treatment, and analysis of single cells, some of which have been applied to investigate analyte release from individual cells or small cellular structures [8, 11-13]. Wei et al. [14] developed a series of microfluidic chips that incorporate cell culture and on-chip pretreatment coupled with electrospray (ESI)-quadrupole-TOF MS for analysis. In order to detect glutamate secreted from stimulated PC12 cells, the cells were cultured and stimulated in microchannels on one chip and then the extracellular fluid was moved through tubing to a miniature extraction chip in which the sample was flowed over polymer solid phase extraction (SPE) beads for pretreatment. After pretreatment, the sample was once again moved through tubing to the ion source. This series of chips could easily be used for the analysis of

peptides released upon stimulation. Microfluidic devices designed for the detection of peptides are used in biomarker detection assays. Yang et al. [15] presented a device in which specific peptides are affinity captured in microchannels lined with antibodies. This particular system allows detection of as few as 300 peptide molecules and can be when applied in targeted analysis of released peptides.

Quantitative analyses of released analytes can also be performed using a microfluidic platform hyphenated to MS. Zhong et al. [19] developed a device for the quantification of peptides released from *A. californica* bag cell neurons. The device consisted of one serpentine channel treated with octadecyltrichlorosilane (OTS), used to collect the peptides at specific locations. A continuous flow of extracellular fluid brought the released peptides into contact with the OTS. This OTS layer with captured molecules was then interrogated using MALDI MSI. The distance that the peptide was detected along the length of the channel correlated with the amount of the peptide in the sample.

3.4 Using SPE During Sample Collection

Collection of the extracellular media and its direct analysis via MALDI-TOF MS is a powerful approach for the analysis of normal and pathological peptide secretion [16]. However, even though MALDI-TOF MS has a high inorganic salt tolerance, the high levels of salts present in the physiological extracellular media hinders effective molecular characterization with MS. Therefore, SPE is often used for sample conditioning as it improves detection, minimizes sample loss, and decreases the salt content before the MS measurement. An analytical system developed by Croushore et al. [17] allowed for the selective stimulation of cultured *A. californica* bag cell neurons through a device in which fluid flow was controlled via applied external pressures and pneumatically

controlled microvalves. Once the cells were stimulated, microliter volumes of the cellular microenvironment were collected, purified using SPE, and analyzed by MALDI-TOF MS analysis. This approach allowed low temporal resolution studies of analyte release from low-density cultures and single cells.

Mao et al. [18] studied intercellular communication through the integration of stimulation, release, and pretreatment steps all on one chip. A microfluidic device capable of culturing two distinct cell populations was used for stimulation of one population and a surface tension plug control was used to control the chemical signaling between the populations. Once the desired stimulation occurred, samples of the extracellular media were moved through the chip and into micro-SPE columns for analyte capture and sample conditioning. After pretreatment, the analysis was performed using ESI-Q-TOF-MS (Fig. 3A).

Commercially available, as well as home built SPE devices, are widely used to desalt and concentrate samples prior to analysis via MS. C18 reversed phase media-packed pipet tips have been used for the conditioning of releasates collected from clusters of bag cell neurons of *A. californica* [16], as well as from low-density bag cell neuron cultures [17]. Due to the large volume of C18 material used, this approach can be utilized when release from multiple cells is investigated. However, reducing the volume of SPE material, therefore, leading to higher analyte preconcentration, aids in the detection of the small amounts of analytes released from a single cell. In one example, a small number of SPE particles were mounted onto the surface of Parafilm M. The ~30 µL volume of collected extracellular media containing cell releasate was deposited onto the particles through a fused silica capillary (Fig. 3B) [16].

Further improvement in the spatial detection of peptide release was achieved by the use of SPE beads placed directly on the processes of cultured *A. californica* bag cell neurons (Fig. 3C) [20]. Alternatively, SPE packed pipette tips or cartridges, as demonstrated by Hatcher et al., can be used to collect peptide release [21]. Finally, to improve both spatial detection and sampling efficiency, lauryl methacrylate-ethylene glycol dimethacrylate porous polymer monolithic columns have been used to investigate both *A. californica* and mammalian systems, attaining sub-picomolar limits of detection with sample volumes of ~ 4 µL [3].

Additional improvements in analyte retention can be realized by acidification, alkylation, or addition of ion-pairing reagents to the sample. However, in most cases these modifications are not easily applied to the extracellular environment without interfering with the physiological activity of the studied cells. Therefore, to increase SPE analyte extraction efficiency in released peptide analysis, Fan et al. [22] customized particle-embedded monolithic capillaries with pyrrolidone or ethylenediamine in poly(stearyl methacrylate-*co*-ethylene glycol dimethacrylate) and used them to collect *A. californica* bag cell neuron releasates. The complete system consisted of two capillaries connected to individual syringe pumps, one for application of the secretagogue to the individual neurons at a rate of 0.25 µL/min and the other for collection and pretreatment of the releasate at the same flow rate for 30 minutes, allowing for low femtomole limits of analyte detection and specific analyte targeting (Figure 3D). This SPE approach was improved in a follow up study [23] with the use of a concentric dual capillary system consisting of an outer capillary that surrounds the stimulation and sampling area, and an inner octadecyl-modified silica nanoparticle-filled capillary to collect and pretreat the ~10 µL sample. The

outer capillary, which delivers the secretagogue, either surrounds the neuron or is positioned above the targeted area of the tissue and remains in that position while the inner sampling capillary can be removed and replaced if multiple collections of releasates are necessary (Fig. 3E). This set-up allows relatively high temporal and spatial resolution of cellular release investigation as well as reduced sample dilution.

3.5 Conclusion

This chapter discusses improved methods for studying the chemical content of extracellular environments and cell-to-cell interactions. These methods are particularly useful when studying chemically complex systems with low analyte amounts. Continual improvement of both sampling and detection techniques prove important to the advancement of fields that rely on such information, including the study of neurochemical systems.

3.6 Figure

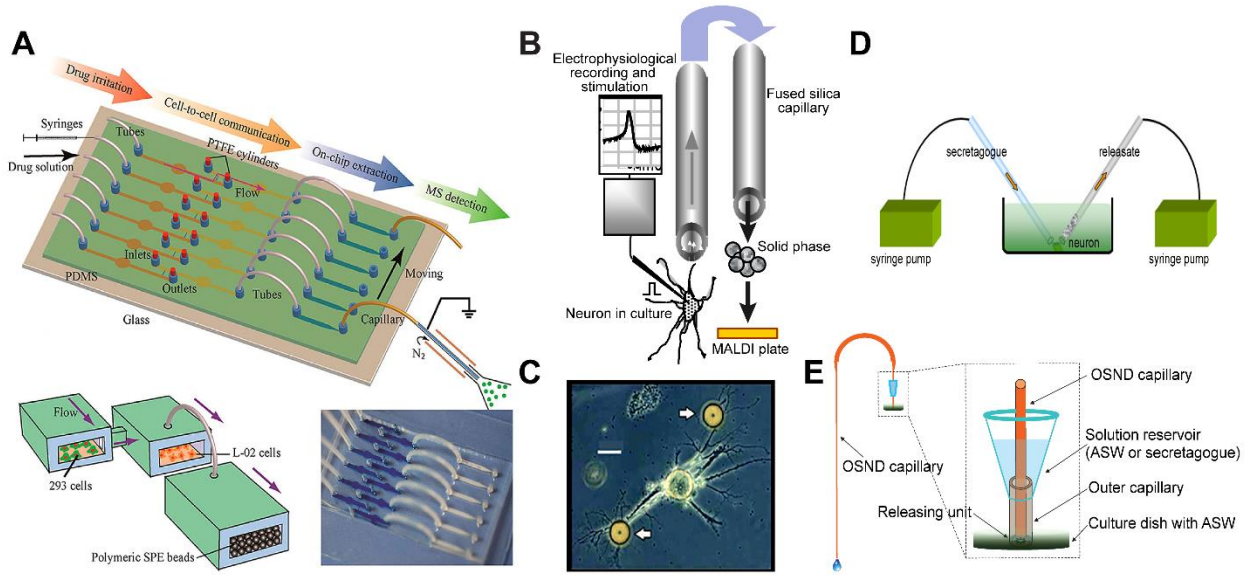

Figure 3.1 A variety of SPE-based analyte collection approaches have been developed and applied to small volume sample analysis. (A) An integrated microfluidic device allowing cell stimulation, cell-cell communication, and sample pretreatment. (Reprinted with permission from reference [18]. Copyright 2012 American Chemical Society). (B) Schematic of sample collection from *A. californica* bag cell neurons and its SPE pre-treatment prior to MALDI MS analysis. (Adapted with permission from reference [16]. Copyright 2001 WILEY-VCH Verlag.) (C) Placement of SPE beads (arrows) directly on neurites of cultured neurons. (Reprinted with permission from reference [20]. Copyright 2005 National Academy of Sciences of the United States of America.) (D) A two-capillary system allowing secretagogue application, released compound collection, and sample processing. (Reprinted with permission from reference [22]. Copyright 2011 American Chemical Society.) (E) A concentric dual capillary system used for temporal and spatial investigation of release. Reduced analyte dilution and flexible sample conditioning using octadecyl-modified silica nanoparticles are important properties. (Reproduced from reference [23] with permission from the Royal Society of Chemistry.)

3.7 Work Cited

1. Ngounou Wetie, A.G., et al., *Automated mass spectrometry–based functional assay for the routine analysis of the secretome.* J. Lab. Autom., 2013. **18**(1): p. 19-29.
2. Skalnikova, H., et al., *Mapping of the secretome of primary isolates of mammalian cells, stem cells and derived cell lines.* PROTEOMICS, 2011. **11**(4): p. 691-708.
3. Iannacone, J.M., et al., *Collecting peptide release from the brain using porous polymer monolith-based solid phase extraction capillaries.* Analytical Chemistry, 2009. **81**(13): p. 5433-5438.
4. Vilim, F.S., et al., *Release of peptide cotransmitters in Aplysia: regulation and functional implications.* Journal of Neuroscience, 1996. **16**(24): p. 8105-8114.
5. Lloyd, P.E., et al., *Release of neuropeptides during intracellular stimulation of single identified Aplysia neurons in culture.* Proc. Natl. Acad. Sci. U.S.A., 1986. **83**(24): p. 9794-9798.
6. Dishinger, J.F., K.R. Reid, and R.T. Kennedy, *Quantitative monitoring of insulin secretion from single islets of Langerhans in parallel on a microfluidic chip.* Analytical Chemistry, 2009. **81**(8): p. 3119-27.
7. Dugan, C.E., et al., *Multiplexed microfluidic enzyme assays for simultaneous detection of lipolysis products from adipocytes.* Analytical and Bioanalytical Chemistry, 2014. **406**(20): p. 4851-9.
8. Reid, K.R. and R.T. Kennedy, *Continuous operation of microfabricated electrophoresis devices for 24 hours and application to chemical monitoring of living cells.* Analytical Chemistry, 2009. **81**(16): p. 6837-42.
9. Wei, D., et al., *Electrochemical biosensors at the nanoscale.* Lab Chip, 2009. **9**(15): p. 2123-31.
10. Li, L., R.W. Garden, and J.V. Sweedler, *Single-cell MALDI: a new tool for direct peptide profiling.* Trends Biotechnol., 2000. **18**(4): p. 151-60.
11. Trouillon, R., et al., *Chemical analysis of single cells.* Analytical Chemistry, 2012. **85**(2): p. 522-542.
12. Dugan, C.E. and R.T. Kennedy, *Measurement of lipolysis products secreted by 3T3-L1 adipocytes using microfluidics.* Methods in Enzymology, 2014. **538**: p. 195-209.
13. Shackman, J.G., et al., *Perfusion and chemical monitoring of living cells on a microfluidic chip.* Lab Chip, 2005. **5**(1): p. 56-63.

14. Wei, H., et al., *Multi-channel microfluidic devices combined with electrospray ionization quadrupole time-of-flight mass spectrometry applied to the monitoring of glutamate release from neuronal cells.* Analyst, 2010. **135**: p. 2043-2050.
15. Yang, M., et al., *Direct detection of peptides and proteins on a microfluidic platform with MALDI mass spectrometry.* Analytical and Bioanalytical Chemistry, 2012. **404**(6-7): p. 1681-1689.
16. Rubakhin, S.S., et al., *Analysis of cellular release using capillary electrophoresis and matrix assisted laser desorption/ionization-time of flight-mass spectrometry.* ELECTROPHORESIS, 2001. **22**(17): p. 3752-3758.
17. Croushore, C.A., et al., *Microfluidic Device for the Selective Chemical Stimulation of Neurons and Characterization of Peptide Release with Mass Spectrometry.* Analytical Chemistry, 2012. **84**(21): p. 9446-9452.
18. Mao, S., et al., *Strategy for signaling molecule detection by using an integrated microfluidic device coupled with mass spectrometry to study cell-to-cell communication.* Analytical Chemistry, 2012. **85**(2): p. 868-876.
19. Zhong, M., et al., *Label-free quantitation of peptide release from neurons in a microfluidic device with mass spectrometry imaging.* Lab Chip, 2012. **12**(11): p. 2037-2045.
20. Hatcher, N.G., et al., *Monitoring Activity-Dependent Peptide Release from the CNS Using Single-Bead Solid-Phase Extraction and MALDI TOF MS Detection.* Analytical Chemistry, 2005. **77**(6): p. 1580-1587.
21. Hatcher, N.G., et al., *Mass spectrometry-based discovery of circadian peptides.* Proc. Natl. Acad. Sci. U.S.A., 2008. **105**(34): p. 12527-12532.
22. Fan, Y., S.S. Rubakhin, and J.V. Sweedler, *Collection of peptides released from single neurons with particle-embedded monolithic capillaries followed by detection with matrix-assisted laser desorption/ionization mass spectrometry.* Analytical Chemistry, 2011. **83**(24): p. 9557-9563.
23. Fan, Y., et al., *Stimulation and release from neurons via a dual capillary collection device interfaced to mass spectrometry.* Analyst, 2013. **138**(21): p. 6337-6346.

Chapter 4

Peptidomics and Secretomics of the Mammalian Peripheral Sensory-Motor System

4.1 Notes and acknowledgements

This chapter is reprinted by permission from Springer Nature: Springer Nature *Journal of The American Society for Mass Spectrometry.* Peptidomics and Secretomics of the Mammalian Peripheral Sensory-Motor System. Emily Tillmaand, Ning Yang, Callie Croushore-Kindt, Stanislav Rubakhin and Jonathan Sweedler, December 2015, Volume 26, Issue 12, pp 2051–2061, doi: 10.1007/S13361-015-1256-1. I specifically worked on characterizing the peptide content of the releasate from cultured dorsal root ganglia (DRG) neurons as well as helped with preparation of DRG and cell extracts for liquid chromatography mass spectrometric analysis. This work was supported by the National Institute of Mental Health under Award No. R21 MH100704A, the National Institute on Drug Abuse under Award No. P30 DA018310 and the National Science Foundation Division of Chemistry under grant Award No. CHE-11-11705 (with co-funding from the Division of Biological Infrastructure). The content is solely the responsibility of the authors and does not necessarily represent the official views of the funding agencies. Technical support by Xiying Wang is gratefully acknowledged. This study involved collaborative efforts with Anika Jain in Martha Gillette's laboratory at the University of Illinois at Urbana-Champaign. The method used for DRG isolation and culture was adapted from procedures partially developed by a former laboratory member, Amy Maduram.

4.2 Abstract

The dorsal root ganglion (DRG) and its anatomically and functionally associated spinal nerve and ventral and dorsal roots are important components of the peripheral sensory-motor system in mammals. The cells within these structures use a number of peptides as intercellular signaling molecules. We performed a variety of mass spectrometry (MS)-based characterizations of peptides contained within and secreted from these structures, and from isolated and cultured DRG cells. Liquid chromatography-Fourier transform MS was utilized in DRG and nerve peptidome analysis. In total, 2724 peptides from 296 proteins were identified in tissue extracts. Neuropeptides are among those detected, including calcitonin gene-related peptide I, little SAAS, and known hemoglobin-derived peptides. Solid phase extraction combined with direct matrix-assisted laser desorption / ionization time-of-flight MS was employed to investigate the secretome of these structures. A number of peptides were detected in the releasate from semi-intact preparations of DRGs and associated nerves, including neurofilament- and myelin basic protein-related peptides. A smaller set of analytes was observed in releasates from cultured DRG neurons. The peptide signals observed in the releasates have been mass-matched to those characterized and identified in homogenates of entire DRGs and associated nerves. This data aids our understanding of the chemical composition of the mammalian peripheral sensory-motor system, which is involved in key physiological functions such as nociception, thermoreception, itch sensation, and proprioception.

4.3 Introduction

A large amount of sensory information within the mammalian nervous system is conveyed from the organism’s periphery to the spinal cord and brain stem via sensory neurons

residing in the dorsal root ganglion (DRG), which consists of the neuron cell bodies and support cells [1, 2]. A sensory neuron has a single axon extending from the cell body that bifurcates, sending one process to the dorsal region of the spinal cord, while the other process innervates a variety of targets [1, 3, 4]. DRG neurons innervate a number of target organs, including skin, muscles, and joints [5, 6], and are involved in mechanoreception, limb proprioception, thermoreception, and nociception. A number of neuropeptides and other cell-to-cell signaling peptides have been identified within DRGs, including substance P and calcitonin gene-related peptide I (CGRP-1) [7]. Many common pain medications (e.g., opioids) target this neuronal network. DRGs are structurally associated the spinal nerve (SN) and its dorsal root (DR) and ventral root (VR). The DR and SN contain neurites from the sensory neurons. The VR possesses mostly terminals of spinal motoneurons and presents an opportunity for a comparative analysis of motor and sensory components of the nervous system.

Both normal and pathological functions of the peripheral sensory-motor system depend on the overall chemical composition of corresponding cells and their extracellular environments. Important studies have been performed to better understand the metabolite, lipid, and protein content of DRGs and their surrounding structures [8-14]. However, the cell-to-cell signaling molecules in these areas and their release have not been completely characterized. Measurements of activity-dependent release are challenging for several reasons. First, cells release a broad range of physiologically active compounds over a wide concentration range. Second, only small amounts of the compounds within the tissue are released, making measurement detection limits important. Moreover, peptide signaling can be terminated by internalization of the signal

or efficient enzymatic extracellular degradation. Therefore, effective capture and accumulation of released peptides is important for successful measurements. Lastly, the collection of the sample should minimally perturb the system and allow for a controlled stimulation of release and efficient analyte collection.

Methods that combine analytical techniques, such as liquid chromatography (LC)-MS, have become mainstream approaches used in proteomic investigations of tissues, organs, and cell cultures [15-23]. In contrast to LC-MS, direct assay of tissues or cells using matrix-assisted laser desorption / ionization (MALDI) time-of-flight (TOF) MS is also effective, either via mass spectrometry imaging [24-26] or by characterization of the isolated cells, nerves and ganglia deposited on a conductive sample plate [27, 28]. Both LC-electrospray ionization (ESI)-MS and direct MALDI MS can be used to investigate peptide release. Direct MS is well suited for the smallest volume samples and can accommodate larger numbers of samples as a separation is not required. However, most released analytes are present at low concentrations and require preconcentration before the MS analysis. Also, the extracellular media contains high inorganic salt levels that are not compatible with direct MS measurements. Therefore, effective methods for collecting released material and conditioning / concentrating the peptides are required. For example, solid phase extraction (SPE) using collection capillaries or probes placed at appropriate locations in close proximity to tissue regions, cell populations in culture, or individual cells enables the measurement of compounds released upon electrical or chemical stimulation [29-31].

Microfluidics-based cell culturing systems can also be used to provide a wealth of information pertaining to tissue and cell biochemistry, growth, and morphology [32, 33].

We previously reported a microfluidic device that permits the culture and maintenance of neurons, temporal application of selective chemical stimuli, and collection of peptide release, with the releasate analyzed using MALDI-TOF MS [34]. The advantages of interfacing microfluidics to MALDI include its small sample-volume requirements, wide dynamic range for peptide characterization [35, 36], and ease of making a large number of measurements, although tandem MS (MS/MS)-based identification of released compounds using direct MALDI MS tends not to be as effective as LC-ESI-MS. Therefore, the separation and preconcentration of peptides on an LC system aids in the identification of endogenous peptides and proteins. Well-known benefits of having LC on the front end of MS include minimized suppression effects from co-eluting ion species and increased dynamic range for better detection of low abundance peptides. The combination of direct tissue measurements with LC-Fourier transform (FT)-ESI-MS and cell release measurements using MALDI-TOF MS is particularly effective in examining peptide release, thereby enabling the assignment of signals detected in release by mass matching to peptides characterized in the larger samples [30, 37].

One of our long-term goals is to recreate different functional networks of well-defined DRG cells within engineered microfluidic devices [38-40] so that we can characterize the biochemical responses, including cellular release, of these networks to different stimuli and changing microenvironments. However, in order to establish and validate our working model and perform the required measurements, it is important to have an inventory of the compounds present within and released from DRGs and their associated structures. Here we present a series of LC-ESI-FTMS/MS investigations of the peptide content of the rat peripheral sensory-motor system, including the DR, VR, SN, and DRG, as well as isolated

DRG cells. In parallel, SPE-assisted MALDI MS and LC-ESI-FTMS were used to characterize the release from semi-intact preparations of DRGs with attached nerves, a robust DRG cell culture was established in miniaturized wells, and a number of peptides identified as being released from the DRG cells and nerves. The data obtained on the peripheral sensory-motor system peptidome and secretome will be used to enable follow-up studies on the function of this complex neuronal system, and on the growth and formation of defined DRG networks in engineered microfluidic devices.

4.4 Experimental

4.4.1 Animals and Tissue Dissection

All procedures related to animal handling and euthanasia were performed in accordance with local, state, and federal regulations, and approved by the Illinois Institutional Animal Care and Use Committee. DRGs, spinal cords, SNs, VRs, and DRs were surgically dissected from 2.5–3 month-old Sprague-Dawley outbred male rats (Harlan Laboratories, Inc., Indianapolis, IN, USA), 21–28 day postnatal Sprague-Dawley outbred male rats (Charles River, St. Constant, QC, Canada), or 6–12 week-old Long-Evans/BluGill male and female rats (University of Illinois at Urbana−Champaign, USA), euthanized by decapitation. To reduce the detrimental metabolic effects of a stopped blood flow, 40–120 mL of ice-cold modified Gey's balanced salt solution (mGBSS) were injected under the skin above the location of the DRGs of interest (the lumbar area) immediately after decapitation. The spinal canal was surgically opened, the spinal cord removed, and DRGs with adjacent nerves were individually isolated and placed into ice cold mGBSS containing (in mM): 1.5 $CaCl_2$, 4.9 KCl, 0.2 KH_2PO_4, 11 $MgCl_2$, 0.3 $MgSO_4$, 138 NaCl, 27.7 $NaHCO_3$, and 0.8 Na_2HPO_4, and 25 HEPES, pH 7.2. In some experiments other

media types were used as described below. Most of the presented work used 2.5–3 month-old Sprague-Dawley outbred male rats (Harlan Laboratories, Inc.). Animals of other strains, sexes, and ages investigated in the DRG peptidomics experiments produced similar results to data obtained from the Sprague-Dawley rats.

4.4.2 DRG Cell Isolation

Immediately after dissection, DRGs were sustained in a volume of ice cold Hibernate A media (BrainBits, Springfield, IL, USA) for up to 48 h. For dissociation, approximately 10 DRGs dissected from 2.5–3 month old Sprague-Dawley outbred rats were digested in a solution of 0.25% collagenase (Worthington Biochemical Corp, Lakewood, NJ, USA) in DRG cell culture media containing Neurobasal A without phenol red (Life Technologies, Carlsbad, CA, USA), 100 U/mL penicillin/streptomycin (Life Technologies), 0.5 mM GlutaMAX (Life Technologies), 50 ng/mL nerve growth factor (Life Technologies), 50 ng/mL brain-derived neurotrophic factor (BDNF) (Prospec Bio, Rehovot, Israel), and 500 µL B27 Growth Supplement (Life Technologies) for 1.5 h at 37 ºC. After digestion, the samples were subjected to centrifugation for 3 min at 200 ×*g*. The supernatant was removed, and the pellet washed with Hank's Balanced Salt Solution (HBSS) (Life Technologies). The sample was centrifuged, the supernatant removed, and the pellet digested using 0.25% trypsin with ethylenediaminetetraacetic acid (Life Technologies) for 15 min at 37 ºC. After incubation, the sample was centrifuged, supernatant removed, and 0.5–1 mL DRG cell culture media + 1% fetal bovine serum (Life Technologies) added to inactivate the trypsin. The pellet was mechanically dissociated by trituration with fire-polished pipettes. Following trituration, some of the pellet was allowed to re-settle. Once a small pellet formed in the bottom of the microcentrifuge tube, the supernatant was

removed and spun for 3 min at 200 ×*g*. After centrifugation, the supernatant was removed and the pellet washed with HBSS. After a final centrifugation, the cell pellet was resuspended in 1 mL of DRG cell culture media per 10 original DRG.

4.4.3 DRG Cell Culture

Polydimethylsiloxane (PDMS) blocks, punched with 1.5 or 2 mm diameter biopsy punches (Acuderm, Inc. Ft. Lauderdale, FL, USA) to create small restricted-space culture wells, were attached to either glass coverslips or PDMS substrates. Prior to cell plating, glass coverslips were treated with concentrated H_2SO_4 for 24 h to remove any contaminants and then washed with distilled water. The PDMS was sterilized in an O_2 plasma cleaner for 30 s at 100 W. After treatment, the substrates were washed with 70% ethanol and air dried in a sterile cell culture hood for 30 min. To functionalize the substrates for neuronal culture, 0.05 mg/mL poly-D-lysine (PDL) (BD Biosciences, Franklin Lakes, NJ, USA) and 0.1 mg/mL laminin (Sigma Aldrich, St. Louis, MO, USA) were placed on the substrates and incubated for at least 1 h at 37 ºC. Prior to seeding, the PDL/laminin solution was removed and substrates were washed with HBSS. A 5–10 µL DRG cell suspension in DRG cell culture media obtained from 2.5–3-month old Sprague-Dawley rat ganglia was seeded into the restricted space wells*.* To regulate evaporation, about 200 mL of HBSS was added to the dish outside of the wells. The seeded cells were cultured at 37 ºC and with 5% CO_2 for 7–10 days before stimulations. DRG cell culture media was added every 2–3 days, or more frequently if levels appeared low due to evaporation.

4.4.4 Release Stimulation and Analysis

Regional whole DRG release sampling. Left and right L4 DRGs, with the roots and spinal nerve attached, were collected from 2.5–3-month old Sprague-Dawley outbred rats after

euthanasia by decapitation. Immediately after decapitation, cold mGBSS (120 ml, 4 ºC) was injected into the subepidermal areas neighboring the SNs and their corresponding DRG. Rat trunks were maintained on ice during the surgical dissection procedure. The collected semi-intact preparations of DRGs with attached nerves were sequentially incubated in ice cold Na^+-free artificial cerebrospinal fluid (aCSF-1) composed of (in mM): KCl 2.5, NaH_2PO_4 1.25, $CaCl_2$ 0.5, $MgCl_2$ 3.5, $NaHCO_3$ 26, glucose 10 and sucrose 233, and HEPES 15 for approximately 3 h, followed by ice cold aCSF-1 supplemented with 63 mM NaCl for 20 min. This series of incubations reduced analyte release induced by surgical isolation. Next, the DRGs and nerves were moved into standard oxygenated artificial cerebrospinal fluid (aCSF-2) (in mM): NaCl 115, KCl 2.5, NaH_2PO_4 1.25, $CaCl_2$ 0.5, $MgCl_2$ 3.5, $NaHCO_3$ 26, HEPES 15, and incubated at 36 ºC for 20–30 min. The structures were placed into an incubation chamber with multiple SPE probes [C18 ZipTip pipette tips (Millipore, Billerica, MA, USA)] mounted near specific areas of the peripheral sensory-motor system. Outward flow of the aCSF-2 through the pipette tips was maintained during the process. Release from the semi-intact preparation was stimulated by replacing aCSF-2 with a high K^+ aCSF-3 (100 mM KCl, with a corresponding reduction in Na^+). Solution flow inside the pipette tips was reversed to inflow, and incubation and analyte collection continued for 20 min at 36 °C. Four experiments were performed using four animals and eight L4 ganglia. Analytes retained on the pipette tips were eluted onto a metal MALDI sample plate and mixed with 2.5 µL of 2,5-dihydroxybenzoic acid (DHB) MALDI matrix solution (10 mg/mL DHB in acetonitrile (ACN)/water (50:50)).

Sampling of release from DRG cell cultures. To chemically stimulate DRG cell release, a high K^+ DRG cell culture media bath (60 mM K^+) was used on the restricted-space

cultures 7–10 days after seeding. Details on the fluid exchanges used to stimulate release were as follows: first, a control sample consisting of DRG cell culture media in which the cells had been incubating was collected. At this point, fresh media was placed on the cells and they were incubated for 30 min. That media was then removed, creating a pre-stimulation sample. Next, the high K^+ DRG cell culture media was added to the cells and removed after 30 min, creating a stimulation sample. A final bath of DRG cell culture media was added to the cells, and collected as the post-stimulation sample after 30 min.

Depending on the experiment and numbers of wells with viable cultures, samples from 1–10 culture wells per dish were combined by sample type before further processing for MALDI MS and/or LC-ESI-FTMS measurements. An initial exploratory release experiment used cells cultured from a single rat; samples obtained from individual cell culture wells were subjected to MALDI analysis. Another experiment, also with a single animal, pooled samples from multiple wells for both MALDI and FTMS analysis. Next, we performed six separate cell culture experiments (using six different animals, with samples collected on six separate days). We collected control, pre-stimulation, stimulation, and post-stimulation samples from each viable well (for a total of 143 wells containing viable cultures), and then combined the samples from individual wells together by dish (18 dishes total). For the combined samples, the analytes were desalted and concentrated using SPE probes [C18 ZipTip pipette tips (Millipore)]. The bound sample was washed with 5% methanol/0.1% TFA in deionized water and eluted, first with 50% ACN/0.1% TFA and then with 75% ACN/0.1% TFA solutions. The eluted samples were mixed 1:1 with the DHB MALDI matrix (10 mg/mL DHB in ACN/water (50:50)) on a metal sample plate. Mass spectrometric profiling was performed using an UltrafleXtreme MALDI-TOF MS

workstation (Bruker Daltonics, Billerica, MA, USA) in the reflectron mode operating at positive polarity. Individual mass spectra were analyzed with flexAnalysis (version 3.3, Bruker Daltonics). External mass calibration was performed using peptide calibration standard II (Bruker Daltonics). Differential comparisons between multiple experiments were done using the ClinProTools (Bruker Daltonics) software. In addition to the MALDI MS measurements, release samples were analyzed with LC-ESI-FTMS; for this experiment, the analytes collected from 34 culture wells from several of the experiments were pre-concentrated and desalted using SPE, pooled, and then subjected to LC-ESI-FTMS (as described below).

4.4.5 Peptide Identification in Biological Samples

Six groups of DRGs and associated nerve tissues were subjected to peptide extraction and analyzed with LC-ESI-FTMS. To extract the peptides, DRGs were immersed in ice-cold acidified acetone (acetone/water/HCl, v/v/v, 40/6/1) immediately after isolation from the animals until all dissections were finished. For groups 1 and 2, the collected DRGs were transferred into 12 mM of ice cold HCl, homogenized, and placed in an ice bath for 1 h. Supernatant was collected and combined with the acidified acetone mentioned above after centrifugation at 20,000 ×*g* for 15 min. For groups 3–6, the DRGs were placed into an 80 ºC water bath for 10 min to stop enzymatic protein degradation. The heat-denatured DRGs were homogenized, placed in an ice bath for 1 h, and centrifuged as described above. The supernatant was saved and tissue pellets were resuspended in 600 µL of 0.25% acetic acid solution and placed on ice for a 1 h peptide extraction. After centrifugation, the saved supernatant was combined with the acidified acetone. The combined peptide extracts from all experiments were cleaned using C18 spin columns

(Thermo Fisher Scientific, Waltham, MA, USA), dried down with a Speedvac concentrator, and reconstituted in H_2O/ACN (95:5).

Each extracted peptide sample was separated on a nanocapillary column (10 cm × 75 µm inner diameter) containing ProteoPep™ II media (C18, 300 Å, 5 µm, New Objective, Inc., Woburn, MA, USA) using an Eksigent nanoLC 1D Plus system (SCIEX, Framingham, MA, USA) and analyzed with an 11 Tesla FT mass spectrometer (LTQ-FT Ultra, Thermo Fisher Scientific). Separation conditions were as follows: 1) buffer A, 95% water, 4.8% ACN, and 0.2% formic acid; 2) buffer B, 95% ACN, 4.8% water, and 0.2% formic acid; 3) gradient conditions were: 0–80 min, 0–30% B; 80–105 min, 30–45% B; 105–120 min, 45–60% B; 120–125min, 60–85%; 125–130 min, 85–85%; 130–145 min, 85–0%; 4) the operating flow rate was 300 nL/min.

Data acquisition on the LTQ-FT mass spectrometer consisted of a full scan event (*m/z* 300–2000 at 50K resolving power) and data-dependent collision-induced dissociation FTMS/MS scans of the five most abundant peaks from the previous full scans. MS/MS settings were as follows: isolation width = *m/z* 10; minimum signal threshold = 5000 counts; normalized collision energy = 35%; activation Q = 0.25; activation time = 50 ms. The RAW files were searched against a lab-built rat proteome database using PEAKS software (version 7.0, Bioinformatics Solutions Inc., ON, Canada) and ProSightPC (Thermo Fisher Scientific). For database search with PEAKS, 15 ppm and 0.1 Da mass tolerances were used for MS and MS/MS modes, respectively. Identified peptides with score (-logP > 15) were kept. For ProSightPC, 81.1 Da and 10 ppm mass tolerance were used for MS and MS/MS modes. Identified peptides with p value < 10^{-4} were kept. A large mass tolerance was used here because of the ProsightPC biomarker search mode, which

involves matching an observed mass to the theoretical masses of possible subsequences in the protein database, and then comparing calculated fragments of those subsequences to observed fragments. A large mass tolerance window allows peptides with post-translational modifications (PTMs) to be matched to the subsequences. The value of 81.1 Da was used here because it can cover the mass shifts related to most common PTMs, including amidation, oxidation, and phosphorylation. Peptide identifications with p value $< 10^{-4}$ were kept.

4.4.6 Calculation of Peptide Signal Intensity Fold Changes across Cell Culture Stimulations

Comparisons of the peptide profiles were performed on the MALDI MS data from the six cell culture experiments in their original format using averaged peak statistics functions (Kruskal-Wallis test for not normally distributed peak signal intensities as determined by the Anderson-Darling normality test) in ClinProTools (version 3.0, Bruker Daltonics). Representative spectra acquired from each culture dish from each of the six experiments were combined into control, pre-stimulation, stimulation, and post-stimulation sample data sets and imported into ClinProTools as separate classes. Each set consisted of 18 spectra. The spectra preparation settings were: a resolution of 800; top hat baseline subtraction of 10% minimal baseline width; 2 cycles of Savitzky-Golay smoothing with a width of 2.0 *m/z*; and a data reduction factor of 3. Peak picking was done on the class average spectrum with a signal-to-noise threshold of 3.00. The Benjamini-Hochberg procedure was automatically applied to correct for the multiple testing hypothesis issue commonly associated with MS data. Peak statistics were calculated by ClinProTools after manual removal of signals originating from the physiological media, and addition of

signals that were not automatically picked. Peak statistic tables were generated and manually analyzed for trends in the change of average peak intensity over the four class types.

4.5 Results and Discussion

4.5.1 Peptidomics of the DRG Tissues

Our first goal was to characterize the endogenous peptides present within the DRG and nerves, and to determine those that were secreted. Accordingly, our initial studies involved characterization of the peptides present within the DRG. Unlike standard bottom up proteomics experiments, we did not digest the proteins and characterize the resulting peptides, but instead, worked with the peptides naturally present within the samples. Here, six groups of DRG tissues were extracted and analyzed with LC-ESI-FTMS, with 2290 peptides from 296 proteins identified after de novo sequencing and database search using the PEAKS software. The database search was performed again using a different search tool, ProsightPC (Thermo Fisher Scientific). The ProsightPC search identified 1650 peptides, 434 of which were unique peptide identifications to the total readout. In summary, 1216 peptides were identified by both PEAKS and ProsightPC; 1074 peptides were exclusively identified by PEAKS and 434 by ProsightPC. Two and four groups of DRG tissues were processed with the two different peptide extraction methods described above. As a result, 145 proteins were observed with both extraction procedures, and 84 and 67 proteins were unique for just one of the extraction procedures, respectively. Our results suggest that peptide and protein coverage is increased by using different sample processing approaches. Identified peptides were categorized into functional classes, as shown in Figure 4.1. The neuronal category represents 40% of all of the peptides detected

and consists of peptides related specifically to neuron structure or processes involved in neuron formation, function, and maintenance. Among them, several peptides originating from proteins involved in neurotransmission and implicated in neurodegenerative diseases were identified, such as complexin-1 [41] and gamma-synuclein [42], as well as those involved in axon growth and myelination, including vimentin [43] and periaxin [44].

Endogenous cell-cell signaling peptides act as neurotransmitters and neuromodulators. Among the results from six experiments, 18 neuropeptides derived from five prohormones were detected. Figure 3.2 shows examples of MS/MS spectra of neuropeptides of various lengths, including LVV-hemophin-7, (mass 1323.10 Da), calcitonin gene-related peptide I 19-37 (CGRP-1 19-37, mass 1921.95 Da), and secretogranin-2 derived peptide (mass 3679.80 Da). Another prohormone described most commonly in the DRG is protachykinin-1. Short forms of neuropeptide K cleaved at dibasic sites and a C-flanking peptide were also detected.

The presence of CGRP-1 and its mRNA in rat DRGs has been previously reported in immunohistochemistry and *in situ* hybridization studies [45, 46]; CGRP-1 has been shown to be essential for pain signaling and increases innervation in DRGs during inflammation [46]. Here, full length CGRP-1 (1-37) was detected and confirmed with MS/MS. In addition, three truncated forms of CGRP-1 (1-37) were identified from the DRG tissues, including CGRP-1 1-17, 18-37, and 19-37. The cleavage site had one arginine, a monobasic site that is often involved in neuropeptide enzymatic processing. Saghatelian and coworkers [47] discovered that the CGRP-1 1-17, 18-37, and 19-37 are produced enzymatically by peptidases. Therefore, those short forms identified in this work are likely

endogenous signaling molecules and not products of degradation of CGRP-1 during sample preparation.

The majority of bioactive peptides are generated from larger precursor proteins. However, in recent years it has been shown that bioactive peptides can also be generated from the cleavage of cytosolic proteins [48]. As a notable example, hemoglobin can be processed to yield multiple bioactive peptides, including the hemorphins [49]. Hemoglobin-derived (Hb) peptides have been found in a number of cells types within the body, from lens and alveolar cells to macrophages, and have also been found within neurons and oligodendrocytes, as well as in the sciatic nerve [49]. We observed several hemoglobin-derived peptides within the tissue samples, including N-terminus extended LVV-hemorphin-3, and lengthened forms of neokyotorphin and LVV-hemorphin-7. Hemorphins are a group of endogenous opioid peptides derived from the β-chain of hemoglobin. They work as signaling molecules by binding to opioid receptors and play roles in pain and inflammation [50, 51]. LVV-H7 produces attenuate hyperalgesia effects at the spinal level. Perhaps the hemorphins detected in these systems participate in the regulation of hyperalgesia given the projection of DRGs toward the spinal cord.

4.5.2 Peptide Profiling of Release

Our next goal was to determine what molecules are released from the DRG and associated nerves, as well as from the cells within the DRG. We used two distinct means to probe release: a semi-intact preparation that consisted of the DRG and nerves, and a separate set of experiments using a miniaturized microfabricated chamber to allow us to culture isolated DRG cells, exchange the culturing fluid to stimulate release, and then efficiently collect releasate for characterization.

4.5.2.1 Regional Release from DRG and Associated Nerves

SPE analyte collection was performed simultaneously at four anatomically defined regions of the mammalian sensory-motor system: the DR, VR, DRG, and SN. After stimulating release with elevated K^+ media and characterizing the releasates using MALDI MS, more than 100 compounds were observed in the releasates, in both metabolite and peptide mass ranges. Although MALDI MS profiling of release from biological structures provides the opportunity for multiplexed, semiquantitative, spatially, and temporally resolved assessment of the chemical composition of release, identifying the compounds using MALDI MS alone can be challenging. In this work we molecular mass-matched the signals observed in releasates with the identities of the compounds characterized using LC-FTMS from similar tissues.

A number of peptides known to be released from nervous tissue were observed. Thymosin beta-4 was detected, which is consistent with the results of prior release experiments from a larger variety of tissues [30, 52, 53]. In fact, the ubiquitous nature of thymosin beta 4 in release experiments suggests it can be used as a marker for effective release stimulation and efficient sample collection. The metabolite and peptide profiles of the releasates we observed from different regions of the mammalian sensory-motor system were similar. Further, since all regions had neuronal termini and only the DRG had the neuronal cell bodies, these results suggest that nerve terminal- and glia-related compounds dominate the profiles. Our previous MS imaging study demonstrated considerable chemical heterogeneity in the chemical content between the DRGs, VRs, DRs, and SNs [54], so it is intriguing that we observed similar compounds released from these regions, as we expect that the content and release profiles would be correlated. In

agreement with the observations of similar release profiles for all regions, principal component analysis of the corresponding data sets did not allow us to separate the analyte profiles of release from these regions. Our inability to distinguish the release profiles from these distinct regions may be explained by the dominant release of peptides originating from neurofilament L and M proteins, myelin-related proteins, and vimentin. Such highly abundant peptides may be obscuring differences in release of much lower concentration peptides.

4.5.2.2 Release from Entire DRG and Cell Culture

The experiments described above used semi-intact preparations, and releasates were collected by placing collection pipettes at specific, spatially defined locations. In the next set of experiments, we investigated release from isolated DRGs and groups of cultured DRG cells within restricted-volume culture wells. The collection system used a flow-through design, and either culture media or stimulation media (with elevated K^+ added to cause secretion) was flowed through the chamber for the designated time period. First, we optimized the collection procedure by measuring release from the entire DRG within the device and ensuring that the ganglion released enough material for characterization. Comparisons between release from a ganglion and cultured cells may yield information about the peptide differences observed from *in vitro* versus *in vivo* measurements. DRGs contain more intact connections between cells and thus, should more closely mimic the semi-intact preparation used above and the *in vivo* environment (Figure 4.3).

Next, pre- and post-stimulation studies from isolated DRGs were performed with DRG cell culture media additions. Elevated K^+ (60 mM) solution was added for two exposure periods: 15 min and 30 min. Signals not observed in the pre-stimulation appeared

following stimulation, and the intensities of a number of signals increased in the mass spectra of the stimulation samples versus mass spectra of the pre-control samples. As one example, a signal corresponding with neurofilament light polypeptide became detectable in the stimulation sample. Finally, intensities of several signals were found to change in the post-control samples, including those that correspond to peptides originating from neurofilament medium polypeptide.

Following isolated ganglion stimulation, a low-density DRG cell culture containing ~20 neurons within a 1.5 mm PDMS well was stimulated with elevated K^+ solution for 30 min. Peptides were characterized with MALDI-TOF MS. A series of mass spectra in the peptide region are shown in Figure 4.4a. Similar to ganglion stimulation data, a number of peaks increased in intensity following the application of elevated K^+, suggesting a potentiation of release in response to stimulation. The peptides from the cultured DRG cell release experiments were also analyzed with LC-ESI-FTMS. The identification results show the presence of 28 peptides from 11 proteins. Peptides having known functions related to cell to cell signaling, including LVV-hemorphin-7, VV-hemorphin-7, and their C-terminus extended forms, were detected.

Interestingly, when compared together (Figure 4.4b), few signals overlap between the ganglion and dispersed cell culture stimulation data. An explanation for this is that the ganglion data contains signals that were released or secreted in abundance within the tissue, obscuring lower-abundance peptides. By having isolated a much smaller subset of cells from the cluster and culturing them, we are able to observe release from fewer cells so that cell-to-cell chemical heterogeneity may have become more obvious.

These results led us to move forward with multiple high-K^+ stimulations using DRG cell cultures. In total, extracellular media was sampled from cultures involving DRGs from six rats on six different days, resulting in the preparation of control, pre-stimulation, stimulation, and post-stimulation samples from cells cultured in multiple wells within 18 different cell culture dishes. Analysis of these samples using MALDI-TOF MS revealed 41 signals of interest. When compared against the LC-ESI-FTMS data of the inventory of characterized compounds from the DRGs, the molecular masses matched 26 peptides from 19 different proteins. These proteins include those involved in axonogenesis and neurite extension such as neurofilament heavy, medium, and light polypeptides [55], and vimentin [56], and those expressed in peripheral neurons and Schwann cells, such as high mobility group protein B1 [57], gamma synuclein [42, 58], and peptidyl-prolyl cis-trans isomerase FKBP1A [59]. In addition, proteins integral to the function of nervous tissue, such as periaxin and myelin protein P0 [60, 61], were detected within the samples. Interestingly, one potential hemorphin peptide, L.LVVYPWTQRYFDSF.G, was detected in the MALDI-TOF MS analysis of samples from the cell stimulation experiment.

The average intensity of the peptides in each condition class was used to determine changes across classes (control, pre-stimulation, stimulation, post-stimulation, and a DRG cell culture media blank). Eight signals showed an upward trend in their relative intensity between pre-stimulation and stimulation or post-stimulation samples (Table 4.1). Of the signals showing an intensity increase, three were identified by mass matching to the LC-ESI-FTMS data. Mast cell protease 1-derived peptide signal increased 1.4 and 1.6 fold from pre-stimulation to stimulation, and pre-stimulation to post-stimulation, respectively, while myelin protein P0-derived peptide increased 1.8 fold for both

conditions. The signal of a peptide derived from histone H2B had a 1.4 fold increase from pre-stimulation to post-stimulation. In addition, 12 signals showed intensity increases between the control and pre-stimulation samples. These include the previously mentioned histone H2B, myelin protein P0, and mast cell protease 1-derived peptides, as well as nine unassigned signals. We do not believe these increases between the pre-stimulation and control are related to K^+-stimulated release, but rather, they may be related to the action of removing the culture media and/or the addition of fresh media, both of which could have induced mechanical and/or chemical stimulation.

4.5.2.3 Peptidomic Analysis of Peptides Released from DRG Cell Culture

In order to aid in identifying the compounds released from these cells, we also performed an LC-ESI-FTMS study of the released peptides. Releasate solutions collected after the stimulation experiments were concentrated and subjected to LC-FTMS analysis as described above. Obtaining enough analyte for an LC-ESI-FTMS-based peptidomic study of released materials was challenging. We expected that high femtomoles to low picomoles of material would be needed for efficient MS/MS peptide sequencing. However, by increasing cell density, performing sample collection in small wells, and combining samples, a number of peptides were identified in the release samples.

As before, we detected several hemorphins, now confidently assigned. Both LVV-hemorphin-7 and VV-hemorphin 7, as well as longer fragments of both peptides, were observed. These observed Hb-derived peptides act on opioid receptors and most have functions relating to antinociception. Thus, from a functional perspective, their presence in release makes sense, although the mechanisms of their synthesis and processing within these cells it not understood. LVV-hemorphin-7 has also been shown to regulate

blood pressure and play a role in learning and memory, as well as cholinergic transmission [49]. Further study into the biosynthetic pathways and release of Hb-derived peptides within DRG tissue and cells is important. Besides Hb-derived peptides, several other classes of peptides were also identified, including thymosin-beta 4, neurofibromin, and myelin basic protein. Neuferricin was also detected and is involved in neuronal apoptosis and plays an important role in neurotrophin signaling during neuronal development [62].

4.6 Conclusions

The DRG and adjacent nerves play an essential role in transmitting sensory information from the periphery to the central nervous system, and are major targets in investigations of mechanisms of pain, mechanical injury, and regeneration. We studied this structurally well-defined system across levels, from isolated cells to whole tissue, and releasates, to investigate the peripheral sensory-motor system's peptidome and secretome. This broad range of sample types, and the cellular and chemical heterogeneity of the samples created measurement challenges that we partially addressed using a range of analytical protocols and platforms.

We used a variety of sample preparation and conditioning steps, and multiple ionization and mass analyzers during this work. The individual workflows and instrumentation have different figures of merit and were selected according to the requirements of the experimental objective. To identify peptides in a complex cellular sample, we used LC-ESI-FTMS, whereas to characterize many samples containing low levels of peptides from volume-limited and concentration-limited release samples, we used direct MALDI-TOF MS. The advantages of LC-ESI-FTMS for obtaining comprehensive peptide profiles are

well established, and direct MALDI MS provides an opportunity to profile large numbers of individual samples without purification in a short period of time. This combined work flow has been shown to be effective in a number of peptidomics experiments [16, 27, 63, 64], and was particularly effective in these experiments. As a result, we generated more complete peptidome and secretome datasets for the peripheral sensory-motor system, providing a better understanding of its chemical composition.

The inventory of peptides and proteins we report here enables a range of follow-up studies using small numbers of cells that form defined networks within engineered structures. This investigation of the peptidomes and secretomes of the peripheral sensory-motor system has revealed new candidates for peptide neuromodulators, hormones, and trophic factors that may have important roles in local and distal intercellular communication. Characterizing the spatiotemporal and chemical parameters of cellular release provides unique functional insights in fundamental and specific mechanisms of peripheral sensory-motor system function.

4.7 Addendum

The studies outlined in this paper are led to the identification of a large number of molecules. One question that remained was: “Where are the neuropeptides in the release?” As was mentioned, even neuropeptides that had been detected previously by our lab through mass spectrometry imaging of tissue slices from the DRG, spinal cord and spinal nerves and are known to be present in these structures were not detected in the release samples. One plausible reason for this lack of expected neuropeptides is not that the peptides are not released in our model, but rather that their detection is limited by both the types of mass spectrometric analysis performed and the sampling approach

due to the relatively low abundance of our target molecules compared to other peptide molecules in the sample. In fact, in later experiments we were able to detect released neuropeptides using the more sensitive and specific enzyme-linked immunosorbent assay coupled with an improved sampling protocol. Since we still believe in the importance of our long-term goals to recreate different functional networks of well-defined DRG cells within engineered microfluidic devices [38-40] so that we can characterize the biochemical responses, including cellular release, of these networks to different stimuli and changing microenvironments, the other aspects of my project addresses ways that we can better detect these neuropeptides within the system.

4.8 Figures

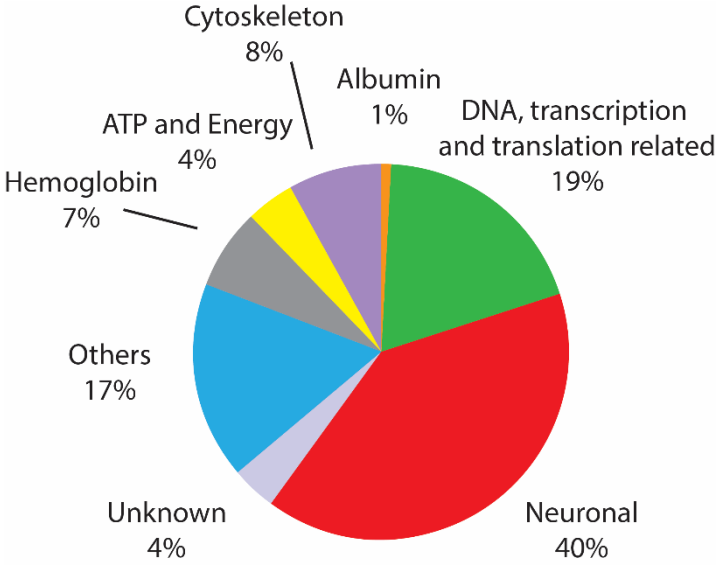

Figure 4.1. Using LC-FTMS, the peptides within DRG tissue extracts have been characterized, identified, and grouped by function, with the largest number of peptides corresponding to neuronal and transcriptionally/translationally related proteins.

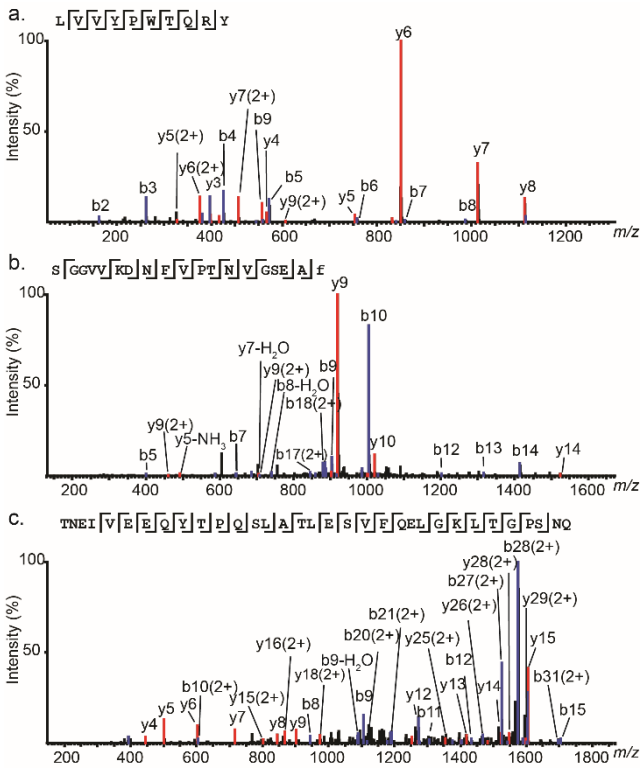

Figure 4.2. Representative MS/MS sequencing of peptides obtained from DRG tissue and release experiments. (**a**) MS/MS fragmentation of LVV-hemorphin (*m/z* 662.86, 2+); (**b**) MS/MS fragmentation of CGRP-1 19-37 (*m/z* 961.98, 2+); (**c**) MS/MS fragmentation of secretogranin-2 derived peptide (*m/z* 1217.61, 3+). The amino acid sequence of each peptide is given above the spectrum.

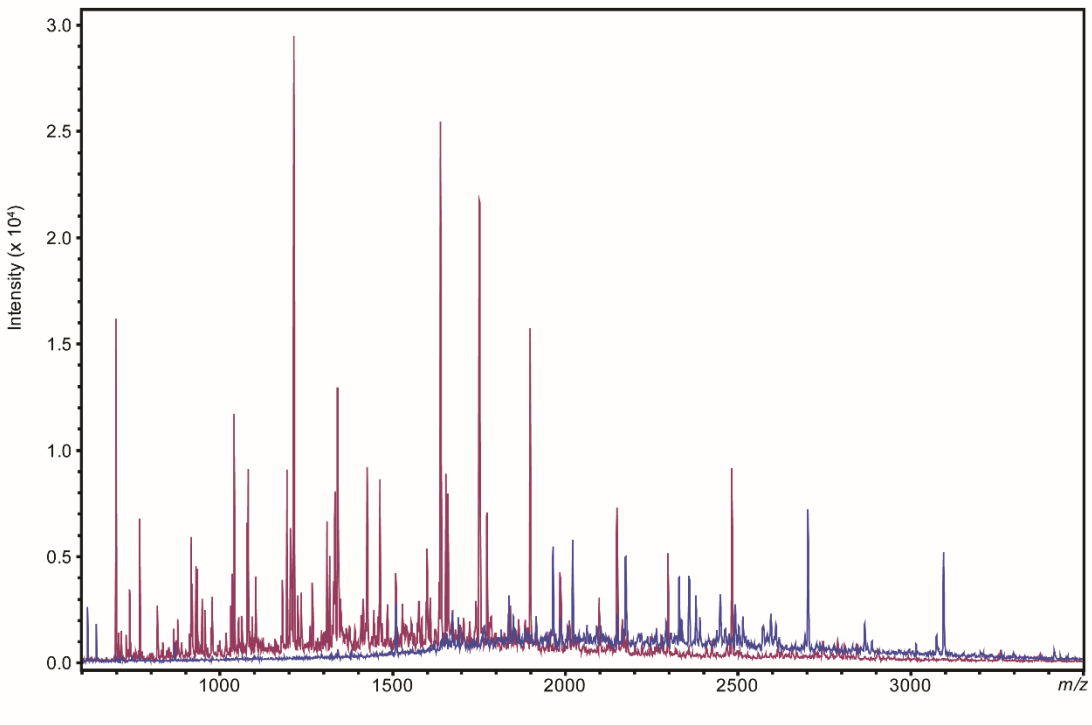

Figure 4.3. Mass spectra comparing peaks from stimulation collections from cluster (maroon) and culture (blue). Although a number of signals in the peptide range were observed for both samples, few peaks overlap.

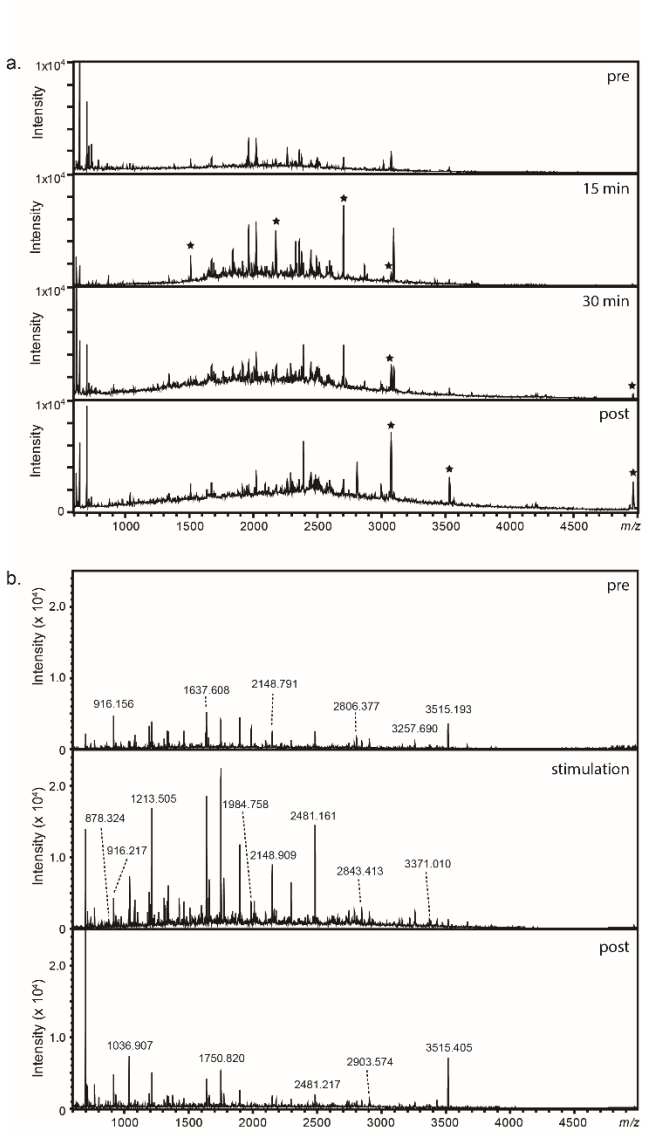

Figure 4.4. Representative mass spectra acquired with MALDI-TOF MS showing relative changes in peak profiles detected within the peptide mass region upon stimulating release from DRG clusters and cultured cells. (**a**) Series of mass spectra showing signals within the peptide molecular mass region following control and stimulation of an entire DRG. Peaks which increased in intensity or newly appeared are highlighted with an asterisk. (**b**) Series of mass spectra of release collected from ~20 DRG neurons within a 1.5 mm PDMS well. Pre- and post- controls were performed with DRG extracellular media; 60 mM elevated extracellular K^+ was added to induce peptide release.

4.9 Tables

m/z (MALDI)	P value for Kruskal-Wallis Test	Identification	Stim/Pre	Post/Pre	Pre/Control
1180.79	0.00337	Histone H2B	0.79	1.43	1.43
1253.72	<0.000001	Mast cell protease 1	1.35	1.63	3.60
916.69	<0.000001	Myelin protein P0	1.75	1.78	4.07
3516.78	<0.000001	Unassigned Peak	1.77	2.26	10.38
1268.75	<0.000001	Unassigned Peak	1.25	1.44	2.30
601.17	0.000432	Unassigned Peak	1.63	1.64	1.71
739.43	0.00000148	Unassigned Peak	1.44	1.43	1.64
3502.77	0.00188	Unassigned Peak	1.65	1.94	1.08
1204.85	0.0000023	Peptidyl-prolyl cis-trans isomerase FKBP1A	0.74	0.73	0.97
1213.86	0.0000151	Gamma-synuclein	0.66	0.72	0.90
1332.81	0.0000059	Myelin protein P0/Neurofilament light polypeptide/Neurofilament medium polypeptide	0.76	0.63	0.84
1575.87	< 0.000001	Vimentin	0.65	0.63	0.68
1820.61	< 0.000001	Hemoglobin subunit beta-1	0.47	0.31	0.54
2010.07	< 0.000001	High mobility group protein B1	0.45	0.32	0.67
2272.3	< 0.000001	Periaxin	0.48	0.35	0.55
2616.13	< 0.000001	Neurofilament heavy polypeptide	0.51	0.41	0.63

Table 4.1. Relative changes in average signal intensities detected in pre-stimulation (pre), stimulation (stim), post-stimulation (post), and control samples. Signals were observed in samples collected in six different experiments performed on six different animals. Refer to Table S5 for average values and standard deviations of the complete list of observed signals.

m/z	Identification	P Value of Kruskal-Wallis Test	Ave Control	Ave Pre	Ave Stim	Ave Post-stim	Ave Blank	Std Dev Control	Std Dev Pre-Stim	Std Dev Stim	Std Dev Post-stim	Std Dev Blank
601.17	Unassigned Peak	0.000432	1.44	2.46	4.02	4.04	2.28	0.83	1.43	2.38	2.85	0.97
616.27	Unassigned Peak	0.0348	1.27	2.39	2.16	2.09	2.48	1.08	2.22	1.27	0.98	1.51
650.86	Unassigned Peak	0.234	2.05	3.76	3.73	3.53	2.21	1.16	2.78	2.75	2.23	0.72
739.43	Unassigned Peak	0.00000148	1.28	2.1	3.02	3.01	2.18	0.78	0.82	1.18	0.93	0.77
768.71	Hemoglobin subunit beta-1	0.00103	4.1	2.68	2.13	1.78	1.84	2.29	1.32	0.87	0.68	0.76
770.68	Unassigned Peak	0.0856	4.14	5.4	4.02	3.61	2.61	2.88	10.95	4.58	4.35	1.29
916.69	Myelin protein P0	< 0.000001	1.04	4.23	7.39	7.54	2.8	0.48	2.14	3.98	3.65	2.94
1180.79	Histone H2B	0.00337	1.5	2.15	1.7	3.08	2.1	0.53	0.67	1.02	1.69	0.95
1204.85	Peptidyl-prolyl cis-trans isomerase FKBP1A	0.0000023	2.6	2.51	1.86	1.82	1.26	1.36	1.75	1.05	0.66	0.24
1213.86	Histone H2B/Gamma-synuclein	0.0000151	3.92	3.52	2.32	2.52	5.63	0.87	0.98	0.61	0.97	6.26
1253.72	Mast cell protease 1	< 0.000001	2.26	8.13	11.01	13.25	3.94	0.75	5.58	6.01	9.11	1.77
1268.75	Unassigned Peak	< 0.000001	1.62	3.73	4.66	5.37	2.35	0.57	1.98	1.92	2.69	0.84

Table 4.2. Peak statistics data from ClinProTools including the averages, standard deviations, and covariance for selected peaks from the DRG cell cultures measured using MALDI-TOF MS.

1332.81	Neurofilament light polypeptide/ Neurofilament medium polypeptide/ Myelin protein P0	0.0000059	8.5	7.16	5.47	4.54	2.15	7.48	7.38	3.38	1.55	0.71
1354.68	Vimentin	0.0000226	2.65	2	1.53	1.33	1.26	1.59	1.07	0.57	0.23	0.16
1573.59	Lumican/Ubiquitin carboxyl-terminal hydrolase isozyme L1	< 0.000001	2.98	2.23	1.38	1.37	0.85	1.42	1.04	0.51	0.42	0.22
1575.87	Mast cell protease 1/Vimentin/ Serum albumin	< 0.000001	2.8	1.9	1.24	1.19	0.82	1.65	0.48	0.43	0.31	0.15
1820.61	Actin cytoplasmic 2/Hemoglobin subunit beta-1	< 0.000001	6.88	3.74	1.75	1.16	0.83	9.67	4.64	1.79	0.75	0.14
1857.81	Unassigned Peak	< 0.000001	3.65	1.9	1.02	0.87	0.65	3.13	1.53	0.38	0.19	0.15
1872.86	Unassigned Peak	< 0.000001	3.59	2.33	1.33	0.91	0.61	2.93	2.32	1.11	0.33	0.16
1898.02	Histone H2B/Cytochrome c oxidase subunit 6A1 mitochondrial	< 0.000001	4.74	2.54	1.26	1.22	0.69	3.26	1.02	0.58	0.53	0.15

Table 4.2 (cont)

1969.98	Nucleoside diphosphate kinase alpha isoform	< 0.000001	4.83	3.03	1.4	1.08	0.6	2.97	2.32	1.14	0.46	0.2
2010.07	High mobility group protein B1/Protein Hmg1l1	< 0.000001	4.87	3.28	1.48	1.06	0.68	5.95	5.13	1.13	0.29	0.33
2060.9	Histone H2B	< 0.000001	3.3	2.06	1.15	0.81	1.02	2.86	2.35	1.32	0.4	0.53
2099.2	Histone H2B	< 0.000001	5.89	3.35	1.53	1.06	0.55	4.83	2.77	1.69	0.67	0.19
2211.15	Unassigned Peak	< 0.000001	5.02	2.22	0.98	0.85	0.51	6.96	0.89	0.43	0.28	0.14
2246.86	Unassigned Peak	< 0.000001	6.16	3.39	1.57	0.9	0.51	6.48	4.43	2.34	0.61	0.15
2272.3	Periaxin	< 0.000001	7.91	4.32	2.07	1.5	0.49	10.69	3.67	2.75	1.26	0.14
2359.82	Unassigned Peak	< 0.000001	4.83	2.57	1.58	1.1	0.87	3.68	1.72	1.37	0.41	0.27
2440.19	Unassigned Peak	< 0.000001	3.05	1.83	0.96	0.79	0.56	1.46	0.84	0.43	0.28	0.13
2482.21	Unassigned Peak	< 0.000001	2.84	1.84	1.21	1.16	1.33	1.24	0.59	0.48	0.39	0.68
2498.08	Unassigned Peak	< 0.000001	3.4	2.05	1.16	0.92	0.61	2.88	0.86	0.65	0.35	0.11
2559.41	Unassigned Peak	< 0.000001	8.97	5.29	2.13	1.12	0.6	5.99	5.46	3.32	0.77	0.09
2595.24	Unassigned Peak	< 0.000001	2.43	1.92	1.04	0.95	0.73	1.13	1.01	0.38	0.38	0.23

Table 4.2 (cont)

2616.13	Neurofilament heavy polypeptide	< 0.000001	2.87	1.82	0.93	0.75	0.5	0.93	0.82	0.38	0.29	0.13
2629.5	Unassigned Peak	< 0.000001	4.69	3.72	1.71	1.3	0.48	2.46	2.31	1.65	0.8	0.14
2722.51	Unassigned Peak	< 0.000001	3.73	1.97	1.02	0.73	0.48	2.6	0.9	0.64	0.25	0.12
2748.43	Heat shock 27kDa protein 1	< 0.000001	3.47	2.35	1.04	0.9	0.47	1.85	1.42	0.45	0.45	0.13
2807.86	Unassigned Peak	< 0.000001	4.83	12.02	7.42	8.13	0.6	6.34	22.65	8.72	11.32	0.26
3502.77	Unassigned Peak	0.00188	1.03	1.11	1.83	2.15	0.68	0.6	0.47	2.14	3.54	0.46
3516.78	Unassigned Peak	< 0.000001	2.01	20.86	36.97	47.14	10.46	2.45	27.54	36.5	40.94	16.13
3807.51	Unassigned Peak	< 0.000001	3.93	1.94	0.75	0.61	0.35	3.1	1.52	0.46	0.36	0.09

Table 4.2 (cont)

Theoretical Mass	m/z (MALDI)	Protein ID	Peptide Sequence	Identification	Stim/ Pre	Post/ Pre	Pre/ Control
600.17	601.17	Unassigned			0.47	0.31	0.54
615.27	616.27	Unassigned			0.47	0.31	0.54
649.86	650.86	Unassigned			0.50	0.48	0.54
738.43	739.43	Unassigned			0.66	0.72	0.90
767.71	768.71	sp|P02091|HBB1_RAT	A.LAHKYH	Hemoglobin subunit beta-1	0.44	0.38	0.68
769.68	770.68	Unassigned			0.79	0.66	0.65
915.69	916.69	sp|P06907|MYP0_RAT	Y.AMLDHSRS.T	Myelin protein P0	0.45	0.32	0.67
1179.79	1180.79	tr|G3V8B3|G3V8B3_RAT	E.RIAGEASRLAH.Y	Histone H2B	0.46	0.32	0.57
1203.85	1204.85	sp|Q62658|FKB1A_RAT	L.VFDVELLKLE	Peptidyl-prolyl cis-trans isomerase FKBP1A	0.50	0.48	0.54
1212.86	1213.86	tr|F1LQ96|F1LQ96_RAT	M(+42.01)DVFKKGFSI.A	Gamma-synuclein	0.56	0.39	0.62
1212.86	1213.86	tr|G3V8B3|G3V8B3_RAT	G.TKAVTKYTSSK	Histone H2B	0.66	0.72	0.90
1252.72	1253.72	sp|P09650|MCPT1_RAT	Y.NFYSNLHDIM.L	Mast cell protease 1	0.56	0.39	0.62
1267.75	1268.75	Unassigned			0.50	0.48	0.54

Table 4.3: Fold changes between sample classes for DRG cell culture MALDI-TOF MS.

1331.81	1332.81	sp|P06907|MYP0_RAT	K.SKGLGESRKDKK	Myelin protein P0	0.56	0.39	0.62
1331.81	1332.81	sp|P19527|NFL_RAT	Y.SAPVSSSLSVRRS.Y	Neurofilament light polypeptide	0.79	1.43	1.43
1331.81	1332.81	tr|G3V7S2|G3V7S2_RAT	E.IIEETKVEDEK.S	Neurofilament medium polypeptide	0.62	0.61	0.75
1353.68	1354.68	sp|P31000|VIME_RAT	L.NDRFANYIDKV.R	Vimentin	1.35	1.63	3.60
1572.59	1573.59	sp|P51886|LUM_RAT	M.SKLPAGLPTSLLTLY.L	Lumican	0.65	0.63	0.68
1572.59	1573.59	sp|Q00981|UCHL1_RAT	MQLKPMEINPEML.N	Ubiquitin carboxyl-terminal hydrolase isozyme L1	1.75	1.78	4.07
1574.87	1575.87	sp|P09650|MCPT1_RAT	R.AAGWGQTGVTKPTSNT.L	Mast cell protease 1	0.76	0.63	0.84
1574.87	1575.87	sp|P31000|VIME_RAT	T.VETRDGQVINETSQ.H	Vimentin	0.51	0.41	0.63
1819.61	1820.61	sp|P02091|HBB1_RAT	L.LVVYPWTQRYFDSF.G	Hemoglobin subunit beta-1	0.76	0.63	0.84
1819.61	1820.61	sp|P63259|ACTG_RAT	M.E(+42.01)EEIAALVIDNGSGMCK.A	Actin cytoplasmic 2	0.76	0.63	0.84
1856.81	1857.81	Unassigned			0.46	0.36	0.63
1871.86	1872.86	Unassigned			0.74	0.73	0.97
1897.02	1898.02	sp|P10818|CX6A1_RAT	L.FHNPHMNPLPTGYEDE	Cytochrome c oxidase subunit 6A1 mitochondrial	0.48	0.35	0.55
1897.02	1898.02	tr|D3ZWM5|D3ZWM5_RAT		Histone H2B	0.45	0.32	0.67

Table 4.3 (cont)

1897.02	1898.02	tr|G3V8B3|G3V8B3_RAT	F.VNDIFERIAGEASRLAH.Y	Histone H2B	0.62	0.61	0.75
1968.98	1969.98	tr|Q9QWQ4|Q9QWQ4_RAT	M.A(+42.01)NLERTFIAIKPDGVQR.G	Nucleoside diphosphate kinase alpha isoform	0.77	0.67	0.75
2009.07	2010.07	sp|P63159|HMGB1_RAT	M.SAKEKGKFEDMAKADKAR.Y	High mobility group protein B1	0.65	0.63	0.68
2009.07	2010.07	tr|D3ZCR3|D3ZCR3_RAT		Protein Hmg1l1	1.63	1.64	1.71
2059.9	2060.9	tr|D4A817|D4A817_RAT		Histone H2B	0.90	0.87	1.88
2059.9	2060.9	tr|G3V8B3|G3V8B3_RAT	F.VNDIFERIAGEASRLAHY.N	Histone H2B	0.99	0.94	1.83
2059.9	2060.9	tr|D3ZWM5|D3ZWM5_RAT		Histone H2B	1.44	1.43	1.64
2098.2	2099.2	tr|D3ZWM5|D3ZWM5_RAT	L.LPGELAKHAVSEGTKAVTKY.T	Histone H2B	0.74	0.67	1.30
2210.15	2211.15	Unassigned			1.25	1.44	2.30
2245.86	2246.86	Unassigned			0.54	0.46	0.52
2271.3	2272.3	sp|Q63425|PRAX_RAT	V.KLPKIPDMAVPDVRLPELQL.P	Periaxin	0.57	0.39	0.65
2358.82	2359.82	Unassigned			0.44	0.38	0.44
2439.19	2440.19	Unassigned			0.46	0.27	0.55
2481.21	2482.21	Unassigned			0.61	0.43	0.53

Table 4.3 (cont)

2497.08	2498.08	Unassigned			0.52	0.43	0.60
2558.41	2559.41	Unassigned			0.66	0.63	0.65
2594.24	2595.24	Unassigned			0.57	0.45	0.60
2615.13	2616.13	tr|F1LRZ7|F1LRZ7_RAT	M(+42.01)MSFGGADALLGAPFAPLHGGGSLHY.A	Neurofilament heavy polypeptide	0.40	0.21	0.59
2628.5	2629.5	Unassigned			0.54	0.49	0.79
2721.51	2722.51	Unassigned			0.46	0.35	0.79
2747.43	2748.43	tr|G3V913|G3V913_RAT	L.RSPSWEPFRDWYPAHSRLFDQA.F	Heat shock 27kDa protein 1	0.52	0.37	0.53
2806.86	2807.86	Unassigned			0.62	0.68	2.49
3501.77	3502.77	Unassigned			1.65	1.94	1.08
3515.78	3516.78	Unassigned			1.77	2.26	10.38
3806.51	3807.51	Unassigned			0.39	0.31	0.49

Table 4.3 (cont)

4.10 Work Cited

1. Altelaar, A.F.M., et al., *Direct molecular imaging of Lymnaea stagnalis nervous tissue at subcellular spatial resolution by mass spectrometry.* Analytical Chemistry, 2005. **77**(3): p. 735-741.
2. Priestley, J.V., *Neuropeptides: Sensory Systems*, in *Encyclopedia of Neuroscience*, L.R. Squire, Editor. 2009, Academic Press: Oxford. p. 935-943.
3. Sugiura, Y., et al., *Visualization of acetylcholine distribution in central nervous system tissue sections by tandem imaging mass spectrometry.* Analytical and Bioanalytical Chemistry, 2012. **403**(7): p. 1851-1861.
4. Strand, F.L., et al., *Neuropeptide hormones as neurotrophic factors.* Physiological Reviews, 1991. **71**(4): p. 1017-1046.
5. Monroe, E.B., et al., *Vitamin E imaging and localization in the neuronal membrane.* Journal of the American Chemical Society, 2005. **127**(35): p. 12152-12153.
6. Su, J., M. Al-Tamimi, and G. Garnier, *Engineering paper as a substrate for blood typing bio-diagnostics.* Cellulose, 2012. **19**(5): p. 1749-1758.
7. Strand, F.L., *Neuropeptides: General characteristics and neuropharmaceutical potential in treating CNS disorders*, in *Progress in Drug Research*, L.P.-T. Prokai, Katalin, Editor. 2003. p. 1-37.
8. Patti, G.J., et al., *Metabolomics implicates altered sphingolipids in chronic pain of neuropathic origin.* Nat Chem Biol, 2012. **8**(3): p. 232-234.
9. Ding, H., et al., *Determination of platinum in rat dorsal root ganglion using ICP-MS.* Biological Trace Element Research, 1999. **67**(1): p. 1-11.
10. Cheng, H., X. Jiang, and X. Han, *Alterations in lipid homeostasis of mouse dorsal root ganglia induced by apolipoprotein E deficiency: a shotgun lipidomics study.* Journal of Neurochemistry, 2007. **101**(1): p. 57-76.
11. Wong, A., et al., *Simultaneous tissue profiling of eicosanoid and endocannabinoid lipid families in a rat model of osteoarthritis.* Journal of Lipid Research, 2014. **55**(9): p. 1902-1913.
12. Zhang, X.-J., et al., *Proteome profiling of spinal cord and dorsal root ganglia in rats with trinitrobenzene sulfonic acid-induced colitis.* World Journal of Gastroenterology, 2012. **18**(23): p. 2914-2928.
13. Komori, N., et al., *Proteomics study of neuropathic and nonneuropathic dorsal root ganglia: altered protein regulation following segmental spinal nerve ligation injury.* Physiol. Genomics, 2007. **29**(2): p. 215-230.

14. Riedl, M.S., et al., *Proteomic analysis uncovers novel actions of the neurosecretory protein VGF in nociceptive processing.* Journal of Neuroscience, 2009. **29**(42): p. 13377-13388.
15. Perry, M., Q. Li, and R.T. Kennedy, *Review of recent advances in analytical techniques for the determination of neurotransmitters.* Analytica Chimica Acta, 2009. **653**(1): p. 1-22.
16. Li, L. and J.V. Sweedler, *Peptides in the brain: mass spectrometry-based measurement approaches and challenges.* Annu Rev Anal Chem (Palo Alto Calif), 2008. **1**: p. 451-83.
17. Fricker, L.D., et al., *Peptidomics: Identification and quantification of endogenous peptides in neuroendocrine tissues.* Mass Spectrometry Reviews, 2006. **25**(2): p. 327-344.
18. Ebner, K., et al., *Increased in vivo release of neuropeptide S in the amygdala of freely moving rats after local depolarisation and emotional stress.* Amino Acids, 2011. **41**(4): p. 991-996.
19. Malcangio, M., et al., *Abnormal substance P release from the spinal cord following injury to primary sensory neurons.* European Journal of Neuroscience, 2000. **12**(1): p. 397-399.
20. Mitsuma, T., et al., *Effects of orexin A on thyrotropin-releasing hormone and thyrotropin secretion in rats.* Hormone and Metabolic Research, 1999. **31**(11): p. 606-609.
21. Li, L.J., et al., *Mass spectrometric investigation of the neuropeptide complement and release in the pericardial organs of the crab, Cancer borealis.* Journal of Neurochemistry, 2003. **87**(3): p. 642-656.
22. Rubakhin, S.S., et al., *Analysis of cellular release using capillary electrophoresis and matrix assisted laser desorption/ionization-time of flight-mass spectrometry.* Electrophoresis, 2001. **22**(17): p. 3752-3758.
23. Svensson, M., et al., *Neuropeptidomics: expanding proteomics downwards.* Biochem Soc Trans, 2007. **35**(Pt 3): p. 588-93.
24. Hanrieder, J., P. Malmberg, and A.G. Ewing, *Spatial neuroproteomics using imaging mass spectrometry.* Biochimica et Biophysica Acta (BBA) - Proteins and Proteomics, 2015. **1854**(7): p. 718-731.
25. Norris, J.L. and R.M. Caprioli, *Analysis of tissue specimens by matrix-assisted laser desorption/ionization imaging mass spectrometry in biological and clinical research.* Chemical Reviews, 2013. **113**(4): p. 2309-2342.
26. Lanni, E.J., S.S. Rubakhin, and J.V. Sweedler, *Mass spectrometry imaging and profiling of single cells.* Journal of Proteomics, 2012. **75**(16): p. 5036-5051.
27. Romanova, E.V., et al., *Small-volume analysis of cell-cell signaling molecules in the brain.* Neuropsychopharmacology, 2014. **39**(1): p. 50-64.

28. Chen, R., et al., *In situ identification and mapping of neuropeptides from the stomatogastric nervous system of Cancer borealis.* Rapid Communications in Mass Spectrometry, 2014. **28**(22): p. 2437-2444.
29. Iannacone, J.M., et al., *Collecting peptide release from the brain using porous polymer monolith-based solid phase extraction capillaries.* Analytical Chemistry, 2009. **81**(13): p. 5433-5438.
30. Hatcher, N.G., et al., *Mass spectrometry-based discovery of circadian peptides.* Proceedings of the National Academy of Sciences of the United States of America, 2008. **105**(34): p. 12527-12532.
31. Fan, Y., S.S. Rubakhin, and J.V. Sweedler, *Collection of peptides released from single neurons with particle-embedded monolithic capillaries followed by detection with matrix-assisted laser desorption/ionization mass spectrometry.* Analytical Chemistry, 2011. **83**(24): p. 9557-9563.
32. Lee, C.Y., E.V. Romanova, and J.V. Sweedler, *Laminar stream of detergents for subcellular neurite damage in a microfluidic device: a simple tool for the study of neuroregeneration.* J. Neural Engineering, 2013. **10**(3): p. 036020.
33. Wang, J., et al., *Microfluidics: A new cosset for neurobiology.* Lab Chip, 2009. **9**(5): p. 644-652.
34. Croushore, C.A., et al., *Microfluidic device for the selective chemical stimulation of neurons and characterization of peptide release with mass spectrometry.* Analytical Chemistry, 2012. **84**: p. 9446-52.
35. Hou, X., F. Xie, and J. Sweedler, *Relative quantitation of neuropeptides over a thousand-fold concentration range.* Journal of the American Society for Mass Spectrometry, 2012. **23**(12): p. 2083-2093.
36. Romanova, E.V., et al., *Comparative peptidomics analysis of neural adaptations in rats repeatedly exposed to amphetamine.* Journal of Neurochemistry, 2012. **123**(2): p. 276-287.
37. Lee, J.E., et al., *Endogenous peptide discovery of the rat circadian clock: a focused study of the suprachiasmatic nucleus by ultrahigh performance tandem mass spectrometry.* Molecular & Cellular Proteomics, 2010. **9**(2): p. 285-297.
38. Millet, L.J., et al., *Microfluidic devices for culturing primary mammalian neurons at low densities.* Lab Chip, 2007. **7**(8): p. 987-994.
39. Croushore, C.A. and J.V. Sweedler, *Microfluidic systems for studying neurotransmitters and neurotransmission.* Lab Chip, 2013. **13**(9): p. 1666-1676.

40. Wei, H., et al., *Multi-channel microfluidic devices combined with electrospray ionization quadrupole time-of-flight mass spectrometry applied to the monitoring of glutamate release from neuronal cells.* Analyst, 2010. **135**(8): p. 2043-2050.
41. Malsam, J., S. Kreye, and T.H. Sollner, *Membrane fusion: SNAREs and regulation.* Cellular and Molecular Life Sciences, 2008. **65**(18): p. 2814-2832.
42. George, J.M., *The synucleins.* Genome Biology, 2002. **3**(1).
43. Asch, W.S. and N. Schechter, *Plasticin, a type III neuronal intermediate filament protein, assembles as an obligate heteropolymer: Implications for axonal flexibility.* Journal of Neurochemistry, 2000. **75**(4): p. 1475-1486.
44. Han, H.J., et al., *Myelin-specific proteins: A structurally diverse group of membrane-interacting molecules.* Biofactors, 2013. **39**(3): p. 233-241.
45. Gibson, S.J., et al., *Calcitonin gene-related peptide messenger RNA is expressed in sensory neurones of the dorsal root ganglia and also in spinal motoneurones in man and rat.* Neurosci. Lett., 1988. **91**(3): p. 283-8.
46. Xu, P., et al., *Activin induces tactile allodynia and increases calcitonin gene-related peptide after peripheral inflammation.* Journal of Neuroscience, 2005. **25**(40): p. 9227-9235.
47. Lone, A.M., Y.-G. Kim, and A. Saghatelian, *Peptidomics methods for the identification of peptidase-substrate interactions.* Current opinion in chemical biology, 2013. **17**(1): p. 83-89.
48. Murillo, L., et al., *Brain processing of hemorphin-7 peptides in various subcellular fractions from rats.* Peptides, 2006. **27**(12): p. 3331-3340.
49. Gomes, I., et al., *Hemoglobin-derived peptides as novel type of bioactive signaling molecules.* AAPS J, 2010. **12**(4): p. 658-669.
50. Cheng, B.-C., et al., *LVV-hemorphin 7 and angiotensin IV in correlation with antinociception and anti-thermal hyperalgesia in rats.* Peptides, 2012. **36**(1): p. 9-16.
51. Honda, M., et al., *Spinorphin, an endogenous inhibitor of enkephalin-degrading enzymes, potentiates leu-enkephalin-induced anti-allodynic and antinociceptive effects in mice.* Japanese Journal of Pharmacology, 2001. **87**(4): p. 261-267.
52. Annangudi, S.P., et al., *Neuropeptide release is impaired in a mouse model of Fragile X mental retardation syndrome.* ACS Chemical Neuroscience, 2010. **1**(4): p. 306-314.
53. Romanova, E.V., et al., *Identification and characterization of homologues of vertebrate β-thymosin in the marine mollusk Aplysia californica.* Journal of Mass Spectrometry, 2006. **41**(8): p. 1030-1040.

54. Rubakhin, S., A. Ulanov, and J. Sweedler, *Mass spectrometry imaging and GC-MS profiling of the mammalian peripheral sensory-motor circuit.* Journal of the American Society for Mass Spectrometry, 2015. **26**(6): p. 958-966.
55. Yuan, A., et al., *Neurofilaments at a glance.* Journal of Cell Science, 2012. **125**(14): p. 3257-3263.
56. Rishal, I. and M. Fainzilber, *Retrograde signaling in axonal regeneration.* Experimental Neurology, 2010. **223**(1): p. 5-10.
57. Müller, S., L. Ronfani, and M.E. Bianchi, *Regulated expression and subcellular localization of HMGB1, a chromatin protein with a cytokine function.* Journal of Internal Medicine, 2004. **255**(3): p. 332-343.
58. Vargas, K.J., et al., *Synucleins regulate the kinetics of synaptic vesicle endocytosis.* Journal of Neuroscience, 2014. **34**(28): p. 9364-9376.
59. Sezen, S., et al., *FK506 binding protein 12 is expressed in rat penile innervation and upregulated after cavernous nerve injury.* International Journal of Impotence Research, 2002. **14**(6): p. 506-512.
60. Gillespie, C.S., et al., *Periaxin, a novel protein of myelinating schwann cells with a possible role in axonal ensheathment.* Neuron, 1994. **12**(3): p. 497-508.
61. Martini, R. and M. Schachner, *Molecular bases of myelin formation as revealed by investigations on mice deficient in glial cell surface molecules.* Glia, 1997. **19**(4): p. 298-310.
62. Kimura, I., et al., *Neuferricin, a novel extracellular heme-binding protein, promotes neurogenesis.* Journal of Neurochemistry, 2010. **112**(5): p. 1156-1167.
63. Buchberger, A., Q. Yu, and L. Li, *Advances in mass spectrometric tools for probing neuropeptides.* Annu Rev Anal Chem (Palo Alto Calif), 2015. **8**(1): p. 485-509.
64. Romanova, E.V. and J.V. Sweedler, *Peptidomics for the discovery and characterization of neuropeptides and hormones.* Trends Pharmacol Sci, 2015.

Chapter 5

Peptide Characterization of Mouse Itch Models and Itch-related Neurons

5.1 Notes

The project outlined in this chapter was born out of a collaboration with Dr. Qin Liu, Associate Professor of Anesthesiology at the Center for the Study of Itch at Washington University School of Medicine in St. Louis. Dr. Liu's insights and understanding of the sensory nervous system have been very useful for this project. Jeff Guo from the Liu lab was instrumental in generating the itch models and helping with dissections. Sheena Chatrath and Nathaniel Grabinski, also in the Liu lab, helped with behavioral analysis. In the Sweedler lab, Krishna Anapindi and Eduardo De La Toba were integral in performing mass spectrometric analysis and data analysis. Ed also helped with behavioral analysis in the second set of experiments. Ashley Lenhart helped with the first set of data analysis.

5.2 Introduction

Disorders of the peripheral sensory system such as chronic pain and itch remain an important health problem for which the full extent of molecular players is not yet understood. These sensory modalities are detected through the primary sensory neurons, with their nerve endings located in the skin and their cell bodies in the dorsal root ganglion (DRG). Primary sensory neurons have a single axon which bifurcates and projects from the peripheral nerve endings to the dorsal horn (DH) of the spinal cord, transmitting important sensory information to the central nervous system via signaling molecules such as neurotransmitters and neuropeptides [1, 2]. While classical neurotransmitters are well studied and have relatively defined roles in information signaling, neuropeptides are more

diverse and wide-acting [3], making it difficult to study the wide range of influences these molecules have on sensory processes.

Through targeted methods such as immunoassays or through studies of RNA expression, we have been able to gain much information about the neuropeptides involved in the system. However, these methods do not provide dynamic information about the wide range of molecules involved in such systems as increased expression does not always translate to increased peptide content and/or release due to the multiple post-translational processing steps performed to make neuropeptides [4, 5] and the limited scope of targeted studies. Therefore, to gain a better understanding of the endogenous peptide content of the DRG, we previously performed peptidomics on healthy DRG tissue from rat [6]. Now, we are extending our study of the peptidomics of the DRG to that of tissue modeling a diseased state, through mouse models of itch.

Chronic itch (pruritis) occurs in over 20% of the population and is associated with various medical conditions [7, 8]. Unfortunately, the molecular mechanisms of itch sensation are not well understood and there are many itch symptoms that are not responsive to common anti-itch treatments [9]. Recent work has begun to delineate pain and itch sensory responses and has shown that Mas-related G-protein coupled receptors (Mrgprs) [10], specifically MrgprA3, MrgprC11, and MrgprD, are important players in the itch sensing pathway [11, 12]. Cells containing these receptors specifically respond to chemical agonists known to cause itch, such as chloroquine and histamine, which are MrgprA3 agonists, bovine adrenal medulla peptide 8-22 (BAM8-22) and SLIGRL-NH2, which are MrgprC11 agonists, and β-alanine, which is an MrgprD agonist [9, 13]. Morphological, immunohistochemical, and functional characterizations of these Mrgpr-expressing

subpopulations of sensory neurons provide useful information. However, the in-depth peptidomic characterization of the cell signaling molecules found within and released from these cells could greatly improve our understanding of the system.

Due to their prevalence in the nervous system and their involvement in multiple physiological processes [3], including sensory responses in the DRG, neuropeptides are important molecules to characterize. The involvement of neuropeptides in pain response is extensive and we expect to find similar complexity in the neuropeptides involved in itch sensation. Already, substance P (SP) [14], endothelin-1 [15, 16], neuromedin B (NMB) [17], calcitonin-gene related peptide (CGRP) [18], natriuretic peptide B and the kappa-opioid dynorphin [19] are implicated in the itch response. A recent study in the Liu lab has shown that NMB is expressed in both MrgprA3+ and MrgprD+ neurons and that NMB deficiency causes impaired itch responses to multiple pruritogens in mice. This impaired, but not completely eliminated response indicates that there may other signaling molecules involved in the transmission of itch sensation. Transcriptomic studies have demonstrated that other neuropeptides, such as natriuretic polypeptide b, agouti-related peptide, neurotensin, and adenylate cyclase activating polypeptide 1 are upregulated in itch sensing neurons [20]. Therefore, a characterization and comparison of the full peptide content of peripheral nervous system tissues within itch models is apt.

There are a few ways to generate itch within a rodent model. The AEW model, utilizing a 15 s application of acetone and diethylether to pre-shaved skin followed with a 30 s application of water, is an established model [21] for pruritis which has also been used to demonstrate changes in DRG cell responsiveness [22] as well as immunohistochemical changes in the dorsal horn of the spinal cord [23] upon development of itch-related

behavior. This model has also been used to investigate the changes in peptidergic fiber accumulation within various itch-producing paradigms and has indeed shown that the number of peptidergic fibers in the skin increases in dry skin models [24].

For a more disease-specific model, the vitamin D analogue, MC903, is applied to the skin to model the disease atopic dermatitis [25, 26]. Atopic dermatitis is a widely prevalent chronic disease of the skin that includes inflammation, skin barrier dysfunction, and a wide IgE immune response [27]. This model triggers a Th1/Th2 immune response within the skin as well as causes increased levels of IgE in the blood and other markers of atopic dermatitis, making it a systemic model rather than the localized dry skin model [28].

This project utilizes both itch models in a hypothesis-forming study. The goal of this work is to find changes in the amount of individual peptides within the DRG and dorsal horn (DH) of the spinal cord on treated versus non-treated sides of the animal.

5.3 Experimental

5.3.1 Itch Model Generation

5.3.1.1 AEW (dry skin) Model

3 B6J WT mice were used to create a dry skin model using acetone, diethylether, and water. The model is created by shaving the skin on the upper flank and treating one side with a 1:1 acetone/diethylether mixture for 15 s followed by an application of water for 30 s. This treatment was continued twice daily for 7 d. The other side of the animal is shaved and treated as a control, providing us with 3 treatment and 3 control samples for each tissue dissected. Scratch bouts were recorded on day 7 and sampling was performed as described below.

5.3.1.2 MC903 (atopic dermatitis) Model

6 B6J WT mice were used to create an atopic dermatitis model. The model is created by shaving the skin on the upper flank of the animal and treating one side with the vitamin D analogue MC903 once daily for 6 d. The other side is shaved and treated as a control, providing 6 treatment and 6 control samples from each tissue dissected. Scratch bouts were recorded on day 5 and sampling was performed as described below.

5.3.1.3 Behavioral Assessment

Animals were video recorded from above in their cages for at least one hour at baseline and after 7 days of treatment for the AEW mice and 5 days of treatment for the MC903 mice. Upon review of the video, the number of scratch bouts per side for each animal were counted and recorded (Table 5.1).

5.3.2 Itch Model Tissue Sampling

DH, DRG, and skin samples corresponding to the correct spinal levels and treatment versus control side were dissected from each animal. Immediately upon dissection, the tissues were stabilized using the Denator Stabilizor system. The tissues were then frozen at -80 °C prior to peptide extraction and analysis.

5.3.3 Itch Model Peptide Extraction and Clean-Up

The frozen tissues were homogenized using a pellet pestle cordless motor after the addition of 200 µL of ice-cold LC-MS grade water. For the first stage of peptide extraction, the homogenized tissue suspensions were placed on ice for 30 min. Following this extraction, the samples were centrifuged at 14000 ×*g* for 10 min and the supernatants were saved. 200 µL of ice-cold acidified methanol (methanol: formic acid: water 90:9:1) were added to the remaining tissue pellets and vortexed for 30 s followed by a 30 min

incubation on ice for the second stage peptide extraction. This procedure was repeated for the third stage peptide extraction using 200 µL of ice-cold acetic acid water solution (0.25%) as the extraction buffer. The supernatants from all extraction steps and were combined and dried using a SpeedVac system (LabConco, MO).

The dried samples were reconstituted in 200 µL of water and loaded onto equilibrated C18 spin columns for desalting (Thermo Fisher Scientific, MA). After clean-up, peptides were eluted four times: twice with 50 µl each of 50%/50% H2O/ACN solution with 0.1 % formic acid (FA) and 0.01 % trifluoroacetic acid (TFA) and twice with 50 µl each 30%/70% H2O/ACN solution with 0.1 % formic acid (FA) and 0.01 % trifluoroacetic acid (TFA). For different regions, either 5 or 10% of the eluted peptide extract were taken out from each of the, pooled and saved in a clean microcentrifuge tube. All samples were evaporated to dryness using a SpeedVac system.

5.3.4 Nanoflow UHPLC for Peptide Identification and Quantitation of Itch Model Samples

For each itch model region, the pooled sample was reconstituted in 10 µl of 99%/1% H2O/ACN solution with 0.1% FA. 10 µl of sample was loaded at 15ul/min onto an Acclaim PepMap100 C18 peptide trap cartridge (Thermo, MA) for pre-concentration. After 3 min, the trap was put in-line with the analytical column and the samples were separated on a C18 column (Acclaim Pepmap, 2Å, 75 µm x 150 mm, Thermo, MA) using a Thermo Ultimate 3000 RSLC system operated at uniform flow rate of 300nL/min. H2O with 0.1% FA and ACN with 0.1% FA were used as solvent A and B, respectively. The peptides were eluted using the following gradients: 0-3 min, 1-1% B; 3-6 min, 1-10% B; 6-90 min, 10-70% B; 90-100 min, 70-99% B; 100-110 min, 99-1% B; 110-120 min, 1-1% B. For

quantitation, the dried samples were reconstituted in 10 µl of 99%/1% H2O/ACN solution with 0.1% FA and centrifuged at 14,000 *xg* for 10 min. 8 µl of the supernatant was collected, transferred to an auto sampler vial and 7 µl of it was used for analysis with a Thermo Ultimate 3000 RSLC (Thermo Fisher Scientific, MA) coupled to high-resolution Impact HD Q-TOF mass spectrometer (Bruker Daltonics, MA). The same LC-conditions were used both for MS/MS and MS analysis.

5.3.5 Mass Spectrometric Instrument Parameters

5.3.5.1 Orbitrap

Top speed data-dependent precursor ion selection was used for all the three modes on Thermo Quadrupole-Iontrap-Orbitrap with a cycle time of 3 s. The parent ions were scanned with an Orbitrap resolution of 120K with an AGC target of 200000. Dynamic exclusion was turned on with the following settings: exclusion time = 60 s; mass tolerance = +/- 10 ppm; repeat count = 2. For the Orbitrap (OT) detection, the parent ions were scanned in the range of 200-1200 *m/z*, the fragment ions were scanned with an Orbitrap resolution of 30K, maximum injection time of 60 ms and AGC target of 50000. Precursor ions with a charge ranging from +1 to +7 were considered. A normalized collision energy (NCE) value of 35% was used for the CID fragmentation.

5.3.5.2 QTOF

The samples were subjected to LC-MS analysis using Bruker IMPACT HD QqTOF outfitted with CaptiveSpray nanosource. The data was acquired in MS1 mode over a range of 290-3000 m/z with a cycle time of 3 s. A fixed MS1 scan rate of 1 Hz was used. An absolute intensity threshold of 694 counts (100 per 1000 sum) was used for spectra collection.

5.3.6 Bioinformatic Search Criteria for Peptide Library Construction

The acquired .RAW files from Thermo Orbitrap Fusion were imported into PEAKS 7.5 or 8 software (Bioinformatics Solutions Inc., Canada) and searched against a mouse proteome database with 81,515 proteins downloaded from UniProt for identification. The following database searching parameters were used: precursor mass tolerance, 20 ppm; fragment mass tolerance, 0.1 Da; no enzymatic cleavage; variable PTMs including acetylation, amidation, phosphorylation, half-disulfide bond, pyroglutamination and Met oxidation; maximum number of variable PTM, 3. A false discovery rate (FDR) threshold of 1% was used to filter the identified peptide sequences. The list was also manually validated to remove possible artifacts such as incorrect post-translational modifications (PTMs), due to statistical sequence assignment by the search engine.

5.3.7 Peptide Quantitation

The peptide quantitation was performed using SKYLINE software developed by the MacCoss lab [29, 30]. A SKYLINE project was built for each region of interest. First, the SKYLINE-compatible .mzxml file was exported from PEAKS using its inbuilt algorithm loaded into its corresponding project to build a peptide library. The following settings were used for importing the PEAKS search data onto SKYLINE: min.length of peptide = 3, max.length of peptide = 60, pick peptides matching: library, rank peptides: intensity, modifications: all the modifications used in bioinformatic search with a maximum of 4 variable modifications per peptide. Regression Fit, Normalization Method and Regression Weighting were all set to none. Only y ions with charge state +1 to +4 were used for peptide library construction. The library contained information including identified peptides and their *m/z*. After peptide library construction, LC-MS data files from different

regions were imported into their corresponding projects. Savitzky-Golay smoothing was applied to all the MS1 chromatograms after import. SKYLINE extracted the ion chromatograms (XIC) for peptides contained in the library from every single imported LC-MS file and the integrated peak areas were used for quantitation. To ensure the correct peaks were picked for quantitation, three criteria were set: the mass error between the detected *m/z* in the LC-MS results and the theoretical peptide *m/z* was less than 20 ppm; the retention time difference between LC-MS and LC-MS/MS experiments was less than 5 min; and the Isotope Dot Product score (idotp), which represents similarity between expected and observed precursor isotope distribution, was over 0.95. Peptides fulfilling all three criteria were kept and quantified by adding the peak areas corresponding to the first three isotopic peak patterns. For peptides with multiple charge states detected, the peak areas for different charge states were summed. The summed peak areas were baseline subtracted, log2 transformed and exported to Microsoft Excel for further statistical analysis.

5.3.8 Statistical Analysis

5.3.8.1 LOESS Normalization to Account for Run-to-run Variability

A locally weighted regression analysis (LOESS) was used normalize the peptide peak areas in different runs using the online tool Normalyzer [31]. Normalization was performed to account for run-to-run variability introduced due to various factors such as sampling artifacts, instrumental variability and pipetting errors. The normalization was performed with the assumption that the sum of all the quantifiable peptide areas matched to the peptide library should be equal/similar across all the biological replicates of a given treatment. The data is transformed into the standard M (log ratio) and A (mean average)

scales within a specific treatment group. The MA plot is constructed using replicates from the same treatment group and fitted with a polynomial using a local regression based weighted least squared (WLS) method. Based on the size of residuals between the individual M values and the WLS curve, a new set of fitted M' values are computed. The weighted regression assigns smaller weights to larger residuals and higher weights to smaller residuals to ensure the data is locally normalized. This process of fitting WLS curve is iterated until there is convergence. The final set of transformed M' values are used to assign the new normalized peak areas for each of the considered peptides. Therefore, LOESS normalization corrects systematic bias present in the sample without removing the biological variability.

5.3.8.2 Student's t-test to Identify the Significantly Changed Peptides and Proteins

To identify the peptides which had a significant change between the treatment and control samples, paired, 2-tailed Student's t-test with equal variance was used. The peptides that show up to be significantly different in both the independent cohorts were compared. The ones that fall below the set value ($p \leq 0.05$) in both the sets were considered significant differences.

5.3.9 Protein Analysis using PANTHER

A PANTHER (Protein ANalysis THrough Evolutionary Relationships) analysis was performed using the protein accession numbers for the detected peptides [32, 33]. Comparisons were made between various groups, including all detected proteins and significantly changed proteins.

5.4 Results

5.4.1 Peptide Quantitation of Itch Models

After the analysis with SKYLINE and the statistical analysis, 53 peptides from 38 precursor proteins were identified to be statistically different in amount between the treated and control samples at a confidence interval of 95%, without a false discovery rate (FDR) correction (Table 5.2). More specifically, in the DH, 9 peptides in the AEW model and 7 in the MC903 model were found to have different expression levels between the treated and control samples. Likewise, in the DRG samples, 19 peptides in the AEW model and 18 peptides in the MC903 models were found to be different in expression levels between the treated and control samples. Some of the peptides determined to be significant by the paired t test did not actually have peak area values for all three samples. Therefore, these peptides were removed from the list leaving 7 significantly different peptides in the DH MC903 model, 8 in the DH AEW model and 14 in both the DRG AEW and MC903 samples, making a total of 43 peptides detected to be significantly different among all models (Figures 5.1- 5.4).

11 of the peptides detected with statistical significance are derived from known prohormones, with 6 being known neuropeptides (somatostatin-28, dynorphin B29, C-terminal flanking peptide TAC1, substance P, nocistatin, PEN), and one, fibrinopeptide A, while not derived from a verified prohormone, has been implicated in neurochemical responses (Table 5.3 and Figure 5.5). It is notable to point out, however, that PEN was only detected in 2 out of the 3 samples.

However, it must be noted that because this study is a hypothesis-driving study, this data has not been corrected for the FDR. Hundreds of peptides were detected by the mass

spectrometer for each group (294 for MC903 DH, 317 for DRG AEW, 181 for DH AEW, and 349 for MC903 DRG), but only a small number of peptides are considered to have changed significantly in each group (7, 14, 8, and 14 respectively). Therefore, an FDR correction would not give any significant changes. Due to the importance of not missing a truly significant result and the expectedly low number of peptides that would be expected to change compared to the number of peptides that can be detected in a sample, we chose to make this particular study a hypothesis-forming study.

PANTHER analysis showed potentially interesting differences between the protein make-up of the significantly changed peptides compared to all detected peptides. Specifically, the changes in the molecular function and protein class classifications proved interesting (Figure 5.6). Within the molecular function group, the ratio of the proteins related to transporter activity increased in the significantly changed groups compared with total. Additionally, proteins with translation regulator activity and structural molecule activity did not show up in the changed groups. Perhaps more interesting is the protein class comparison, in which the protein make-up of the significantly increased group looks very different than the protein make-up of the significantly decreased and not changed groups. Within these groups, there is an increase in the ratio of enzyme modulators and signaling molecules in the significantly increased group while there is an increased ratio of nucleic acid binding proteins and oxidoreductase observed in the significantly decreased group.

5.5 Discussion

The goal of this project was to determine changes in the neuropeptide content of DRG within the context of an itch model. Encouragingly, changes in a few key neuropeptides were observed between the treatment and control model, namely substance P,

somatostatin-28, dynorphin B-29 and PEN. Additionally, there were quite a few statistically significant changes in levels of other peptides that may be of note, even if they are not specifically neuropeptides.

Substance P (RPKPQQFFGLM(-.98)) is an undecapeptide cleaved from the prohormone protachykinin-1 and is found in and released from both peripheral and central sensory neuron terminals in response to noxious stimuli [34]. Substance P acts on target neurons by inducing slow, long-lasting depolarizations which cause hypersensitization and can also act on blood vessels and immune cells to increase the inflammatory response [3, 34, 35]. Specific to itch-related functions, substance P has been shown to elicit scratching upon injection into the rostral back of mice [14], has been specifically implicated in the transmission of non-histaminergic itch signals in the spinal cord [36], and has been shown to be increased in the plasma of patients with atopic dermatitis [37].

A shortened form of the neuropeptide Somatostatin-28 (89-100) was also significantly decreased in the atopic dermatitis model. However, this peptide was detected in the DRG rather than the DH. Somatostatin has long been implicated in the pain response, but has recently also been specifically investigated for its role in itch transmission, particularly due to its expression in a subpopulation of sensory neurons known to respond to itch [38-40]. It was found that somatostatin plays an important role in the transmission of itch by inhibiting the peptide dynorphin, which has been shown to inhibit itch response [19, 40]. It is unclear from these publications which length of somatostatin is involved in these systems. Perhaps our use of mass spectrometry and exact peptide sequencing can shed some clarity on this situation. Interestingly, a shortened form of Dynorphin B-29 was

significantly increased in the dorsal horn of AEW models, perhaps indicating an itch-inhibitory counter-reaction.

The relationship of the neuroendocrine peptide, PEN, to itch is less straightforward. PEN is significantly increased in AEW-treated DRG. A role for this peptide in sensory response, however, has not been determined as it is usually associated with feeding or appetite-related behaviors.

Peptides derived from prohormones also implicated in sensory responses and/or signaling such as proenkephalin A, secretogranins 1 and 3, and pronociceptin were also increased in the AEW model DRG samples. A peptide from thymosin beta-10 was decreased in the MC903 DRG samples.

While some of the peptide changes detected in this project seem to fit into the narrative we would expect, others seem to be paradoxically changing. MS measures the amount of peptide in the tissue; if a peptide undergoes activity dependent release, its amount within the tissue will first decrease. However, a longer-term use of a peptide can result in more synthesis and accumulation. Thus, an increase in the use of a specific peptide during our itch model will change the amount detected, but the direction of change depends on peptide release/synthesis dynamics and is difficult to predict. Neuropeptide signaling is a dynamic system in which location, timing, and sampling methods all influence which peptides are more or less present as well as if we can detect that change. The purpose of this preliminary study is for us to get a feel for which peptides we should be looking at more closely within itch model systems and why. Once those peptides are determined, we can look further into understanding timing, location, and release patterns. Toward this end, the results of the PANTHER study provide insight into which functions

the changing peptides may be involved in, helping us to determine if the changes we are seeing make biological sense.

Additionally, it is also important to look at the nerve endings to fully understand the neuropeptide response. Detection of peptide content and release at the nerve endings is challenging, due to the low amount of peptide material in such samples and the high amount of other material, such as skin peptide content. So far, we have not been successful in analyzing the skin samples for neuropeptides from these animals for these reasons. However, the incorporation of such data is very important to the understanding of this system.

5.6 Future Directions

The project described in this chapter is a hypothesis-driving study. Therefore, the experiments are being repeated to test their validity and reproducibility before more labor-intensive validation studies are undertaken. For the second study, we increased the number of animals to 20. This number allows for 5 replicates for each treatment group (MC903 and AEW) with 2 animals per replicate. The treatment, sample collection, and behavioral analysis (Table 5.4) has been performed for these samples. As a result of the behavioral data, we did remove two animals per set, leaving 4 replicates of 2 animals each. The samples are currently being analyzed. If the hypothesis is correct, we will choose the most interesting neuropeptides for validation studies.

5.7 Figures

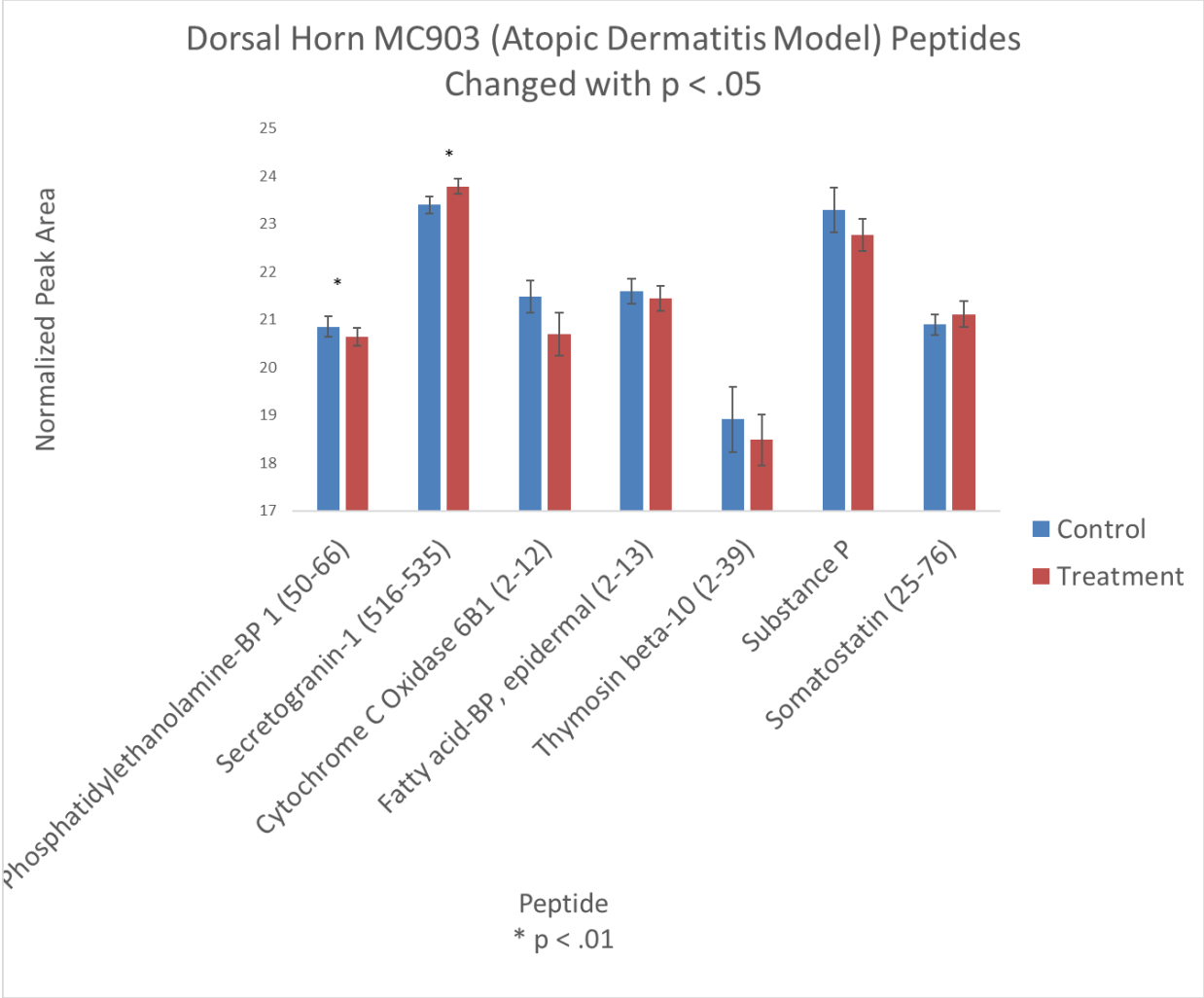

Figure 5.1: All statistically significantly changed peptides in the dorsal horn MC903 model (normalized peak area is log2 transformed).

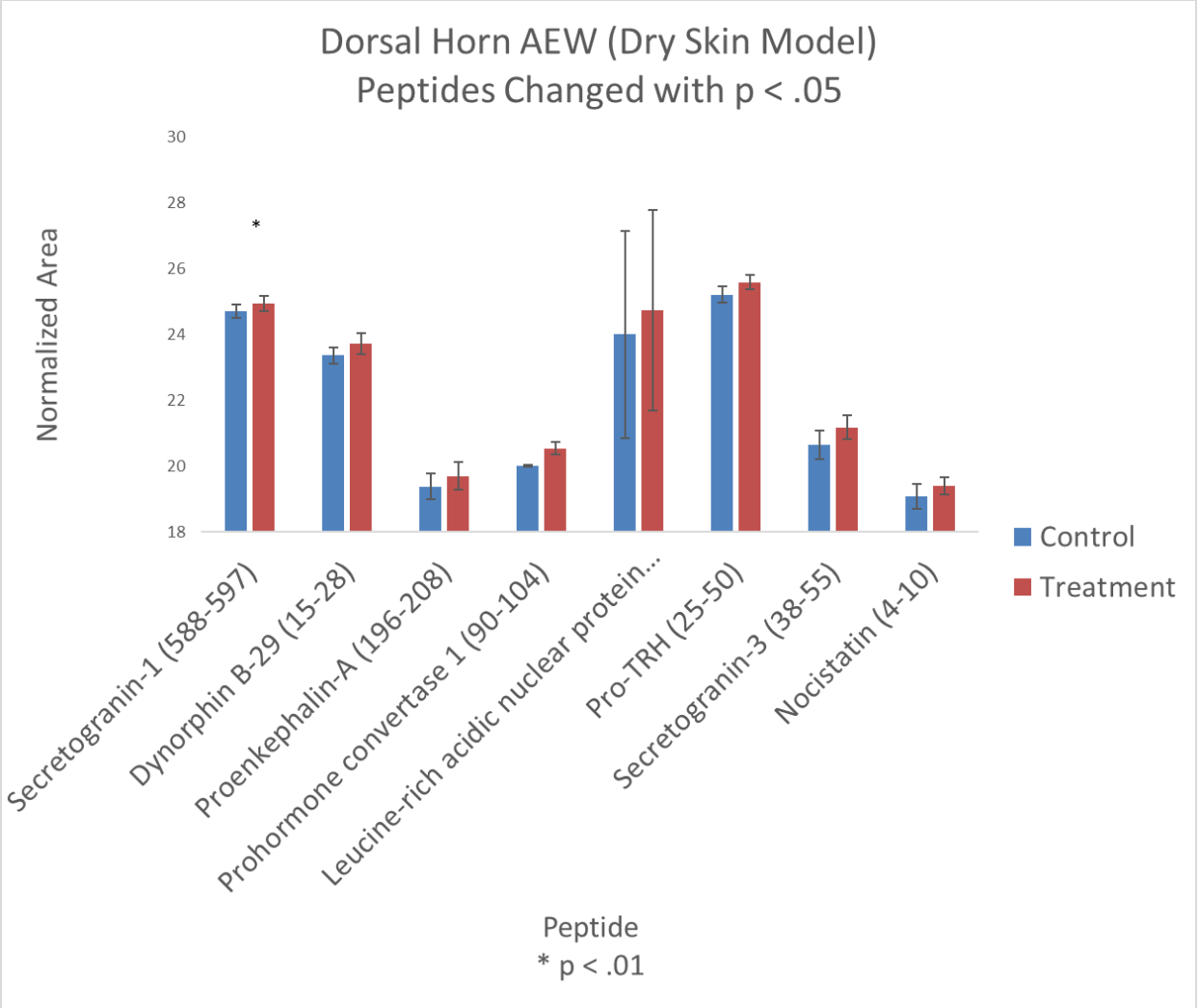

Figure 5.2: All statistically significantly changed peptides in the dorsal horn AEW model (normalized peak area is log2 transformed).

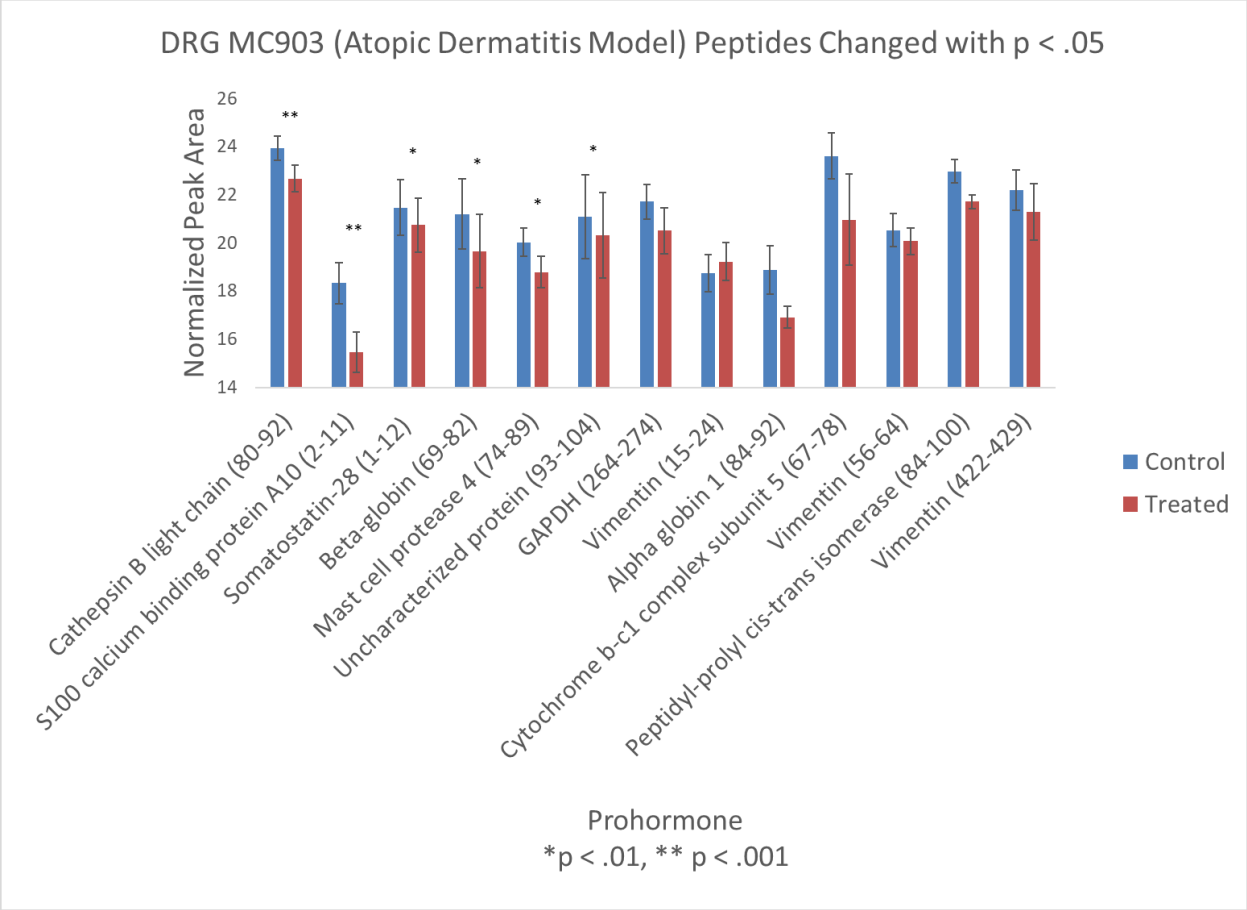

Figure 5.3: All statistically significantly changed peptides in the DRG MC903 model (normalized peak area is log2 transformed).

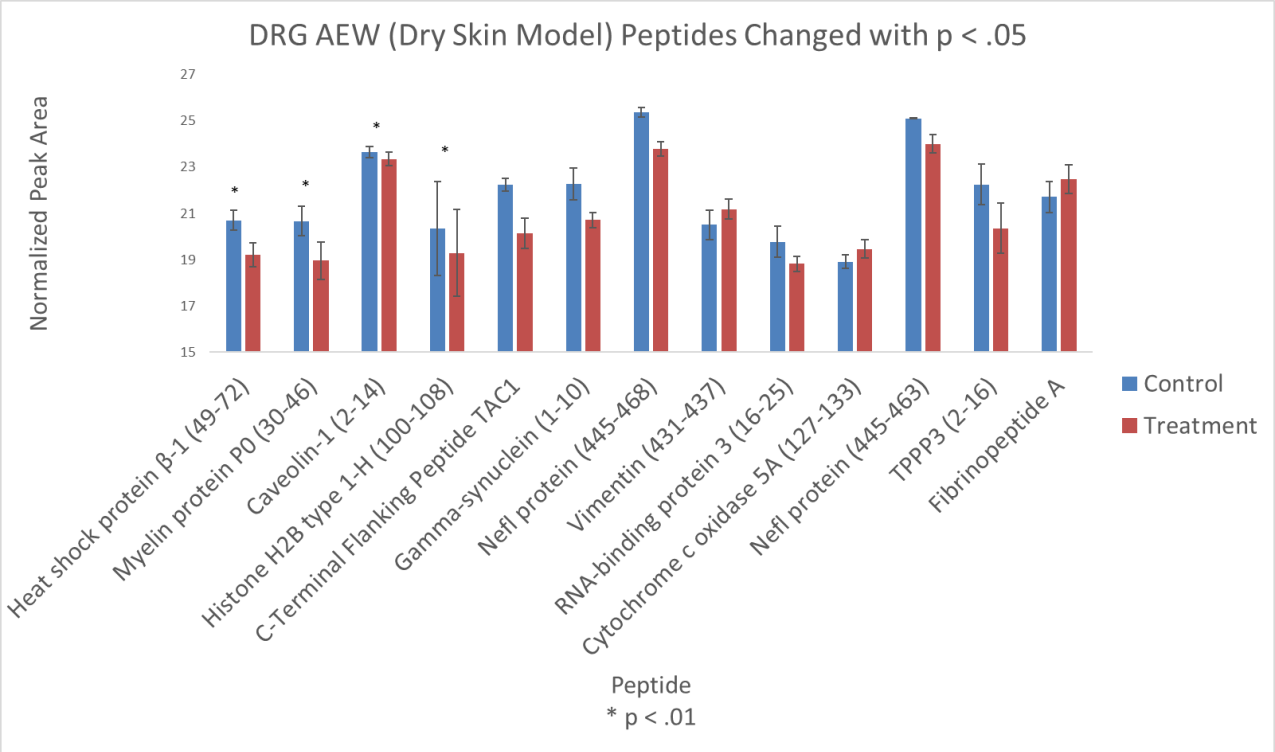

Figure 5.4: All statistically significantly changed peptides in the DRG AEW model (normalized peak area is log2 transformed).

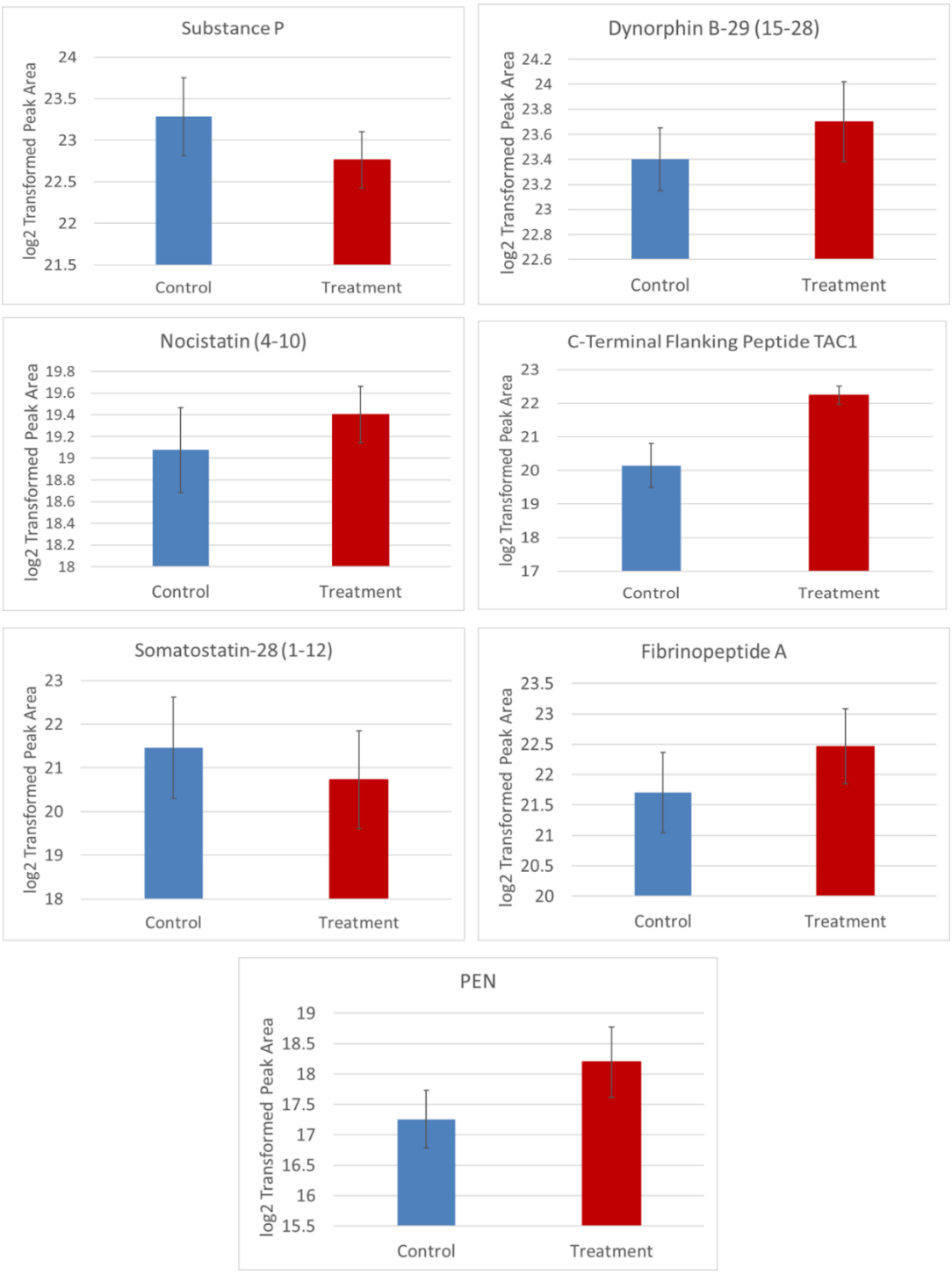

Figure 5.5: Changes in peptides that are classified as known neuropeptides between control and treatment models. Substance P is from DH MC903 model, dynorphin B-29 and nocistatin from DH AEW model, C-terminal flanking peptide, fibrinopeptide A, and PEN from DRG AEW model and somatostatin-28 from DRG MC903 model.

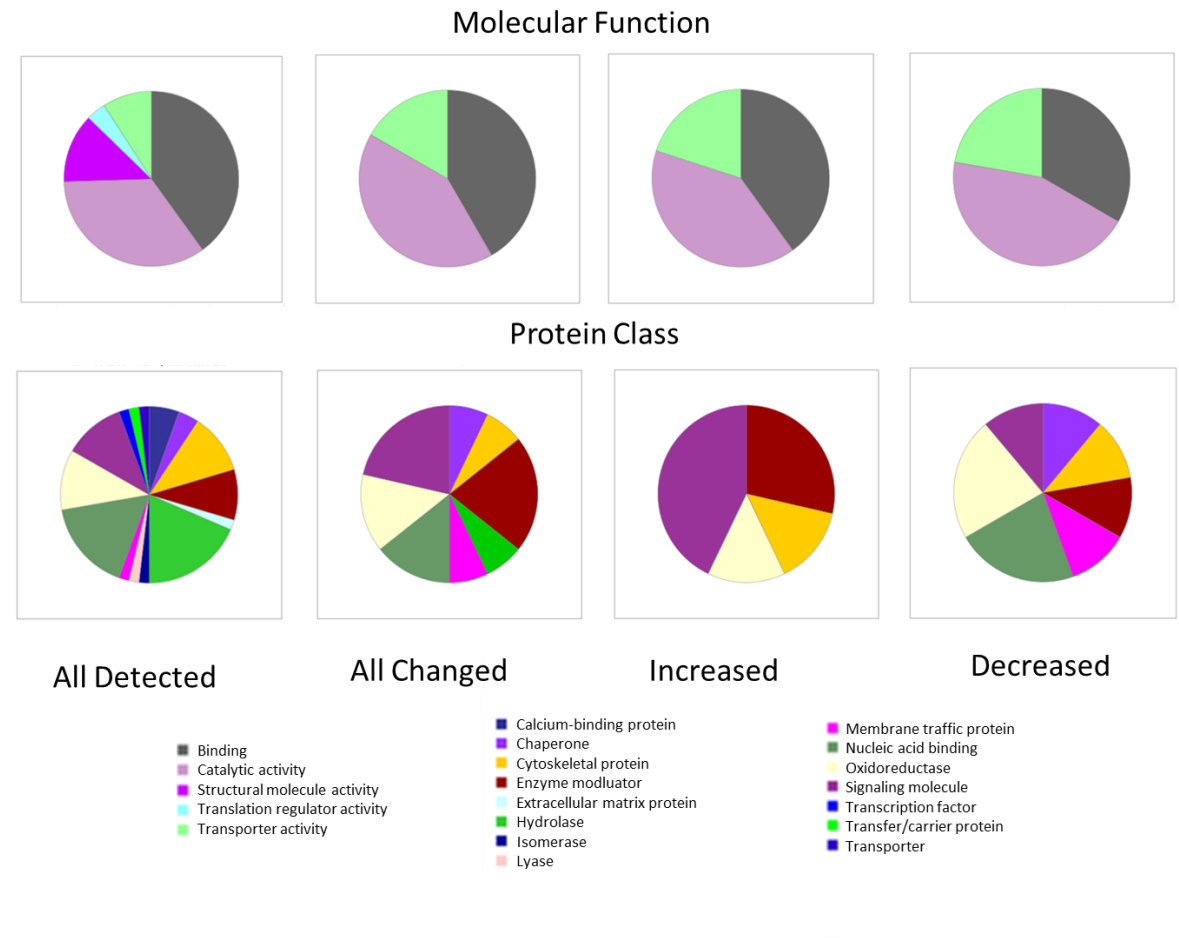

Figure 5.6: PANTHER Analysis of the proteins that all detected peptides are derived from (left column) , the proteins that all significantly changed peptides are derived from (2nd column), the proteins that all significantly increased peptides are derived from (3rd column), and the proteins that all significantly decreased peptides are derived from (right) as related to Molecular Function and Protein Class.

5.8 Tables

Mouse ID	Genotype	Sex	Treatment	Bouts of Scratching (30 min)			
				Day 5		Day 7	
				L Flank	R Flank	L Flank	R Flank
WT424	B6/J	F	AEW (L Flank)	X	X	107	62
WT442	B6/J	F	AEW (L Flank)	X	X	109	38
WT443	B6/J	F	AEW (L Flank)	X	X	37	10
WT421	B6/J	F	MC903 (R Flank)	0	55	X	X
WT422	B6/J	F	MC903 (R Flank)	2	90	X	X
WT423	B6/J	F	MC903 (R Flank)	18	7	X	X
WT450	B6/J	F	MC903 (R Flank)	0	1	X	X
WT451	B6/J	F	MC903 (R Flank)	0	0	X	X
WT452	B6/J	F	MC903 (R Flank)	0	3	X	X

Table 5.1: Scratch counts per side per animal.

Table 5.2 Peptide Changes in Mouse Itch Models							
Tissue	Model	Peptide Sequence	Average Normalized Areas		Pvalue	Protein ID	Peptide ID
DH			Control	Treated			
	AEW						
		SFARAPQLDL	24.7	24.9	0.007	Secretogranin-1	---
		SQENPNTYSEDLDV	23.4	23.7	0.012	Preprodynorphin:Proenkephalin-B	shortened form of dynorphin B-29
		V(+42.01)NPTVFF	21.5	22.1	0.012	peptidyl-prolyl cis-trans isomerase A	---
		RSPQLEDEAKELQ	19.4	19.7	0.031	Proenkephalin-A	part of the propeptide
		LSDDDRVTWAEQQYE	20.0	20.5	0.032	Neuroendocrine convertase 1	part of the propeptide
		M(+42.01)EMDKRIYLEL	24.0	24.7	0.033	Acidic leucine-rich nuclear phosphoprotein 32 family member A	---
		LLEAAQEEGAVTPDLPGLEKVQVRPE	25.2	25.6	0.039	thyrotropin releasing hormone preproprotein	---
		ELSAERPLNEQIAEAEAD	20.6	21.2	0.041	Secretogranin-3	---

Table 5.2: Peptides Changed in Mouse Itch Models

		VRSLVQV	19.1	19.4	0.047	Prepronociceptin	shortened form of nocistatin
	MC 903						
		PSSISWDGLDPGKLYTL	20.9	20.6	0.007	Phosphatidylethanolamine-binding protein 1	---
		LGALFNPYFDPLQWKNSDFE	23.4	23.8	0.010	Secretogranin-1	---
		A(+42.01)EDIKTKIKNY	21.5	20.7	0.020	Cytochrome C Oxidase subunit 6B1	---
		A(+42.01)SLKDLEGKWRL	21.6	21.4	0.025	Fatty acid-binding protein, epidermal	---
		A(+42.01)DKPDMGEIASFDKAKLKKTETQEKNTLPTKETIEQEK	18.9	18.5	0.034	Thymosin beta-10	---
		RPKPQQFFGLM(-.98)	23.3	22.8	0.043	Tachykinin 1	Substance P
		APSDPRLRQFLQKSLAAATGKQELAKFLAELLSEPNQTENDALEPEDLPQA	20.9	21.1	0.044	Somatostatin	antrin plus propeptide
DRG							
	AEW						
		SLKQTPLSR	18.4	18.0	0.002	Clathrin Light Chain	---

Figure 5.2 (cont)

		AAGWPGYVRPLPAATAEGPAAVTL	20.7	19.2	0.003	Heat shock protein beta-1	---
		IVVYTDREIYGAVGSQV	20.7	19.0	0.004	Myelin protein P0	---
		GKDFTPAAQAAFQKVVAGVAAALAHKYH	19.5	17.1	0.005	Beta-globin	---
		S(+42.01)GGKYVDSEGHLY	23.7	23.3	0.007	Caveolin-1	---
		RLLLPGELA	20.3	19.3	0.009	Histone H2B type 1-H	---
		NDIFERI	20.2	18.0	0.014	Histone H2B type 1-H	---
		ALNSVAYERSAMQNYE	22.2	20.1	0.015	Tachykinin 1	C- terminal flanking peptide
		M(+42.01)DVFKKGFSI	22.3	20.7	0.017	Gamma-synuclein	---
		TSHVQEEQTEVEETIEATKAEEAK	25.4	23.8	0.022	Nefl protein	---
		QELRPTLNELGISTPEELGLDKV	19.3	20.5	0.028	Cytochrome c oxidase subunit 5A, mitochondrial	---
		GEGILPDGGEYKPPSDS	20.3	19.0	0.035	Epsilon-Sarcoglycan splicing variant 3B	---
		LPLVDTH	20.5	21.2	0.036	Vimentin	---

Figure 5.2 (cont)

		NTDEQALEDHF	19.8	18.8	0.037	RNA-binding protein 3	---
		RPTLNEL	18.9	19.5	0.039	Cytochrome c oxidase subunit 5A, mitochondrial	---
		TSHVQEEQTEVEETIEATK	25.1	24.0	0.042	Nefl protein	---
		A(+42.01)ASTDIAGLEESFRKF	22.2	20.4	0.043	Tubulin polymerization-promoting protein family member 3	---
		TDTEDKGEFLSEGGGVR	21.7	22.5	0.047	Fibrinogen alpha chain	fibrinopeptide A
		SVDQDLGPEVPPENVLGALLRV	17.3	18.2	0.049	ProSAAS	PEN
	MC 903						
		LPETFDAREQWSN	23.9	22.7	0.001	Cathepsin B light chain	---
		PSQMEHAMET	18.3	15.5	0.001	S100 calcium binding protein A10	---
		SANSNPAMAPRE	21.5	20.7	0.001	Somatostatin	shortened form of Somatostatin-28
		ITAFNDGLNHLDSL	21.2	19.7	0.002	Beta-globin	---

Figure 5.2 (cont)

		NLDWGDNGF	17.9	18.6	0.006	Uncharacterized protein	---
		FQKVVAGVAA	21.1	20.9	0.007	Beta-globin	---
		TLGAHDVSKTESTQQK	20.0	18.8	0.007	Mast cell protease 4	---
		RVDPVNFKLLSH	21.1	20.3	0.008	Uncharacterized protein	---
		SHHPADFTPAVH	18.2	17.6	0.012	Uncharacterized protein	---
		SEGPLKGILGY	21.7	20.5	0.018	Glyceraldehyde-3-phosphate dehydrogenase	---
		FGGSGTSSRP	18.7	19.2	0.022	Vimentin	---
		M(+42.01)DIAIHH	19.0	17.4	0.026	Alpha-crystallin B chain	---
		LSDLHAHKL	18.9	16.9	0.027	Alpha globin 1	---
		TVGLNVPASVRF	23.6	21.0	0.040	Cytochrome b-c1 complex subunit Rieske, mitochondrial	---
		SNLHDIM	22.0	18.6	0.040	Mast cell protease 4	---
		SPGGAYVTR	20.5	20.1	0.044	Vimentin	---

Figure 5.2 (cont)

		EDENFILKHTGPGILSM	23.0	21.7	0.047	Peptidyl-prolyl cis-trans isomerase	---
		NLRETNLE	22.2	21.3	0.048	Vimentin	---

Figure 5.2 (cont)

Peptide Name	Region	Itch Model	Peptide Sequence	P-Values
Somatostatin-28 (1-12)*	DRG	MC903	SANSNPAMAPRE	0.001
Secretogranin-1 (588-597)	DH	AEW	SFARAPQLDL	0.007
Secretogranin-1 (516-535)	DH	MC903	LGALFNPYFDPLQWKNSDFE	0.010
Dynorphin B-29 (15-28)*	DH	AEW	SQENPNTYSEDLDV	0.012
C-Terminal Flanking Peptide TAC 1*	DRG	AEW	ALNSVAYERSAMQNYE	0.014
Proenkephalin A (196-208)	DH	AEW	RSPQLEDEAKELQ	0.031
Secretogranin-3 (38-55)	DH	AEW	ELSAERPLNEQIAEAEAD	0.041
Substance P*	DH	MC903	RPKPQQFFGLM(-.98)	0.043
Somatostatin (25-76)	DH	MC903	APSDPRLRQFLQKSLAAATGKQELAKYFLAEL LSEPNQTENDALEPEDLPQA	0.044
Nocistatin (4-10)*	DH	AEW	VRSLVQV	0.047
Fibrinopeptide A*	DRG	AEW	TDTEDKGEFLSEGGGVR	0.047
PEN*	DRG	AEW	SVDQDLGPEVPPENVLGALLRV	0.049

Table 5.3: List of peptides from known prohormones and/or known signaling molecules that were found to be significantly different in expression levels between the treated and the control itch model samples (* means known neuropeptide/signaling molecule).

Animal	**Treatment**	**Baseline Bouts of Scratching**		**Day 7 Bouts of Scratching**	
1-1	AEW (Right Side)	L: 2	R: 4	L: 2	R: 0
1-2	AEW (Right Side)	L: 4	R: 0	L: 15	R: 27
1-3	AEW (Right Side)	L: 0	R: 6	L: 8	R: 58
1-4	AEW (Right Side)	L: 0	R: 6	L: 37	R: 64
1-5	AEW (Right Side)	L: 2	R: 3	L: 5	R: 14
2-1	AEW (Left Side)	L : 0	R: 0	L: 50	R: 8
2-2	AEW (Left Side)	L: 1	R: 0	L: 82	R: 19
2-3	AEW (Left Side)	L: 0	R: 1	L: 1	R: 4
2-4	AEW (Left Side)	L : 0	R: 0	L: 5	R: 2
2-5	AEW (Left Side)	L: 1	R: 0	L: 117	R: 10
3-1	MC903 (Right Side)	L: 3	R: 0	L: 0	R: 33
3-2	MC903 (Right Side)	L: 0	R: 4	L: 2	R: 27
3-3	MC903 (Right Side)	L: 1	R: 2	L: 0	R: 26
3-4	MC903 (Right Side)	L: 1	R: 4	L: 0	R: 3
3-5	MC903 (Right Side)	L: 0	R: 2	L: 3	R: 17
4-1	MC903 (Left Side)	L : 6	R: 5	L: 61	R: 25
4-2	MC903 (Left Side)	L: 0	R: 0	L: 22	R: 13
4-3	MC903 (Left Side)	L: 2	R: 4	L: 98	R: 21
4-4	MC903 (Left Side)	L : 0	R: 3	L: 32	R: 2
4-5	MC903 (Left Side)	L: 10	R: 2	L: 64	R: 8

Table 5.4: Counts of scratching bouts in 30 minutes per treatment and side for second set of experiments.

5.9 Work Cited

1. Priestly, J., *Neuropeptides: Sensory Systems*, in *Encyclopedia of Neuroscience*, L.R. Squire, Editor. 2009, Academic Press: Oxford. p. 935-943.
2. Devor, M., *Unexplained peculiarities of the dorsal root ganglion.* Pain, 1999. **Suppl 6**: p. S27-35.
3. Strand, F.L., ed. *Neuropeptides: Regulators of Physiological Processes*. 1998, The MIT Press: Cambridge.
4. Maier, T., M. Güell, and L. Serrano, *Correlation of mRNA and protein in complex biological samples.* FEBS Letters, 2009. **583**(24): p. 3966-3973.
5. Wilhelm, M., et al., *Mass-spectrometry-based draft of the human proteome.* Nature, 2014. **509**(7502): p. 582-7.
6. Tillmaand, E.G., et al., *Peptidomics and Secretomics of the Mammalian Peripheral Sensory-Motor System.* J Am Soc Mass Spectrom, 2015.
7. Matterne, U., et al., *Incidence and determinants of chronic pruritus: a population-based cohort study.* Acta Derm Venereol, 2013. **93**(5): p. 532-7.
8. Akiyama, T. and E. Carstens, *Neural processing of itch.* Neuroscience, 2013. **250**: p. 697-714.
9. Han, L., et al., *A subpopulation of nociceptors specifically linked to itch.* Nat Neurosci, 2013. **16**(2): p. 174-182.
10. Dong, X., et al., *A diverse family of GPCRs expressed in specific subsets of nociceptive sensory neurons.* Cell, 2001. **106**(5): p. 619-32.
11. Liu, Q., et al., *Sensory neuron-specific GPCRs Mrgprs are itch receptors mediating chloroquine-induced pruritus.* Cell, 2009. **139**(7): p. 1353-1365.
12. Liu, Q., et al., *The distinct roles of two GPCRs, MrgprC11 and PAR2, in itch and hyperalgesia.* Sci Signal, 2011. **4**(181): p. ra45.
13. Liu, Q., et al., *Mechanisms of Itch Evoked by β-Alanine.* The Journal of Neuroscience, 2012. **32**(42): p. 14532-14537.
14. Andoh, T., et al., *Substance P induction of itch-associated response mediated by cutaneous NK 1 tachykinin receptors in mice.* Journal of Pharmacology and Experimental Therapeutics, 1998. **286**(3): p. 1140-1145.
15. Katugampola, R., M.K. Church, and G.F. Clough, *The neurogenic vasodilator response to endothelin-1: a study in human skin in vivo.* Experimental Physiology, 2000. **85**(06): p. 839-846.

16. Trentin, P.G., et al., *Endothelin-1 causes pruritus in mice.* Exp Biol Med (Maywood), 2006. **231**(6): p. 1146-51.
17. Sukhtankar, D.D. and M.-C. Ko, *Physiological Function of Gastrin-Releasing Peptide and Neuromedin B Receptors in Regulating Itch Scratching Behavior in the Spinal Cord of Mice.* PLoS One, 2013. **8**(6): p. e67422.
18. Rogoz, K., et al., *Multimodal use of calcitonin gene-related peptide and substance P in itch and acute pain uncovered by the elimination of vesicular glutamate transporter 2 from transient receptor potential cation channel subfamily V member 1 neurons.* J Neurosci, 2014. **34**(42): p. 14055-68.
19. Kardon, Adam P., et al., *Dynorphin Acts as a Neuromodulator to Inhibit Itch in the Dorsal Horn of the Spinal Cord.* Neuron, 2014. **82**(3): p. 573-586.
20. Usoskin, D., et al., *Unbiased classification of sensory neuron types by large-scale single-cell RNA sequencing.* Nat Neurosci, 2015. **18**(1): p. 145-153.
21. Miyamoto, T., et al., *Itch-Associated Response Induced by Experimental Dry Skin in Mice.* The Japanese Journal of Pharmacology, 2002. **88**(3): p. 285-292.
22. Akiyama, T., M.I. Carstens, and E. Carstens, *Enhanced scratching evoked by PAR-2 agonist and 5-HT but not histamine in a mouse model of chronic dry skin itch.* PAIN®, 2010. **151**(2): p. 378-383.
23. Nojima, H., et al., *Spinal c-fos expression associated with spontaneous biting in a mouse model of dry skin pruritus.* Neuroscience Letters, 2004. **361**(1): p. 79-82.
24. Schüttenhelm, B.N., et al., *Differential Changes in the Peptidergic and the Non-Peptidergic Skin Innervation in Rat Models for Inflammation, Dry Skin Itch, and Dermatitis.* Journal of Investigative Dermatology, 2015. **135**(8): p. 2049-2057.
25. Li, M., et al., *Topical vitamin D3 and low-calcemic analogs induce thymic stromal lymphopoietin in mouse keratinocytes and trigger an atopic dermatitis.* Proceedings of the National Academy of Sciences, 2006. **103**(31): p. 11736-11741.
26. Choi, J., et al., *The Atopic Dermatitis-Like Symptoms Induced by MC903 Were Alleviated in JNK1 Knockout Mice.* Toxicological Sciences, 2013. **136**(2): p. 443-449.
27. Mark, B. and L.D.Y. M., *Atopic dermatitis: a disease of altered skin barrier and immune dysregulation.* Immunological Reviews, 2011. **242**(1): p. 233-246.
28. Moosbrugger-Martinz, V., M. Schmuth, and S. Dubrac, *A Mouse Model for Atopic Dermatitis Using Topical Application of Vitamin D3 or of Its Analog MC903*, in *Inflammation: Methods and Protocols*, B.E. Clausen and J.D. Laman, Editors. 2017, Springer New York: New York, NY. p. 91-106.

29. Schilling, B., et al., *Platform-independent and Label-free Quantitation of Proteomic Data Using MS1 Extracted Ion Chromatograms in Skyline*. Vol. 11. 2012. 202-14.
30. MacLean, B., et al., *Skyline: an open source document editor for creating and analyzing targeted proteomics experiments.* Bioinformatics, 2010. **26**(7): p. 966-968.
31. Chawade, A., E. Alexandersson, and F. Levander, *Normalyzer: A Tool for Rapid Evaluation of Normalization Methods for Omics Data Sets.* Journal of Proteome Research, 2014. **13**(6): p. 3114-3120.
32. Mi, H., A. Muruganujan, and P.D. Thomas, *PANTHER in 2013: modeling the evolution of gene function, and other gene attributes, in the context of phylogenetic trees.* Nucleic Acids Research, 2013. **41**(Database issue): p. D377-D386.
33. Thomas, P.D., et al., *PANTHER: A Library of Protein Families and Subfamilies Indexed by Function.* Genome Research, 2003. **13**(9): p. 2129-2141.
34. Xu, X.-J. and Z. Wiesenfeld-Hallin, *Neuropeptides: Pain*, in *Encyclopedia of Neuroscience*, L.R. Squire, Editor. 2009, Academic Press: Oxford.
35. Squire, L., et al., eds. *Fundamental Neuroscience*. Third ed. 2008, Elsevier.
36. Akiyama, T., et al., *Roles of glutamate, substance P, and gastrin-releasing peptide as spinal neurotransmitters of histaminergic and nonhistaminergic itch.* PAIN®, 2014. **155**(1): p. 80-92.
37. M., T., et al., *Nerve growth factor and substance P are useful plasma markers of disease activity in atopic dermatitis.* British Journal of Dermatology, 2002. **147**(1): p. 71-79.
38. Kuraishi, Y., et al., *Evidence that substance P and somatostatin transmit separate information related to pain in the spinal dorsal horn.* Brain Research, 1985. **325**(1–2): p. 294-298.
39. Stantcheva, K.K., et al., *A subpopulation of itch-sensing neurons marked by Ret and somatostatin expression.* EMBO reports, 2016. **17**(4): p. 585-600.
40. Huang, J., et al., *Circuit dissection of the role of somatostatin in itch and pain.* Nature Neuroscience, 2018. **21**(5): p. 707-716.

Chapter 6

Characterization of Neuropeptide Release from Dorsal Root Ganglion Neurons upon Chemical Stimulation

6.1 Notes

Throughout the project described in this chapter, Ashley Lenhart worked diligently to improve our sample preparation methods for neuropeptide detection and helped with the stimulations and sample preparation. Krishna Anapindi helped with LC-MS/MS analysis and provided great insights on peptide detection, Jeff Guo at the Liu Lab at Washington University in St. Louis helped with calcium imaging of experiments, Dr. Stanislav Rubakhin helped with DRG dissections, Yujin Lee helped with cell culture, and Dr. Thanh Do provided encouragement and revived my search for substance P by helping with the tissue homogenate samples.

6.2 Introduction

The initial goal of this project was to detect and characterize a wide range of neuropeptides released from sensory neurons in a spatially and temporally relevant manner. Matrix-assisted laser desorption/ionization time of flight (MALDI-TOF) mass spectrometry (MS) was chosen due to its ability to provide quick and accurate information about chemicals detected in the peptide mass range without a need for large sample sizes or targeted analysis [1-3]. Unfortunately, we have been unable to detect known neuropeptides released from cultured sensory neurons in this manner [4]. What follows is our attempt to rectify this issue.

To address the difficulty of detecting the pico-femtomolar concentration of neuropeptide within the release samples, one of the most well-known neuropeptides in the sensory

nervous system, substance P, was used as a goal for detection. Substance P is a peptide that is released both peripherally and centrally in response to changes in pH, temperature, cytokine activity, and other inflammatory responses which sensitizes the neurons upon which it acts [5-7]. Substance P has been detected via immune-based assays in releasates from sensory neurons upon high potassium activation [8-10] and, therefore, should be detected upon high potassium stimulation of our DRG cell cultures. This chapter outlines a series of changes implemented to our procedures and protocols to troubleshoot the detection of substance P in released samples. Multiple methods were employed, with one aim to ensure correct stimulation and sampling protocols and the other aim to improve detection of substance P using standards. Toward the first aim, calcium imaging was implemented to verify stimulation of the cells, cell culture amounts were increased, immunostaining was used to verify the presence of substance P, and release and homogenized samples were analyzed using MALDI, liquid chromatography (LC)-MS/MS and enzyme-linked immunosorbent assay (ELISA). Toward the second aim, a series of dilutions of substance P standard in water and cell culture media were performed, solid phase extraction parameters were tested, and new matrix application techniques were employed.

6.3 Experimental

6.3.1 DRG Cell Dissociation and Seeding

Dorsal Root Ganglia (DRG) were isolated from adult or neonatal rats and sustained in a bath of ice cold Hibernate A (BrainBits Springfiled, IL) for up to 24 h before dissociation. For postnatal day 2-5 rats, DRG were digested in a solution of 0.2% type II collagenase and 0.6% protease in DRG serum-free media containing Neurobasal A without phenol

red (Life Technologies Carlsbad, CA), 100 U/mL penicillin/streptomycin (Life Technologies), 0.5 mM GlutaMAX (Life Technologies), 50 ng/mL NGF (Life Technologies), 50 ng/mL BDNF (Prospec Bio Rehovot, Israel), and 500 µL B27 Growth Supplement (Life Technologies) for 30 min at 37 ºC. After digestion, the samples were subjected to centrifugation for 2-3 min at 200 *xg*. The supernatant was removed, and the pellet washed with Hank's Balanced Salt Solution (HBSS) (Life Technologies). Upon centrifugation using the same parameters, the supernatant was removed and the pellet triturated using fire-polished pipets. Following trituration, the supernatant was removed and centrifuged after the debris was allowed to settle at the bottom of the tube. After centrifugation, the supernatant was removed and the pellet washed with HBSS. A final centrifugation was performed after which the pellet was resuspended in 200 µL of media and 20 µL of cell suspension was added to the cell seeding well of a device treated with poly-D-lysine (BD Biosciences Franklin Lakes, NJ) and Laminin and incubated for 30 min at 37 ºC. If appropriate, the device is tilted to enhance movement of cells toward the microchannels. After 30 min, all wells were filled with 150 µL of media. The cells were incubated at 37 ºC, with a media change at 24 h and then every 3 d until needed for experiments.

For adult rats, DRGs were digested in a solution of 0.25% collagenase (Worthington Biochemical Corp, Lakewood, NJ, USA) in DRG cell culture media for 1.5 h at 37 ºC. After digestion, the samples were treated the same as the neonatal rat samples, with the final cell pellet being resuspended in 1 mL of DRG cell culture media per 10 original DRG.

6.3.2 Chemical Stimulation for Release

To stimulate nonspecific peptide release from DRG cells, cell culture media with 60mM K^+ was used, rather than the normal 5mM K^+ that is present in the cell culture media. First, a control sample consisting of the media in which the cells were incubated was collected. Next, fresh media was added through the inlet port and the cells were incubated at 37 °C for 5 min. After incubation, that media was removed through the outlet port, creating a wash sample. Next, media containing 60 mM KCl was added to the cells. After 5 min, the high potassium media was removed and labeled the stimulation sample. A final wash of media was added to the cells and collected as the post-stimulation sample 5 min after addition to the cells (Figure 6.1).

To stimulate nonspecific peptide release from DRG cells cultured in standard dishes, the same media stimulation steps were used, except the media was carefully added and removed as bath stimulations rather than flown through the inlet and outlet ports. Additionally, a few experiments were performed in which one set of cells were not stimulated at all. These samples were used as a non-stimulation sample.

6.3.3 Calcium Imaging of Stimulated Cells

DRG cells were cultured for 24 h and then washed with calcium imaging buffer (in mM: 130 NaCl, 3 KCl, 0.6 MgCl2, 10 HEPES, 10 Glucose, 1.2 NaHCO3, 2.5 CaCl2, ~290 mOsm, pH 7.4) twice before incubation with Fura2-AM for 30 min. After incubation, the cells were washed twice and then stimulated with 60 mM KCl in both calcium imaging buffer and DRG culture media. The 340/380 ratio was captured on an inverted Nikon TI-E microscope.

6.3.4 Immunofluorescent Imaging of Cultured Cells

DRG media was replaced with a 4% paraformaldehyde (Ted Pella, CA) fixation bath at room temperature for 15-20 min. The cells were then washed with PBS (Life Technologies Carlsbad, CA) five times, with the last wash lasting five min with shaking. 0.25% Triton X (Sigma-Aldrich St. Louis, MO) was added to the cells for 10 min to permeabilize the membranes. A wash was performed and a blocking solution of 5% normal goat serum (NGS) (Life Technologies) in PBS was added for 30 min for dish cultures and 1 h for devices with shaking. Another wash step was performed and the primary antibody in a 2% NGS solution was added and incubated overnight at 4 ºC. After incubation, a wash was performed, and the second primary antibody was added and incubated overnight. After that incubation, another wash was performed and the secondary antibody in a 2% NGS solution was added to the culture for 1-2 h. If 4',6-Diamidino-2-Phenylindole, Dihydrochloride (DAPI) was used, the culture was rinsed and DAPI added to the culture and incubated for 20 min. Finally, the cells were subjected to a final wash step, rinsed with DI water for 30 s, and mounted with ProLong Gold Antifade (Life Technologies) onto a glass slide. If not visualized immediately, the slides were kept in the dark at 4 ºC until imaging with a Zeiss Axio Imager M2 (Carl Zeiss AG, Oberkochen, Germany). Primary Antibodies: Substance P polyclonal antibody (Enzo Life Sciences), β3 tubulin monoclonal antibody (Santa Cruz Biotechnology), and DAPI nuclear stain (Thermo Fisher Scientific). Secondary antibodies: Alexa Fluor (Life Technologies) goat antibodies with excitation maxima of 488 and 594, 20 µg/mL.

6.3.5 Released Sample Preparation for MALDI MS

Samples were processed via a series of desalting and concentrating steps using Zip Tip C18 pipet tips (Millipore, Billerica, MA) and eluted onto a ground steel MALDI target (Bruker Daltonics Inc., Billerica, MA) with 75% ACN/0.1% TFA solution, as outlined in a previous publication [4]. Initially, final eluted samples were combined on the MALDI target in a 1:1 ratio of DHB using a dry droplet method. To improve analyte detection, dilutions of a peptide standard were subjected to various matrix application methods, including sample:DHB ratios of 5:1 and 10:1, changing the matrix to α-Cyano-4-hydroxycinnamic acid (CHCA), and implementing a triple layer MALDI matrix application which consists of first applying CHCA in a thin layer, allowing it to crystalize, applying it in a dried droplet form, adding the sample, and washing the sample with cold, acidified water once it has dried.

6.3.6 Released Sample Preparation for LC-MS and ELISA

200 µL of sample were removed per dish per sample set and immediately acidified using 10% volume of 5% TFA in water. The samples were kept on ice until all samples were collected, after which they were spun down to remove any solid debris and then dried using a SpeedVac concentrator. After drying, the samples were re-suspended in a 98:2 water:ACN with 0.1% FA and 0.01% TFA solution, vortexed vigorously, and spun again to remove any remaining solid debris. The supernatant was taken and desalted with 95:5 water:ACN with 0.1% FA and 0.01% TFA solution using a pre-equilibrated C18 spin column. The sample was then eluted twice with 50:50 water:ACN with 0.1% FA and 0.01% TFA and three times with 30:70 water:ACN with 0.1% FA and 0.01% TFA. After elution, the samples were once again dried in a SpeedVac concentrator. For LC-

triplequadrupole(QQQ)-MS analysis, the samples were re-suspended in 20 µL 50:50 ACN:water solution with 1% FA. For ELISA analysis, the samples were re-suspended in 50 µL assay buffer and the ELISA methods were carried out according to the manufacturer's instructions.

6.3.7 Homogenized Sample Preparation for MALDI-TOF, LC-MS and ELISA

Homogenized sample preparation followed a previously published protocol [11]. Briefly, 200 µL of ice-cold acidified methanol (90% methanol, 9% water, 1% HCL) were added to each cell culture dish. The cells were scraped and rinsed twice using additional ice-cold acidified methanol, then added to a conical tube and kept on ice until all dishes in the sample set were harvested. The samples were then subjected to homogenization, separated into 200 µL aliquots and dried via a SpeedVac concentrator. After drying, the samples were re-suspended in 98:2 water:ACN with 0.1% FA and 0.01% TFA and prepared for LC-MS and ELISA analysis as indicated above. For MALDI analysis, the dried sample was mixed with 50 mg/mL 2,5-dihydrobenzoic acid (DHB) in 50:50 ethanol:water with 1% TFA and spotted onto a ground steel MALDI plate for analysis.

6.3.8 MALDI-TOF Analysis

A select group of samples were analyzed using an ultrafleXtreme TOF mass spectrometer (Bruker Daltonics). Mass calibration is performed using peptide calibration standard II (Bruker Daltonics). Individual mass spectra were analyzed with flexAnalysis (version 3.3, Bruker Daltonics).

6.3.9 LC-MS Analysis

Samples were analyzed with a UHPLC system coupled with an EVOQ QQQ-MS (Bruker Daltonics, Billerica, MA, USA). For separation, Solvents A and B were water/0.1% FA and

ACN/0.1% FA respectively. The gradient for elution was 5% B for 0-1 min, increased to 85% B for 1-8 min, 85% B for 8-9 min, decreased to 5% B for 9-10 min, and 5% for 10-12 min at a 500 µL flow rate.

6.3.10 ELISA Analysis

A Substance P competitive ELISA kit (Enzo Life Sciences, Farmingdale, NY) was used according to the manufacturer's instructions. The 405 wavelength was read using an Epoch plate reader (BioTek, Winooski, VT, USA) without correction, and the standard curve was fitted with the appropriate nonlinear or polynomial regression using Gen5 software (BioTek, Winooski, VT, USA). Sample concentrations were calculated based on the best fit curve, usually a non-linear 5PL, 4PL regression or second order polynomial.

6.4 Results

6.4.1 DRG Cell Culture

Neonatal rat DRGs were successfully dissociated, seeded, and cultured within various microfluidic devices (Figure 6.2). Neonatal and adult rat DRGs were successfully dissociated, seeded, and cultured within cell culture dishes.

6.4.2 High Potassium Stimulation of Cells in Dishes and Microfluidic Devices

High potassium stimulation of cells dissociated from adult and neonatal rat DRG resulted in calcium influx into the cells as shown by calcium imaging, both in normal bath culture stimulations as well as when stimulation media was flown across both axons and cell bodies within microfluidic devices (Figure 6.3). Additionally, stimulation with capsaicin resulted in calcium influx into the correct subset of small-diameter sensory neurons, validating that the cell culture contains nociceptive TRPV1 neurons, which would release substance P upon activation (Figure 6.3) [7].

6.4.3 Detection of Substance P in Homogenized DRG Tissue, Cultured DRG Cells, and Release Samples

Substance P was detected in cultured DRG cells via immunofluorescent imaging (Figure 6.4), LC-QQQ-MS analysis, and ELISA. Substance P was also detected in homogenized DRG tissue via LC-QQQ-MS analysis, ELISA, and MALDI-TOF analysis (Figure 6.5).

Two sets of stimulation experiments were performed using microfluidic devices and analyzed via ELISA and MALDI MS. The first experiment pooled 9 sets of samples while the second pooled 16. In both experiments, the MALDI analysis showed no identifiable substance P peak, whereas the ELISA did provide results (Table 6.1, Figure 6.6). The stimulation sample had the highest concentration of substance P with 4.9 pg/mL and 4.5 pg/mL, respectively. Both controls contained no substance P, washes contained 2.3 pg/mL and 2.9 pg/mL, respectively, and post sample contained 0 and 1.3 pg/mL, respectively. Due to the low concentrations of these release samples, further experiments were performed with larger cell amounts and with glass bottomed dishes, which allow for more complete sample collection. One set of these results shows control and stimulation samples containing similar amounts of SP (448 and 375 pg/mL, respectively), while the other shows control, stimulation, and post samples as exceeding the amount detectable by the assay (>10,499 pg/mL). Encouragingly, the wash, blank, and no stimulation samples (Figures 6.6 and 6.7) show low concentrations of substance P, except for in one instance in which the wash may have stimulated the cells, while the cell homogenate sample contains five times the amount of substance P as the stimulation sample for that experiment.

LC-QQQ-MS analysis shows similar signal intensity of substance P for all stimulation samples (in the hundreds of counts per second), with a ten-fold increase in intensity for the substance P detected in the cellular homogenate (Figure 6.8).

6.4.4 Detection of Substance P Standard Dilutions using MALDI MS

Substance P standard solutions were best detected using a triple-layer CHCA matrix application method with a cold, acidified water wash of the sample (Figure 6.9). They were not detected in media samples, even when detected in water samples diluted at the same time (Figure 6.10A and B). SPE did improve detection of substance P standards diluted with cell culture media, but not with water (Figure 6.10C and D).

6.5 Discussion and Future Directions

While it is unfortunate that we are yet unable to detect substance P in DRG release samples using MALDI MS, the data show that our cells do contain substance P, are being stimulated by our stimulation paradigms, and do release substance P in a detectable amount upon 60 mM K^+ stimulation. We have targeted detection of substance P using QQQ-MS but have not been able to detect appropriate levels allowing for quantitation. While an obvious solution to this issue would be to increase sample amount, the eventual goal is to be able to detect release within small, specialized cell culturing systems. Therefore, sampling from ever-increasing amounts of cells does not seem like the best way forward.

We have used multiple improvements to our sample preparation techniques for MALDI MS with the goal of detecting substance P (and, hopefully, other neuropeptides) at a physiologically relevant concentration. Through performing serial dilutions of a standard, we began simply, with diluted standard in water using our standard detection methods

with DHB in a 1:1 ratio. We quickly learned that this was not the best method for detection of substance P in our samples and tried a variety of matrix applications before settling on the triple layer CHCA application method.

Since the actual cell release samples are not diluted in water but are instead collected within cell culture media, the next step was to test the detection of the standard dilutions in cell culture media. As expected, the salt content of the media masked the substance P in the samples, which was only detected after application of a solid phase extraction method, Zip Tipping the samples. However, the Zip Tipping of the samples only resulted in the detection of the standard at the highest concentration, leading us to believe that too much sample was being lost during the Zip Tip procedure itself. To curb sample loss during Zip Tipping, we decided to use a nonspecific blocking agent, bovine serum albumin, to block any surface that the sample came into contact with to decrease nonspecific or irreversible binding of the analyte to the various surfaces within the experiment. Unfortunately, this blocking step did not help with the analyte detection.

While our current technology does not allow us to effectively use mass spectrometry for untargeted detection of neuropeptides released from sensory neurons in a spatially relevant manner, we are encouraged by the robustness of our current cell culture model to behave as expected. Once we gain the ability to detect expected neuropeptides at physiologically relevant levels, it should be straightforward to apply the sample preparation and detection methods to the sampling protocols to look for spatial differences in peptide release from the devices, differences in peptide release in cells co-cultured with skin and/or spinal cord cells, and differences in peptide release based on pruritogen stimulation.

6.6 Figures

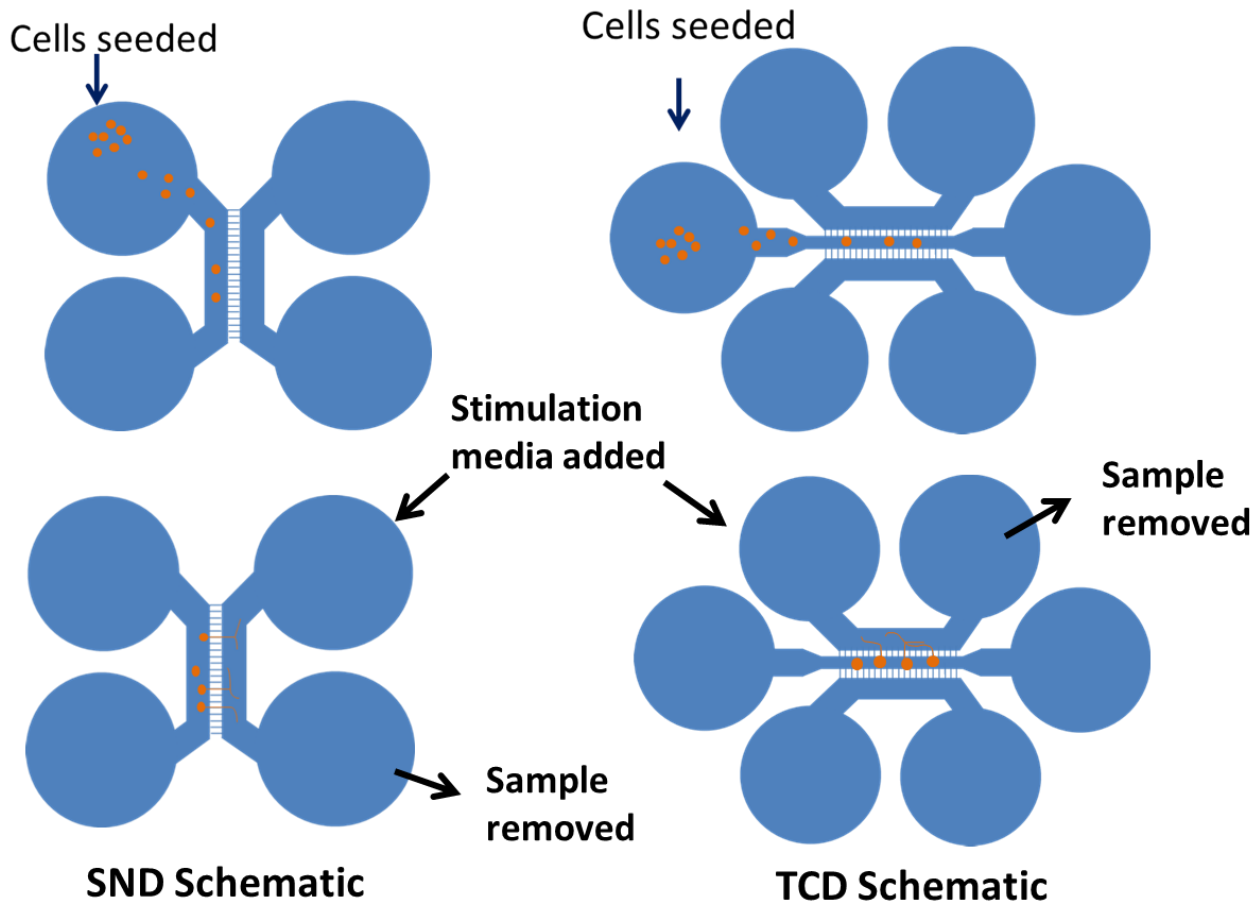

Figure 6.1: Microfluidic device schematics with explanation of seeding and sampling locations.

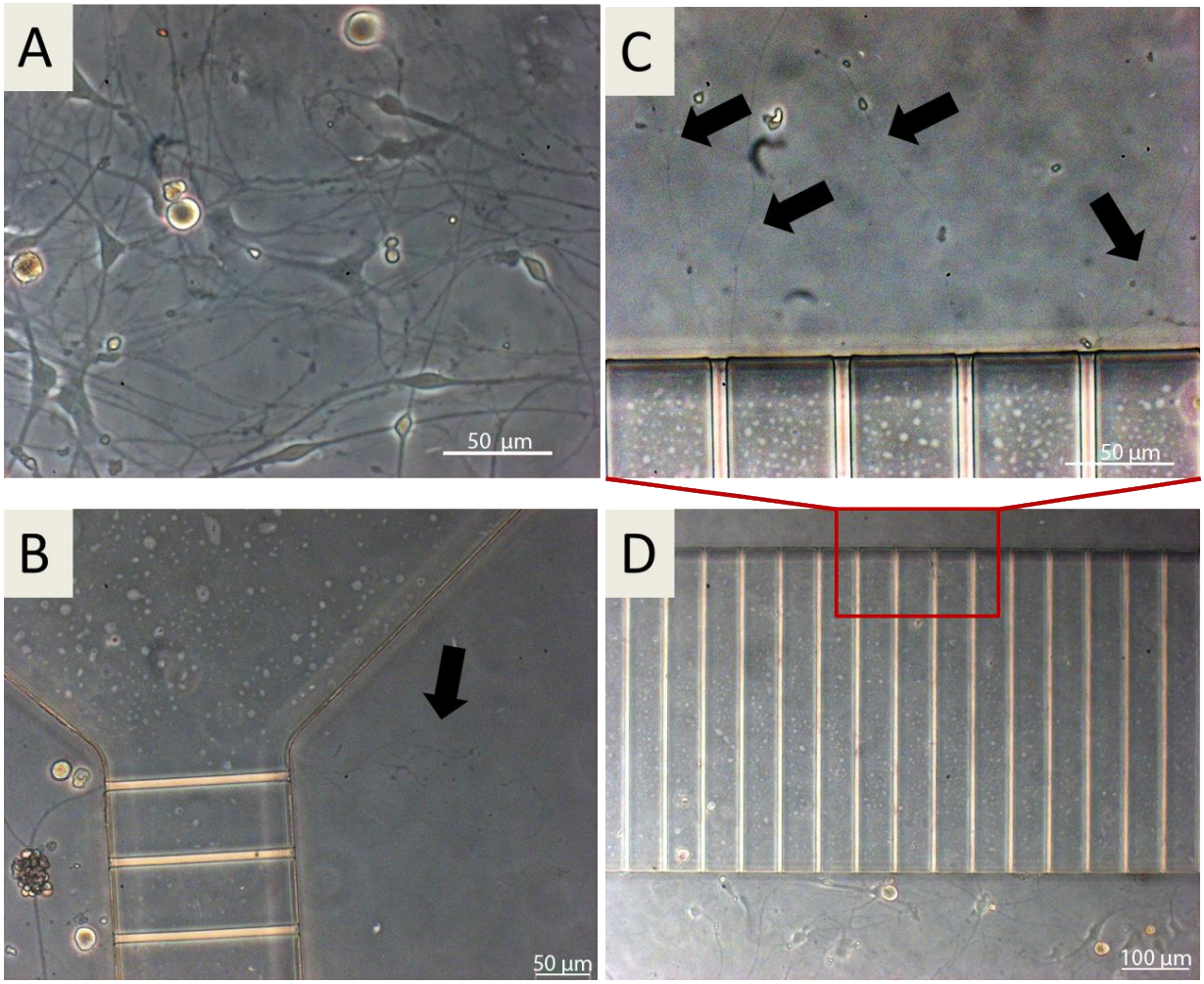

Figure 6.2: DRG cells were successfully cultured in microfluidic devices. A: DRG cells in the cell culture well of an SND150, DIV 7. B: SND150 with axons crossing through the microchannels to the axon side (black arrow). C: axons (black arrows) can be seen crossing through the microchannels in the TCD500, DIV 7. D: cell seeding channel of the TCD500 with microchannels.

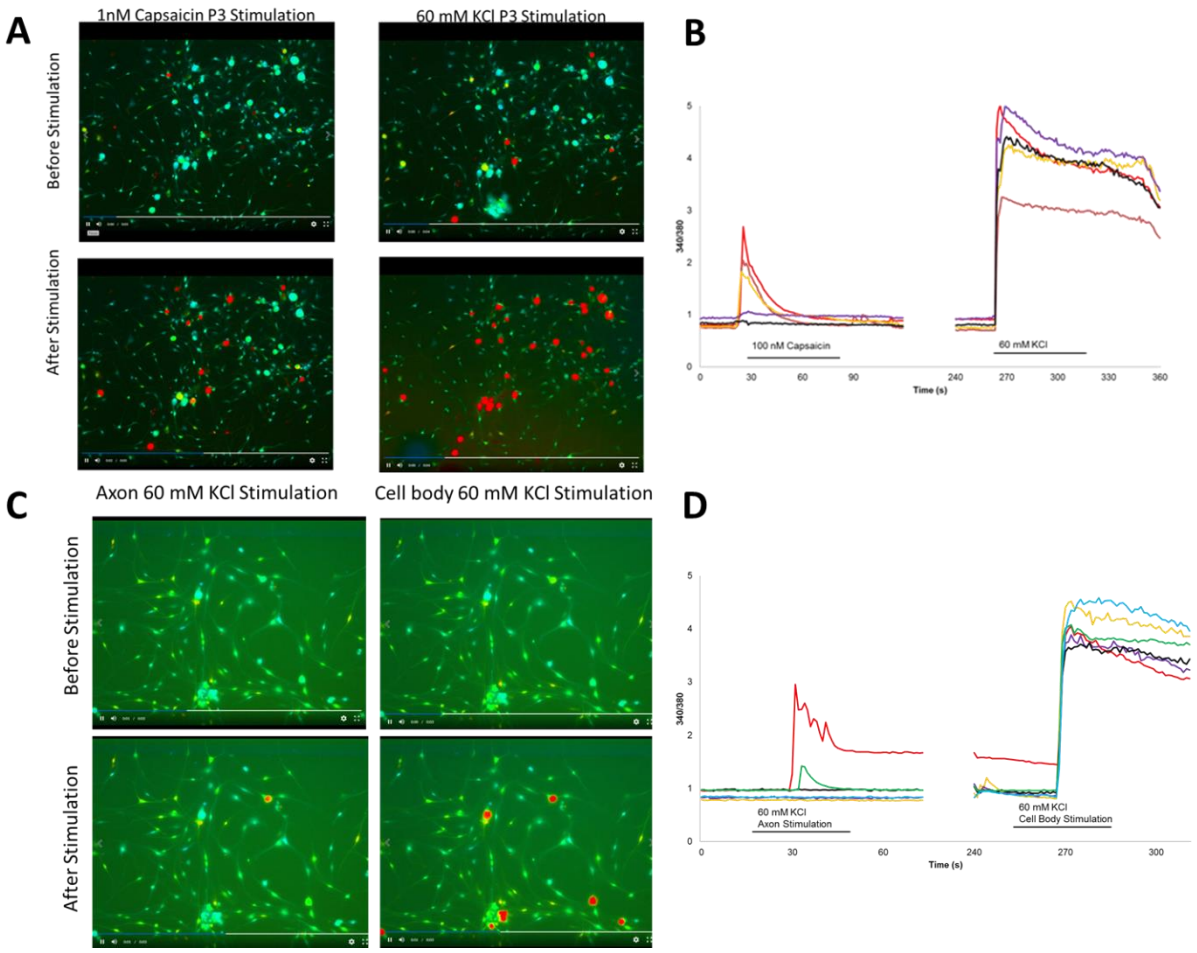

Figure 6.3: Calcium imaging of adult and P3 DRG cells cultured after 24 hours. A: appropriate sensory neuron stimulation via 1nM capsaicin versus 60 mM KCl, red denotes calcium influx into the cell. B: plot of 340/380 ratio over time for specific neuronal cell bodies. C and D: stimulation of axonal side of microfluidic device, led to activation of two sensory neuron cell bodies. Stimulation of cell body side of the device activated all neuronal cell bodies.

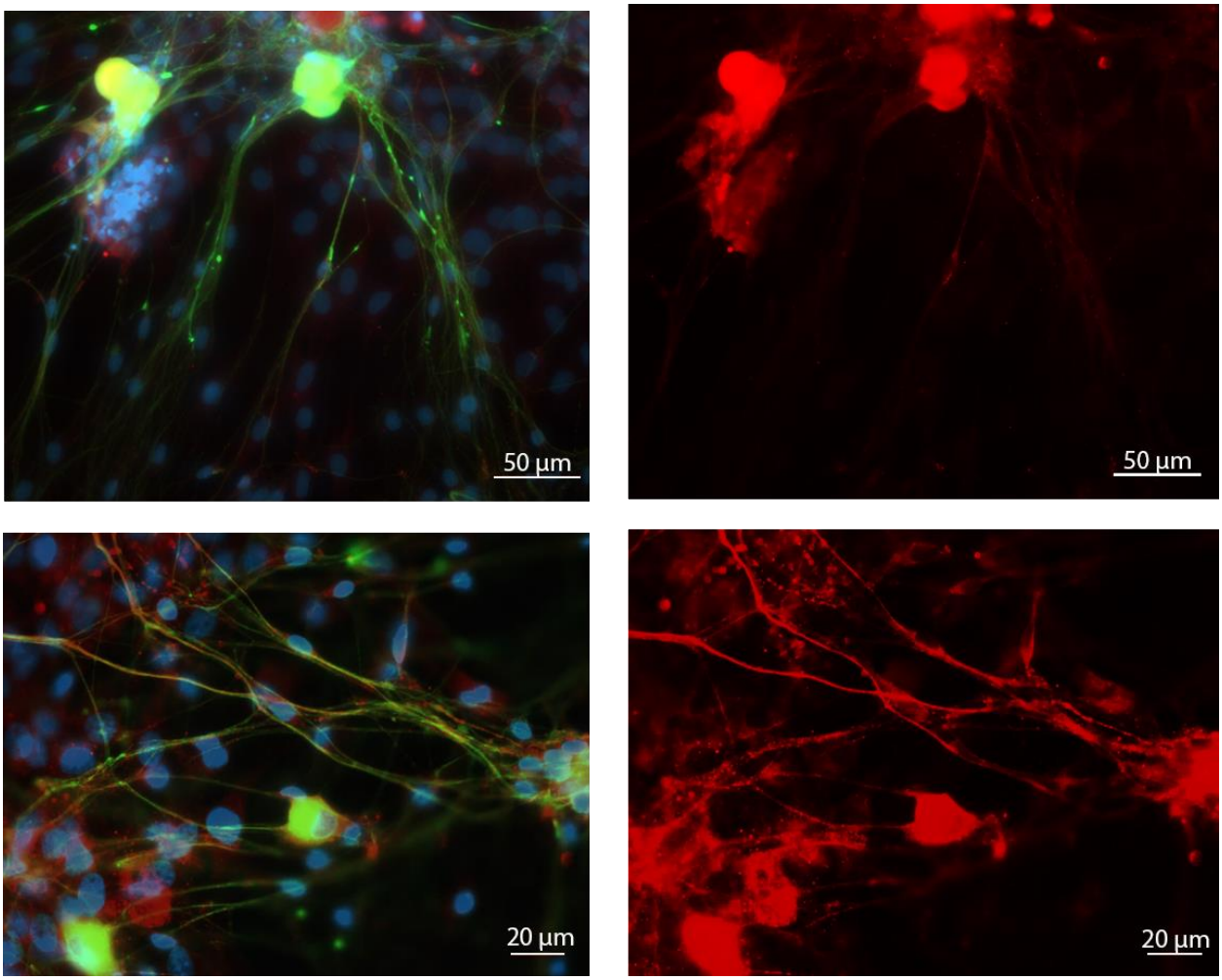

Figure 6.4: Immunofluorescent staining of DRG cells in culture. Red: substance P; Green: β3 tubulin (neuronal marker); Blue: DAPI (nuclear stain).

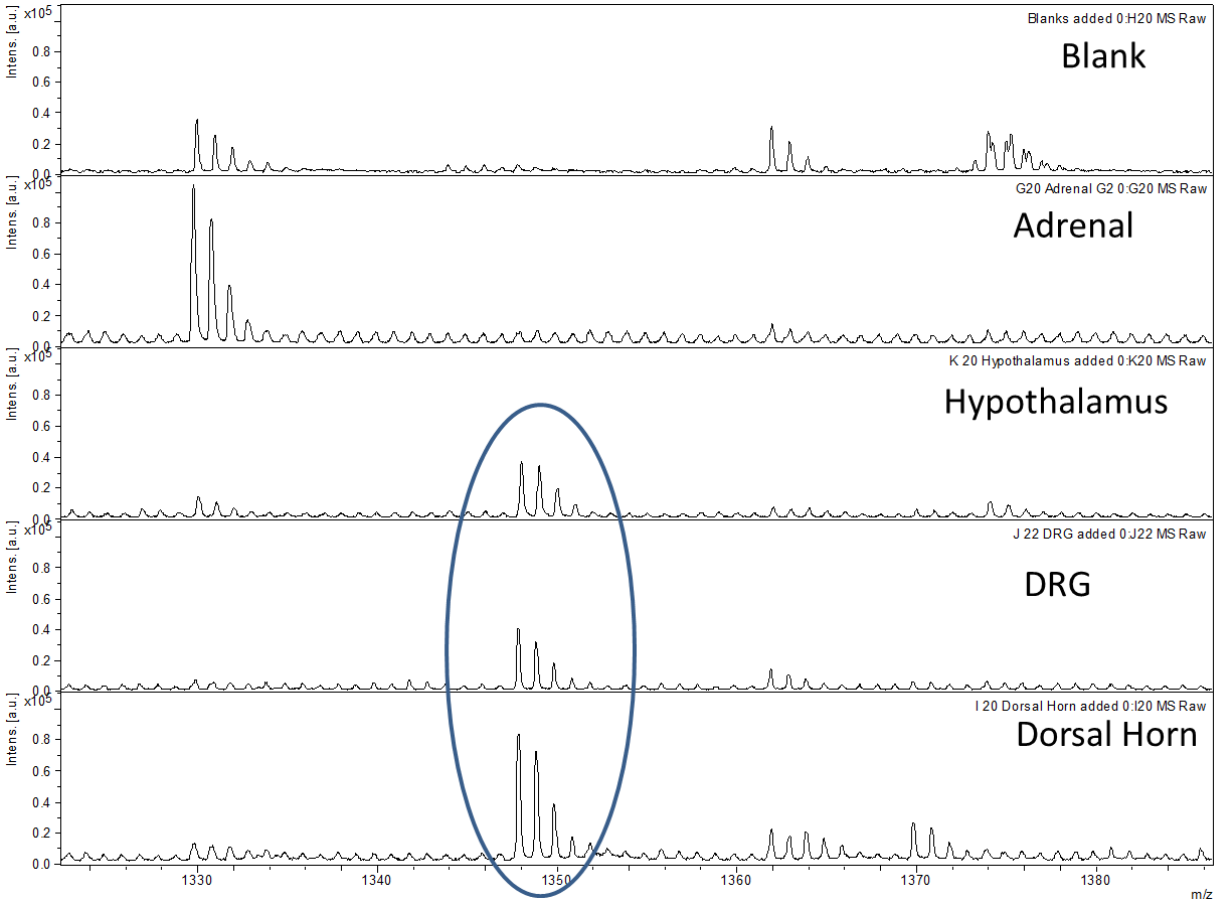

Figure 6.5: Substance P (*m/z* 1347, circled) was detected using MALDI-TOF MS analysis in homogenates from the hypothalamus, dorsal root ganglia, and dorsal horn of the rat.

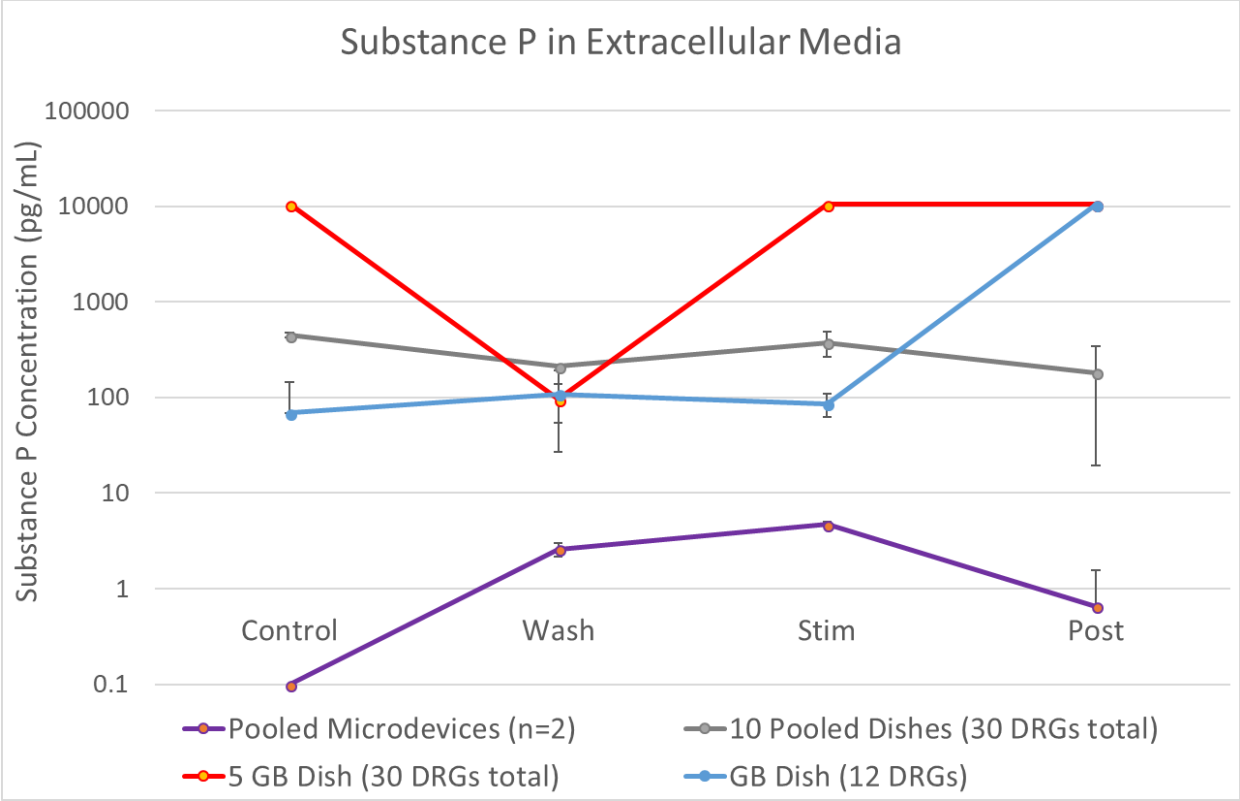

Figure 6.6: Concentrations of substance P measured by ELISA in cell culture releasates at different points in the experiment. GB = glass bottomed.

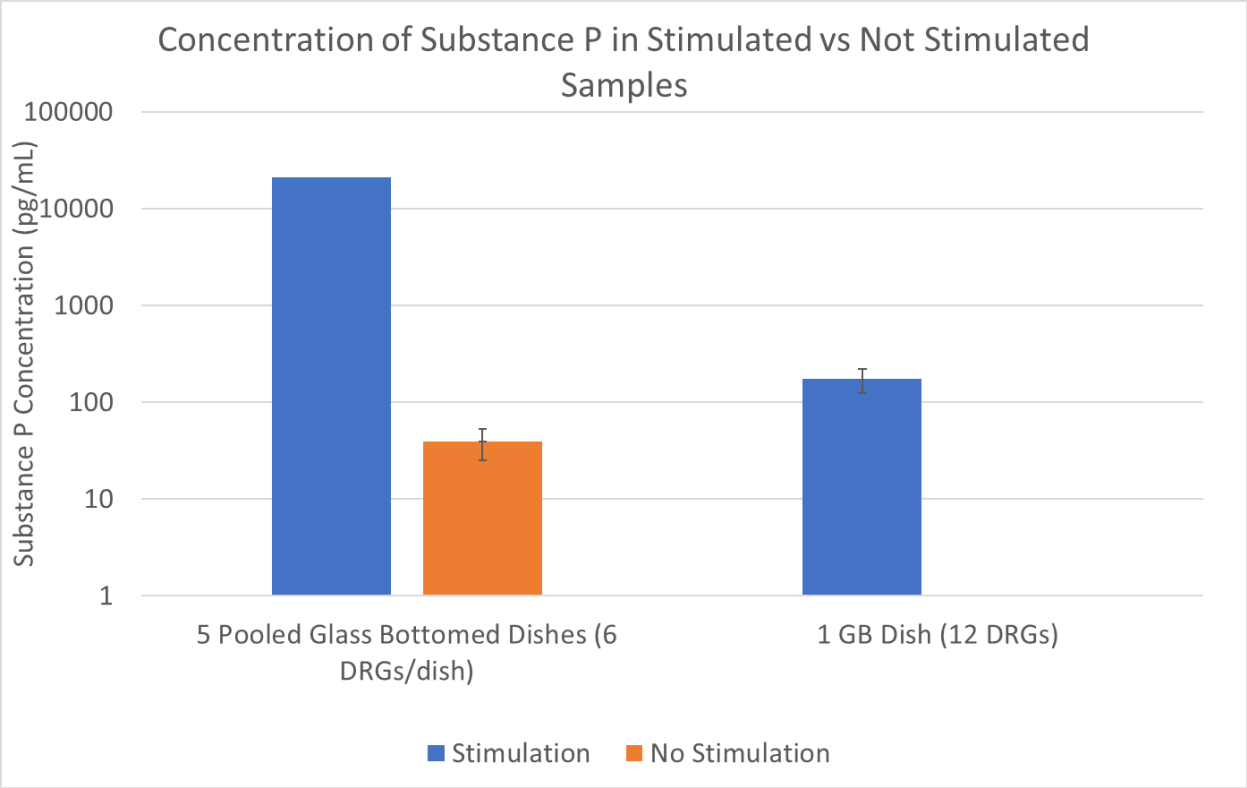

Figure 6.7: Comparison of stimulation versus no stimulation concentrations of substance P released using ELISA. GB = glass bottomed.

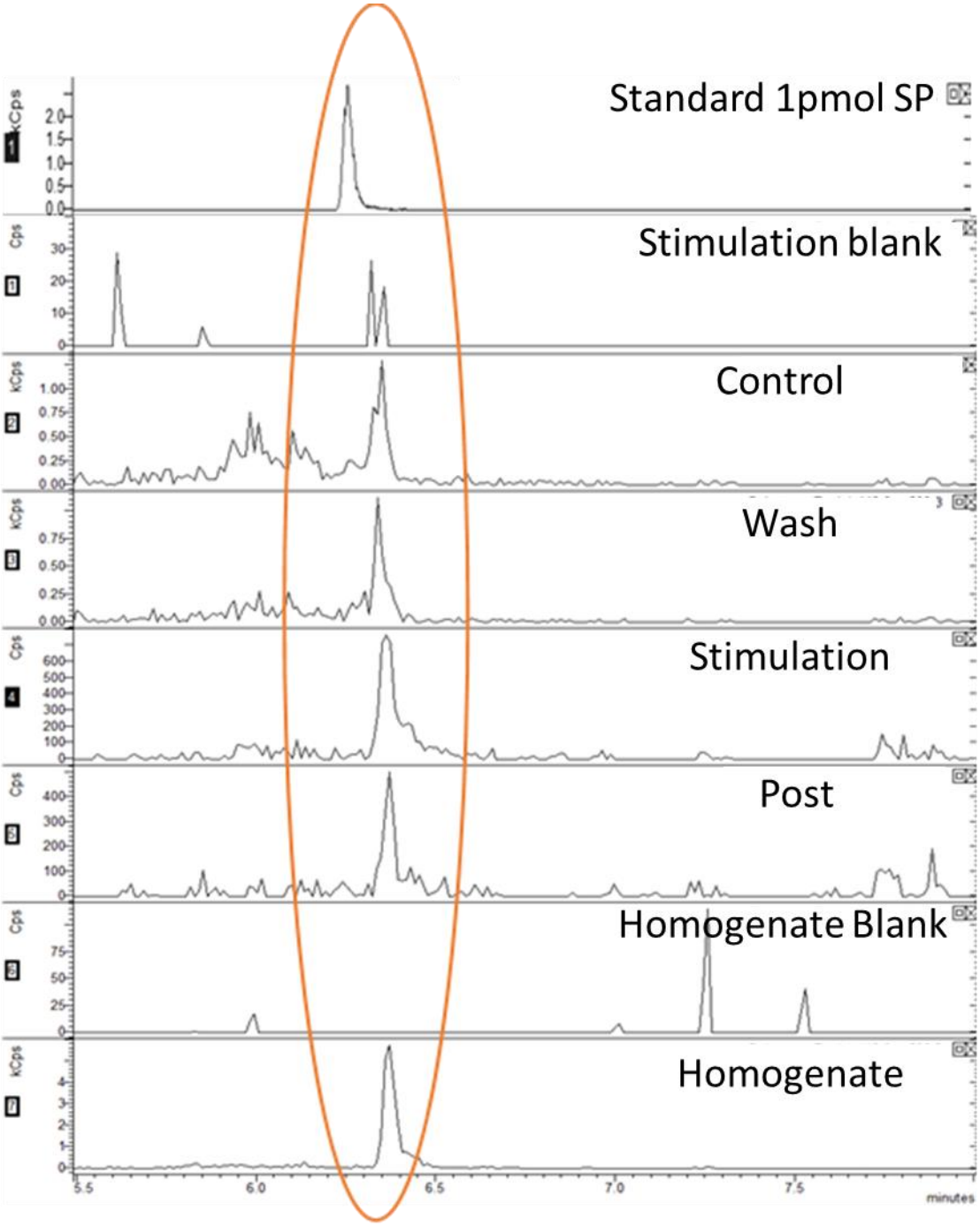

Figure 6.8: Representative spectra of substance P was detected in stimulation release samples and cultured cell homogenate samples using LC-QQQ-MS. Peaks with similar intensities were detected for control, wash, stimulation, and post samples while the cultured cell homogenate sample had a 10-fold increase in intensity.

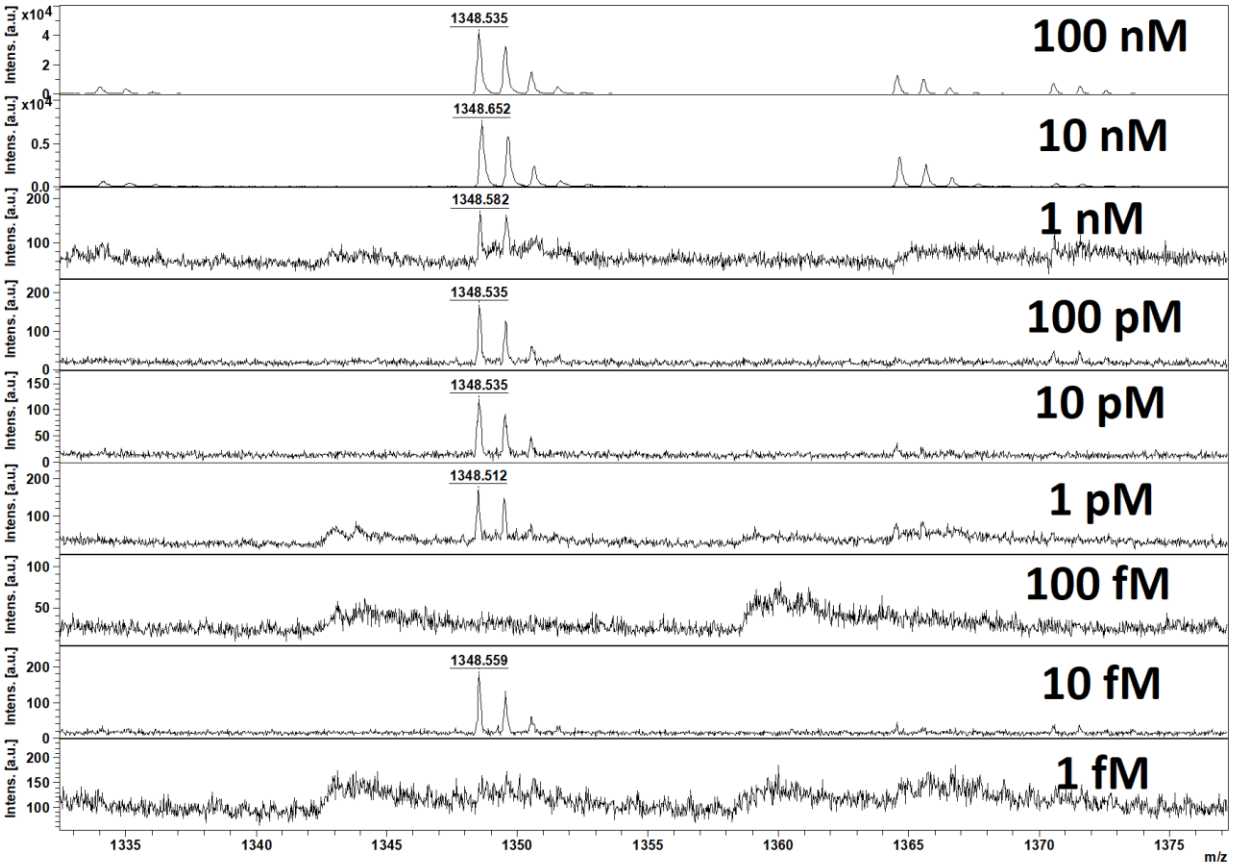

Figure 6.9: Substance P (*m/z* = 1348.5) peak detected in 7 out of 9 dilutions using the CHCA triple-layer method with acid wash.

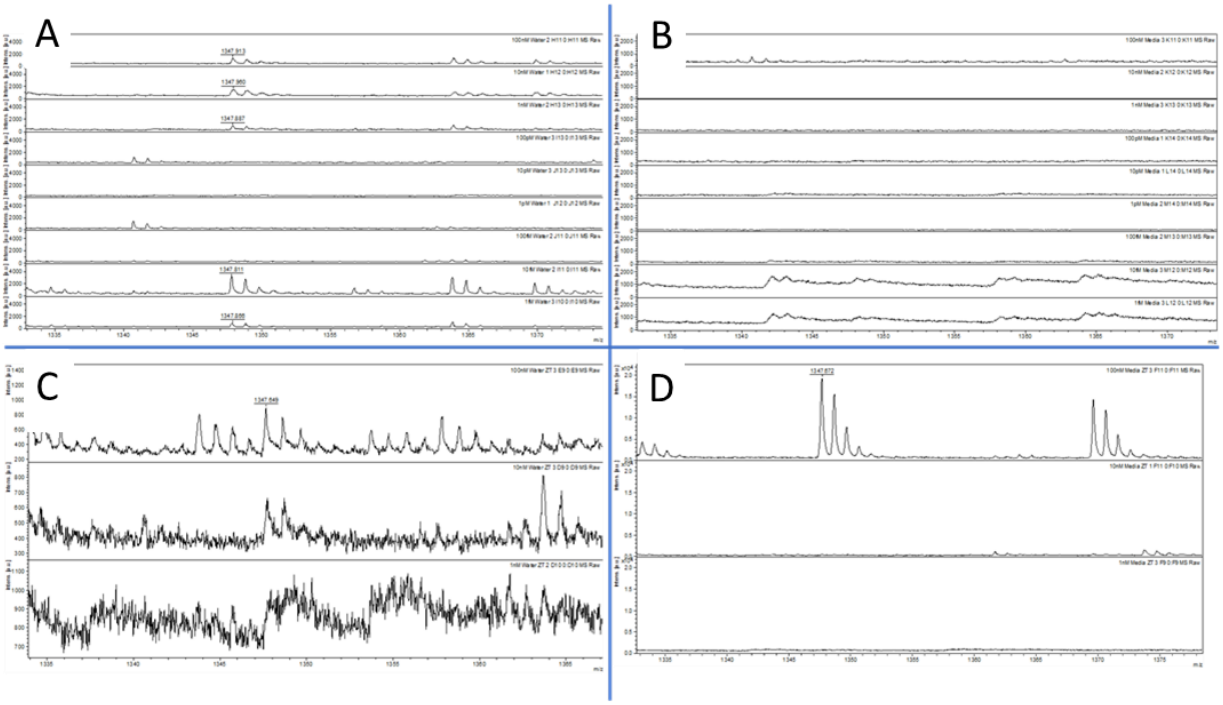

Figure 6.10: Substance P dilutions in water (A and C) and media (B and D). Substance P (*m/z* 1347.8) can be detected in 100nM, 10 nM, 1nM, 10 fM, and 1fM dilutions in water (A), but cannot be detected in any dilutions in media (B). After using solid phase extraction, Substance P could be slightly detected in 100 nM and 10 nM dilutions in water (C), and well detected in 100 nM dilution in media (D).

6.7 Tables

ELISA Results					
	Microdevices		30 DRGs in dishes		12 DRGs in GB dish
	9 pooled	16 pooled	Normal	Glass-bottomed	
Blank	---	---	223	1.42	---
Control	0	0	448	>10500	69
Wash	2.3	2.9	211	96	109
Stimulation	4.9	4.5	375	>10500	86
Post	0	1.3	182	>10500	>10500
No Stimulation	---	---	---	19.5	0
Homogenized Cells	---	---	2532	---	---

Table 6.1: Compilation of ELISA results from various stimulation experiments, all values in pg/mL.

6.8 Work Cited

1. Hillenkamp, F. and M. Karas, *The MALDI Process and Method*, in *MALDI MS*. 2007, Wiley-VCH Verlag GmbH & Co. KGaA. p. 1-28.
2. Dreisewerd, K., *Recent methodological advances in MALDI mass spectrometry.* Analytical and Bioanalytical Chemistry, 2014. **406**(9): p. 2261-2278.
3. Watson, J.T. and O.D. Sparkman, *Introduction to Mass Spectrometry: Instrumentation, Applications, and Strategies for Data Interpretation*. 2013: Wiley.
4. Tillmaand, E.G., et al., *Peptidomics and Secretomics of the Mammalian Peripheral Sensory-Motor System.* J Am Soc Mass Spectrom, 2015.
5. Strand, F.L., ed. *Neuropeptides: Regulators of Physiological Processes*. 1998, The MIT Press: Cambridge.
6. Squire, L., et al., eds. *Fundamental Neuroscience*. Third ed. 2008, Elsevier.
7. Xu, X.-J. and Z. Wiesenfeld-Hallin, *Neuropeptides: Pain*, in *Encyclopedia of Neuroscience*, L.R. Squire, Editor. 2009, Academic Press: Oxford.
8. Helke, C.J., D.M. Jacobowitz, and N.B. Thoa, *Capsaicin and potassium evoked substance P release from the nucleus tractus solitarius and spinal trigeminal nucleus in vitro.* Life Sciences, 1981. **29**(17): p. 1779-1785.
9. Mudge, A.W., S.E. Leeman, and G.D. Fischbach, *Enkephalin inhibits release of substance P from sensory neurons in culture and decreases action potential duration.* Proceedings of the National Academy of Sciences, 1979. **76**(1): p. 526-530.
10. Tang, H.-B., Y.-S. Li, and Y. Nakata, *The Release of Substance P From Cultured Dorsal Root Ganglion Neurons Requires the Non-neuronal Cells Around These Neurons*. Vol. 105. 2007. 264-71.
11. Yin, P., et al., *Neuropeptidomics: Mass Spectrometry-Based Qualitative and Quantitative Analysis*, in *Neuropeptides: Methods and Protocols*, A. Merighi, Editor. 2011, Humana Press: Totowa, NJ. p. 223-236.

Chapter 7

Advancements Toward a Biologically Relevant DRG Culture System

7.1 Notes

Much of the cell culture and imaging described in this chapter was performed by undergraduate assistants Yujin Lee, Ashley Lenhart, and Zachary Daniels. Yujin also created the CAD designs for our microfluidic device prototypes. Additionally, this project relies on the microfabrication expertise of Dr. Mikayla Yoder and Hanxiao Su, 3D printing expertise of Dr. Sean Lehman, the patience of photomask maker Jeff Grau, and the guidance and advice of Drs. Adina Badea, Joselle McCracken, Ralph Nuzzo, and Stanislav Rubakhin.

7.2 Introduction

As discussed in Chapter 2, there are many reasons why creating a physiologically relevant system is important for the study of neurochemistry, particularly when the goal is to characterize molecules that are released from cells at low concentrations under specific conditions. For this reason, and because of marked differences between the morphology of DRG cells in culture versus *in vivo* [1-3], we decided it is important to move away from bath stimulations of DRG cells in culture and move toward systems that are more physiologically and structurally relevant. We have worked toward accomplishing this goal by focusing on a few areas of cell culture improvement: growing aligned axons, spatial separation of nerve endings and cell bodies, and co-culture with relevant cell types.

When DRG cells are dissociated and seeded onto a flat surface, they extend more than one axon and these axons grow in many directions (Figure 7.1). This increased axonal output and lack of directionality does not provide a structurally relevant model for chemical

release. Within the body, the axons of primary sensory neurons travel together in parallel within the nerve either toward the nerve endings of the skin and viscera or toward the secondary sensory neuron within the spinal cord [1, 2]. This set-up allows the nerve endings of the primary sensory neurons to detect stimuli and communicate that information from the periphery to the spinal cord [2]. Neuropeptide release occurs both at locations within the skin and within the spinal cord, facilitating this communication [4]. Therefore, to accomplish the goal of understanding neuropeptide release from sensory neurons upon specific stimulation, it is important to replicate the structural relationship found *in vivo*. To do so, it is helpful to create a culture system which promotes growth of straight and aligned axons as well as separates the cell bodies spatially from the nerve endings.

Microfluidic devices are devices that utilize the physics of small volume fluidics for a specific outcome. In biological applications, microfluidic devices can be used for small volume cell culture applications using micrometer size features, such as channels and patterns. These features are useful for providing growth guidance as well as spatial separation of DRG neuron cell bodies and axonal endings [5-8]. Microfluidic devices used for the culture of neurons usually consist of separate compartments for cell seeding and axonal growth connected by a series of microchannels. The microchannels are small enough to allow only the axons and cell bodies of small glial cells through them, providing structural separation. Additionally, fluidic isolation can be achieved between the different cell culture chambers by keeping the fluid levels within the cell culture chambers equal.

Another application of microfluidic devices is that they are useful for guiding, compartmentalizing, and controlling interactions between different types of cells cultured

within the same device [5, 9-11]. This functionality is one that we considered in our design of the new device, since the DRG neurons interact with multiple cells, especially keratinocytes and secondary sensory neurons. Creating a device in which these cells can be cultured within separate compartments in an appropriate structural paradigm is paramount to the relevance of in-device cellular stimulation and release studies.

Keratinocytes, a type of skin cell, are a target for sensory neuron innervation, particularly by C-fibers [12]. Various studies have demonstrated successful co-culture of keratinocytes and dorsal root ganglion cells as well as functional interactions between the two cell types [12-15]. Particularly useful to our project is the demonstration that sensory nerve endings can influence the growth of keratinocytes through specific release of the neuropeptide CGRP [15] and that the presence of keratinocytes in cultures with sensory neurons changes the neuropeptide content of the innervating fibers [12].

At the other end of the system, secondary sensory neuron cell bodies are located in the dorsal horn of the spinal cord and are what the primary sensory neurons synapse onto to communicate information from the periphery to the higher order brain structures [4]. Co-cultures of both DRG cells and explants with dorsal horn neurons from the spinal cord have also been successful at demonstrating functional connections between the cell types *in vivo* [16-19] and researchers have even gone so far as to use these co-cultures for potential therapeutic studies [20].

With DRG, it is also possible to culture the entire structure as an explant [16, 21, 22]. While the explant method is helpful for maintaining the correct cell ratios and structure of the ganglia, both sustaining the viability of the tissue and supporting robust axonal outgrowth can be challenging. However, improved methods of three-dimensional

culturing, such as those discussed in Chapter 2, may improve upon those challenges and make DRG explant culture a viable option for future work performed in these devices.

7.3 Experimental

7.3.1 DRG Cell Isolation and Culture

DRG were isolated from postnatal day 2-5 rats and sustained in a bath of ice cold Hibernate A (BrainBits Springfiled, IL) for up to 24 h before dissociation. DRG were digested in a solution of 0.2% type II collagenase and 0.6% protease in DRG serum-free media containing Neurobasal A without phenol red (Life Technologies Carlsbad, CA), 100 U/mL penicillin/streptomycin (Life Technologies), 0.5 mM GlutaMAX (Life Technologies), 50 ng/mL NGF (Life Technologies), 50 ng/mL BDNF (Prospec Bio Rehovot, Israel), and 500 µL B27 Growth Supplement (Life Technologies) for 30 min at 37 ºC. After digestion, the samples were subjected to centrifugation for 2-3 min at 200 *xg*. The supernatant was removed, and the pellet washed with Hank's Balanced Salt Solution (HBSS) (Life Technologies). Upon centrifugation using the same parameters, the supernatant was once again removed and the pellet triturated using fire-polished pipets. Following trituration, some of the pellet was allowed to re-settle. Once a small pellet was formed in the bottom of the microcentrifuge tube, the supernatant was removed and centrifuged. After centrifugation, the supernatant was removed and the pellet washed with HBSS. A final centrifugation was performed after which the pellet was resuspended in 200 µL of media and 20 µL of cell suspension was added to the cell seeding well of a device treated with poly-D-lysine (BD Biosciences Franklin Lakes, NJ) and laminin and incubated for 30 min at 37 ºC. If appropriate, the device was tilted to enhance movement of cells toward the microchannels. After 30 min, all wells were filled with 150 µL of media. The cells were

incubated at 37 ºC, with a media change at 24 h and then every 3 d until the cells were used for experiments.

7.3.2 Keratinocyte Isolation and Culture

Keratinocyte dissociation followed the protocols outlined in two recent papers [5, 23]. Briefly, the skin was removed from 2-d old rats and stretched dermis side down onto an untreated polystyrene cell culture dish and kept cold for approximately 1 h. Next, the skin was transferred dermis side down onto a 0.25% solution of trypsin without EDTA in HBSS and incubated floating on the solution overnight at 4 ºC. After incubation, the skin was stretched epidermis side down onto an untreated polystyrene cell culture dish in a sterile cell culture hood and the dermis was carefully removed using forceps. The dermis was moved into 10 mL of cold DMEM and cut with sterilized scissors until the skin pieces were small enough to be triturated by a 10 mL pipet. After trituration, the triturated solution was transferred into a 15 mL conical tube while leaving behind as many sheets of tissue as possible. The solution was centrifuged at 200 *x*g for 5 min, the supernatant was aspirated and pellet was re-suspended in DMEM and passed through a 70 µm cell filter. The filtrate was centrifuged again, supernatant aspirated, and the pellet was resuspended in 200 µL of a media consisting of 2:1 solution of DMEM:F12 supplemented with 5% FBS and 10% Pen/Strep. Cells were counted and the sample was adjusted to 50,000 cells per 10 µL solution and 10 µL solution was seeded into the prepared well of the microfluidic device. After 30 min of seeding, 100 µL of the DMEM/F12 media was added to each keratinocyte well of the device and cells were monitored every day with media changes every 3 d.

7.3.3 Secondary Sensory Neuron Isolation and Culture

Secondary sensory neuron isolation was carried out following a process outlined by Vikman et. al. [17]. First, the spinal cord was dissected out of the rat. Then, the dorsal third of each side of the spinal cord was removed and incubated in 0.25% Trypsin for 20 min at 37 ºC. After incubation, the spinal cords were rinsed with HBSS and triturated in cell culture media containing 1% FBS. After a final centrifugation, the cells were re-suspended in cell culture media and seeded at 20,000 cells per well. Media changes occurred every 3 d.

7.3.4 Explant Cultures

DRG explants were placed on a PDL and laminin coated glass surface, PDMS slab, or PDMS slab with microchannels, and media was carefully exchanged every 1-3 d. So as not to disturb the explant, the media exchange was performed as slowly and as far away from the explant as possible.

7.3.5 Stamping

A PDMS mold with various sized microgroves was used as the stamp. The stamp was incubated in a 100 µg/mL PDL and laminin solution for 1.5 h, dried, and placed onto an ethanol-cleaned glass coverslip. Initial tries used fluorescent PDL and lines were detected on the coverslip after stamping. Cells were seeded onto glass slides at various densities.

7.3.6 Microfluidic Device Design and Preparation

The commercially available microfluidic devices used in this project were purchased from Xona Microfluidics. The devices included the Standard Neuron Device (SND) 150 and 450 and the Tri-Chamber Device (TCD) 500. Device preparation for cell culture followed the protocol outlined in the product manual. Briefly, the microscope slides upon which the

devices were placed were cleaned with 70% ethanol or isopropanol in a sterile cell culture hood for 30 min and then air dried for 30 min in the sterile cell culture hood. They were then incubated with 0.5 mg/mL PDL in sterile water at 37 °C for at least 4 h. After incubation with PDL, the surfaces of the slides were washed 3 times with sterile water and the slides were incubated in sterile water for at least 3 h and dried in the sterile cell culture hood, usually overnight, but for at least 2 h.

The in-house designed microfluidic devices used in this project were designed using CAD software. The design includes cell culture chambers divided by microchannels and an elongated axonal growth area which will house 3D printed poly-2-hydroxyethyl methacrylate (HEMA) laponite constructs for axonal guidance and improved nerve-like growth (Figure 7.2). The first iteration consists of a central DRG cell culturing channel with a “central” (left) and “peripheral” (right) cell culture chamber, each separated by an axonal growth chamber, all separated by microchannels (10 µm wide, 3 µm high, 200 µm long for the outside microchannels, 100 µm long for the inside microchannels). The second iteration consists of three cell culture chambers separated by microchannels (10 µm wide, 3 µm tall, 200 µm long for the outside microchannels, 100 µm for the inside microchannels) and one large 5 mm axon growth chamber, in which the poly-HEMA laponite constructs are placed to encourage axonal growth. The cell culture and growth chambers are 50-100 µm high, 5-6 mm long and 0.5-5 mm wide. The device requires a two-layer photolithography mask process, which means that two photomasks were created, one with the microchannels, which are 3 µm high, and the other consisting of the rest of the features, with the SU-8 spun to 100 µm. Once the SU-8 mask was created, the devices were molded using sylgard-187 poly-dimethylsiloxane (PDMS) and allowed to

cure for at least 24 h at 65 °C. Once fabricated, the devices were treated in the same manner as the commercial devices.

On cell culture day, the microfluidic devices were removed from their packaging and extra dust was removed using scotch tape. Then, the devices were incubated in 70% ethanol for 30 minutes and air dried in the sterile cell culture hood for 1 h. Once the devices were dry, they were placed onto the PDL-coated, dried microscope slides and pressure was applied to form a seal. 0.2 mg/mL laminin was flown through the device in a sequential manner to allow full coverage of the cell culture surfaces with laminin. Full incubation time for laminin is 1 h at 37 °C. After laminin incubation, the laminin was washed out with either sterile water or media, and cell culture media was added to the wells and incubated for at least 1 h, or until the cells were ready for seeding. If the device was also used for keratinocytes, the side of the device that held keratinocytes was additionally coated with 30 µg/mL collagen and 10 µg/mL fibronectin for 30 min.

For DRG cell seeding, the cell pellet was re-suspended in 200 µL of media and 20 µL of cell suspension was added to the cell seeding well of the device and incubated for 30 min at 37 ºC. If appropriate, the device was tilted to enhance movement of cells toward the microchannels. After 30 min, all wells are filled with 150 µL of media. The media was exchanged 24 h after cell seeding and then once every 3 d after that.

For keratinocyte seeding, the cell pellet was re-suspended so that there are 50,000 cells per 10 µL of solution and 10 µL were added to the keratinocyte side of the device. After the 30 min incubation period, 100 µL of media was added to the wells leading to the keratinocyte channel, to ensure flow from the neuronal channels to the keratinocyte channel and not vice versa.

7.3.7 Immunohistochemistry

DRG media was replaced with a 4% paraformaldehyde (Ted Pella, CA) fixation bath at room temperature for 15-20 min. The cells were then washed with PBS (Life Technologies Carlsbad, CA) five times, with the last wash lasting 5 min with shaking. 0.25% Triton X (Sigma-Aldrich St. Louis, MO) was added to the cells for 10 min to permeabilize the membranes. A wash was performed and a blocking solution of 5% normal goat serum (NGS) (Life Technologies) in PBS was added for 30 min for dish cultures and 1 h for devices with shaking. Another wash step was performed and the primary antibody in a 2% NGS solution was added and incubated overnight at 4 ºC. After incubation, a wash was performed, and the second primary antibody was added and incubated overnight. After that incubation, another wash was performed and the secondary antibody in a 2% NGS solution was added to the culture for 1-2 h. If 4',6-Diamidino-2-Phenylindole, Dihydrochloride (DAPI) was used, the culture was rinsed and DAPI added to the culture and incubated for 20 min. Finally, the cells were subjected to a final wash step, rinsed with deionized water for 30 s, and mounted with ProLong Gold Antifade (Life Technologies) onto a glass slide. If not visualized immediately, the slides were kept in the dark at 4 °C until imaging with a Zeiss Axio Imager M2 (Carl Zeiss AG, Oberkochen, Germany). Primary Antibodies: Rabbit monoclonal glutamine synthetase antibody (Thermo Fisher Scientific), mouse monocolonal anti-beta-III tubulin (Santa Cruz Biotechnology, Santa Cruz, CA); rabbit anti-cytokeratin 5 (ab53121) (Abcam, Cambridge, MA) and DAPI nuclear stain (Thermo Fisher Scientific). Secondary antibodies: Alexa Fluor (Life Technologies) goat antibodies with excitation maxima of 488 and 594, 20 µg/mL.

7.4 Results and Discussion

7.4.1 Stamping

The stamping of PDL onto glass slides was successful. After the addition of cells, a trend can be seen in which the cells align and grow along the PDL in straight lines. However, there is too much cross over between axons that grow on one line and then move toward another as well as too many cell bodies located throughout the culture (Figure 7.3) for stamping to remain a viable method for growing sensory neuron axons in a straight line.

7.4.2 Microfluidic Devices

Successful growth of axons through the microfluidic device microchannels was difficult to obtain. For over a year, we worked to improve axonal migration through the channels by optimizing many parameters including cell seeding concentration, device position, growth factor gradients, use of bovine serum albumin during the dissociation procedure, and more. We finally obtained success by switching to neonatal animals. Once the switch was made, no adjustments were needed to the cell culture protocol to encourage axon growth through the microchannels. At that point, we worked to determine which type of device and microchannel length was best for our purposes (Fig 7.4). The cell growth occurs quite quickly through the SND 150 and the exchange of fluids may be difficult to control during the stimulation protocol. The SND 450 and TCD 500 both provide good separation while maintaining successful cultures. The TCD 500 allows for even greater control as there are 3 cell culture channels.

7.4.3 Co-cultures

Keratinocyte co-culture was attempted once with success (Figure 7.5). The main issue is that only a small portion of the cells on the keratinocyte side of the device stained with

anti-cytokeratin 5, an appropriate marker for keratinocyte cells. Therefore, we need to identify the other cells in the culture are and if it is appropriate to have them in the co-culture system or if we need to find ways to remove them.

Spinal cord co-culture has been attempted, but not been met with success. However, the culture was attempted using whole spinal cord tissue. The prospect of only dissecting and dissociating the dorsal horn of the spinal cord is not only biologically sound, but also seems promising due to published results of both embryonic and neonatal dorsal horn tissue being used for successful studies [17-20].

7.4.4 Explant Cultures

Successful culture of DRG explants is well documented in the literature [21, 22, 24]. Initial forays into explant cultures were unsuccessful due to limited axonal outgrowth. However, recent attempts to culture explants along a series of microgroves within a PDMS block has been met with modest success (Figure 7.6). While there are no signs of direct axonal outgrowth from the explants, there are areas of cell growth along the microgrooves that may have been where the explants were connected to the device at one point. In addition, there is evidence of cellular outgrowth from some, although not all, of the explants.

7.4.5 Primary Sensory Microphysiological System Iteration 1

The first iteration of our primary sensory microphysiological system was designed to address the limited length of axonal outgrowth allowed for in the commercial devices. Therefore, our system consisted of five chambers fluidically isolated by microchannels (Figure 7.7). More specifically, the chambers included a central chamber for primary sensory neuron culture, two middle chambers for axonal growth and two outer chambers for target cells such as skin and spinal cord cells. The central and outer chambers were

connected to inlet and outlet ports for cell and media addition and sample collection. We were able to successfully fabricate the devices as well as culture and sustain cells within the device for up to 1.5 weeks. One challenge raised by this design was that it was difficult to get the axons to travel through the middle chambers to the outer microchannels. Therefore, it was ultimately decided that the device could benefit from axonal guidance through the middle chambers, so a second iteration was designed.

7.4.6 Primary Sensory Microphysiological System Iteration 2

The goal of the second device design was to provide axonal guidance through the elongated axonal culture area. This ability is necessary for the re-creation of the *in vivo* structural relationships of primary sensory neurons. To do this, we introduced poly(2-hydroxyethyl) methacrylate (pHEMA) laponite XLG (LAP) (LAP; $Na^{+0.7}$ $[(Si_8\ Mg_{5.5}\ Li_{0.3})\ O_{20}(OH)_4]^{-0.7}$) scaffolds to our device. pHEMA is a neutral hydrophilic polymer hydrogel material amenable to 3D printing by direct ink-writing, which makes it useful for printing a scaffold design onto a slide which will house the microdevice [25]. LAP is a silicate nanoclay inorganic composite that, when incorporated into HEMA-based inks, increases the buildability of the ink, providing more options for scaffold shape design. On-going work in the Nuzzo group shows that pHEMA-LAP ink is a promising guidance structure for nerve-like growth of DRG cells in culture [26].

We also lengthened the axonal chamber within which the scaffold would be placed and re-imagined the device to have four chambers: one for primary sensory neuron cell culture, one for axonal outgrowth, and two for target cell culture (Figure 7.8). The left-most chamber is separated from the middle chamber by 100 µm length microchannels, which represent the relatively short distance that the axons travel into the spinal cord. The

middle chamber with inlet and outlet ports is for primary sensory neuron cell culture, while the 5 mm long middle chamber without inlet and outlet ports is the axonal growth chamber, where the scaffolds are placed. The right-most chamber is separated from the axon chamber by 50 μm length microchannels and is meant for the culture of skin target cells.

The assembly of this device requires printing the scaffold onto a glass slide, functionalizing it, and then placing the microfluidic device over the scaffold so that the scaffold fits inside the axonal elongation chamber (Figure 7.8). Preliminary cell culture of primary sensory neurons within this device was also successful, although moving fluid into the large axonal chamber is challenging. We now include the punching of media inlet holes into the PDMS as part of our procedure to add cell culture media directly to the axonal chamber.

7.5 Conclusion

This chapter has outlined our movement toward building a more physiologically relevant system for growth, stimulation, and release of neurochemicals from DRG cells. First with the transition to using microfluidic devices and then through each new device design, we moved closer to the desired functionality. The success of culturing neonatal DRG cells in the newly designed microfluidic devices allows us to move forward with further characterizing axonal growth along the incorporated scaffolds. Of course, our ultimate goal is to use the device to build a complete microphysiological system, including DRG, DH, and skin cells, allowing us to study cellular stimulation and release utilizing relevant structural and functional relationships between the cultured cells. Our initial success with

both the first and second iterations of our new device is encouraging, and we are excited to continue to study the growth of primary sensory neurons within the device.

7.6 Figures

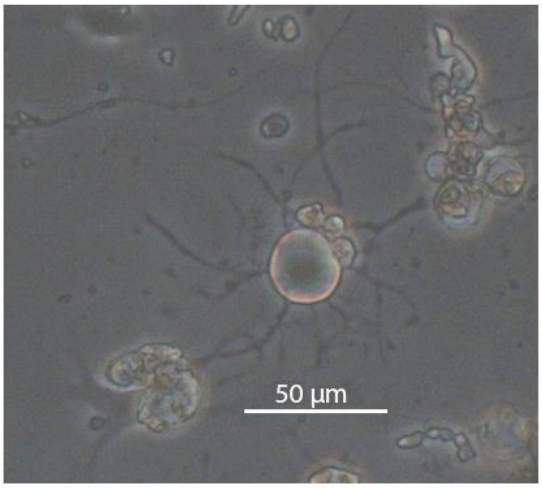

Figure 7.1: DRG neuron in culture with multiple axonal outgrowths.

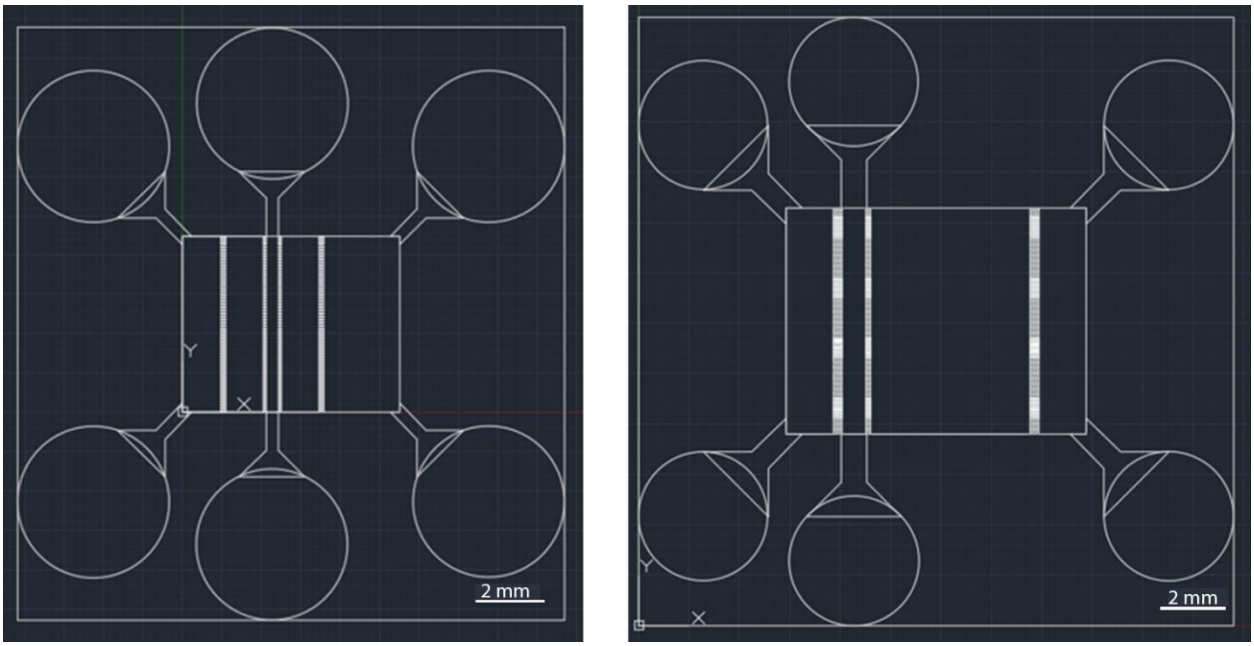

Figure 7.2: The first (left) and second (right) iterations of the microfluidic portion of the primary sensory system microphysiological device. The first iteration consists of a central DRG cell culturing channel with a “central” (left) and “peripheral” (right) cell culture chamber, each separated by an axonal growth chamber, all separated by microchannels (10 µm wide, 3 µm high, 200 µm long for the outside microchannels, 100 µm long for the inside microchannels). The second iteration consists of three cell culture chambers separated by microchannels (10 µm wide, 3 µm tall, 200 µm long for the outside microchannels, 100 µm for the inside microchannels) and one large 5 mm axon growth chamber, in which the poly-HEMA laponite constructs will be placed to encourage axonal growth. The cell culture and growth chambers are 50-100 µm high.

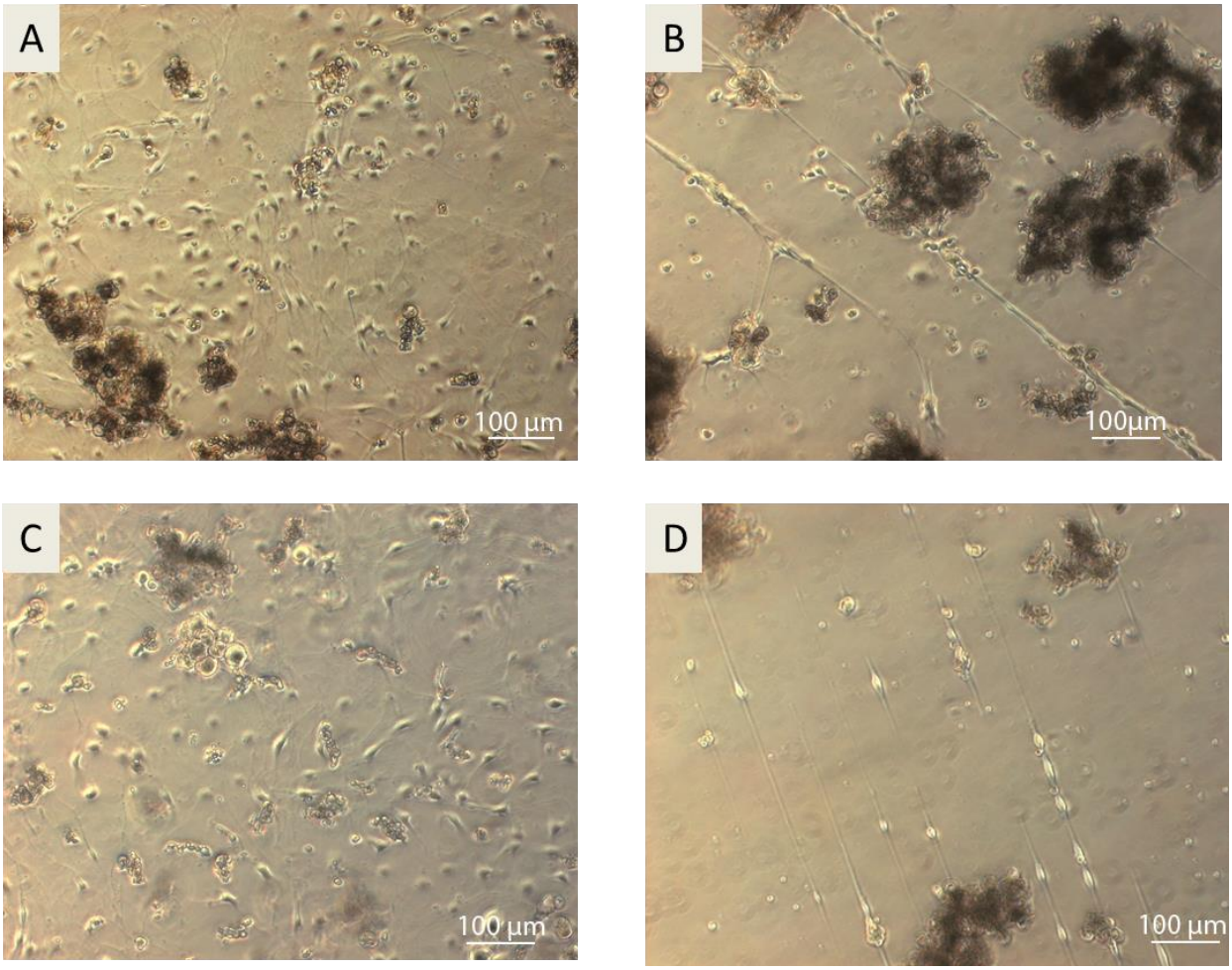

Figure 7.3: DRG cells plated at high concentration (A and B) and low concentration (C and D) on normal surface (A and C) versus stamped surface (B and D).

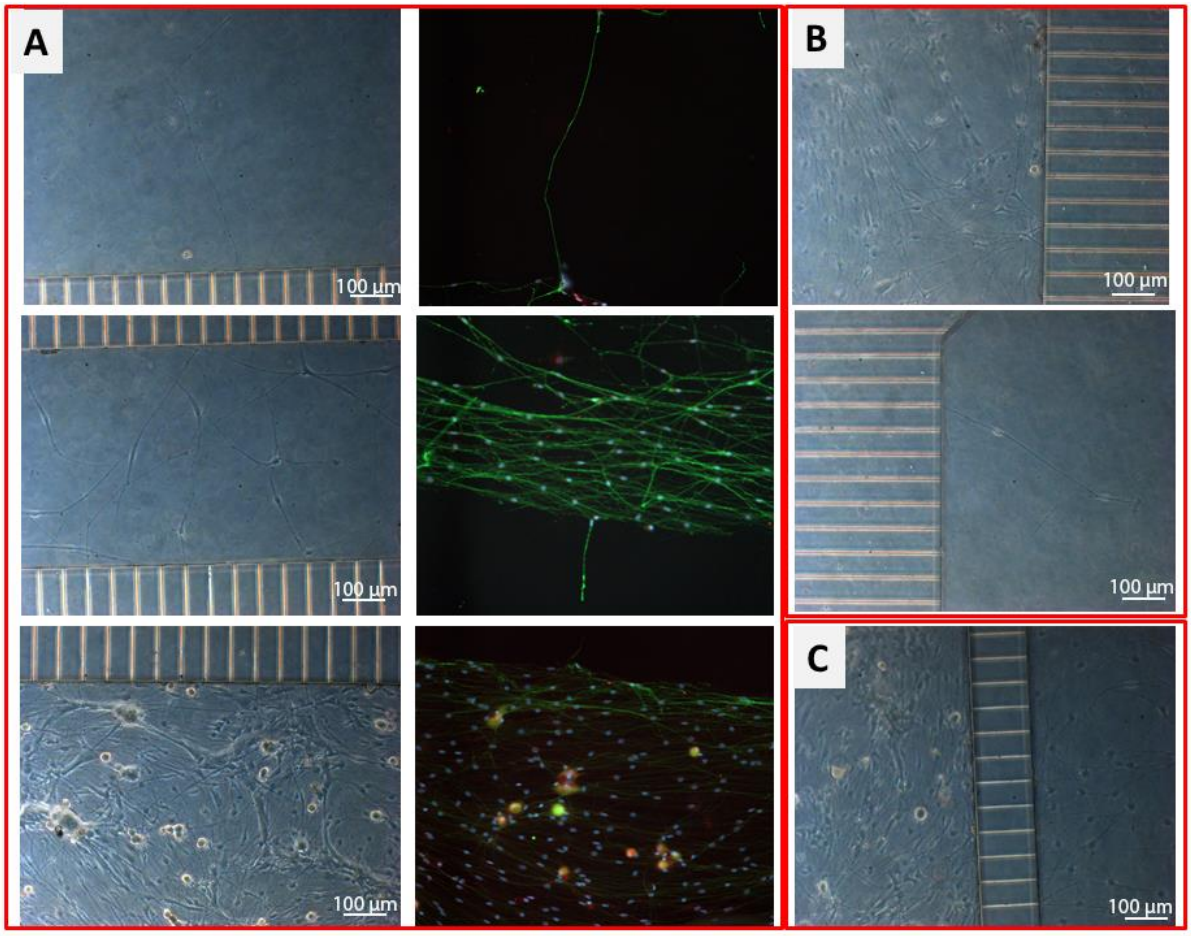

Figure 7.4: Panel A: DRG cells cultured in TCD 500. Top to Bottom: Far axonal well, middle well, cell seeding well. Left are brightfield images at DIV 6, right side are representative fluorescent images from similar areas of the device, at the same magnification. Green: Beta 3 tubulin, neuronal marker; red: glutamine synthetase, glial marker; blue: DAPI, nuclear marker. Panel B: DRG cells cultured in SND 450 DIV 6; top: cell seeding well; bottom: axonal well. Panel C: DRG cells cultured in SND 150 DIV 6. Left side of image: cell seeding well; right side of image: axonal well.

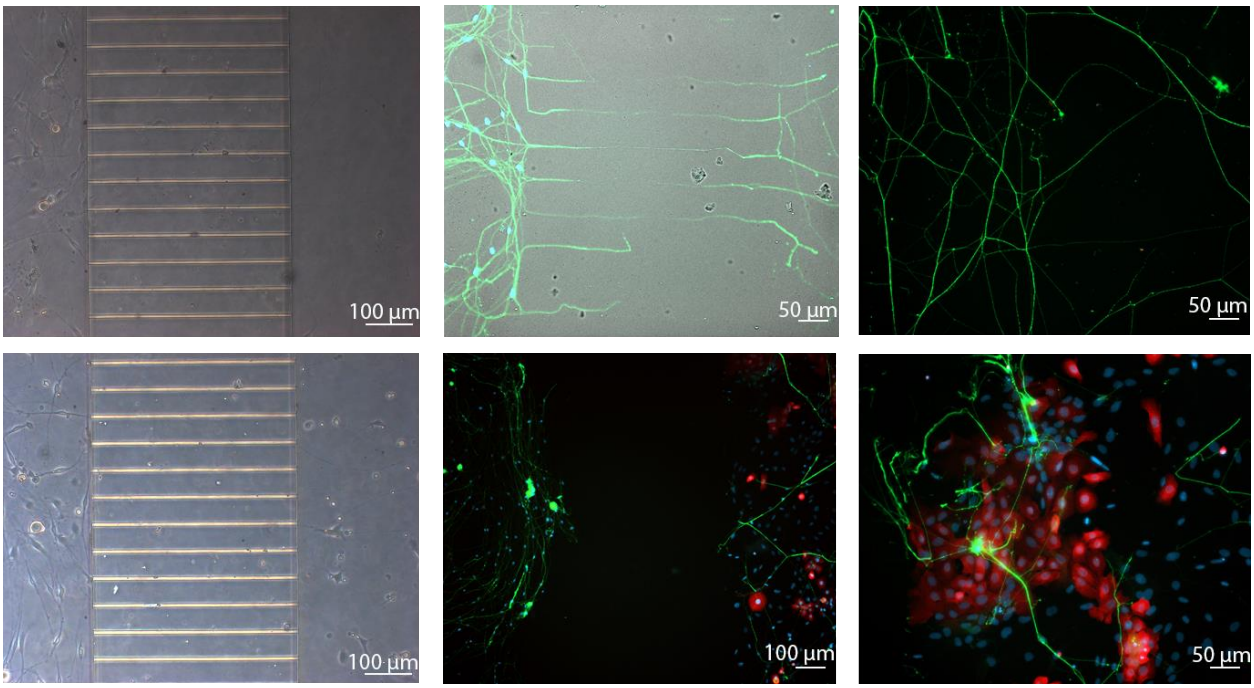

Figure 7.5: DRG cell-Keratinocyte co-culture in SND450. Green: beta-III tubulin neuronal marker; red: cytokeratin 5 keratinocyte marker; blue: DAPI nuclear stain. Top (L-R): Control DRG cell culture brighfield image with cells on left and axons on right; overlay of brightfield and immunofluorescent images; axonal side of microfluidic device. Bottom (L-R): DRG cell-keratinocyte co-culture with DRG cells seeded on left side and keratinocytes seeded on right; immunofluorescent image of both sides of co-culture with keratinocytes are only on right side of device; immunofluorescent image of axonal/keratinocyte side of microfluidic device.

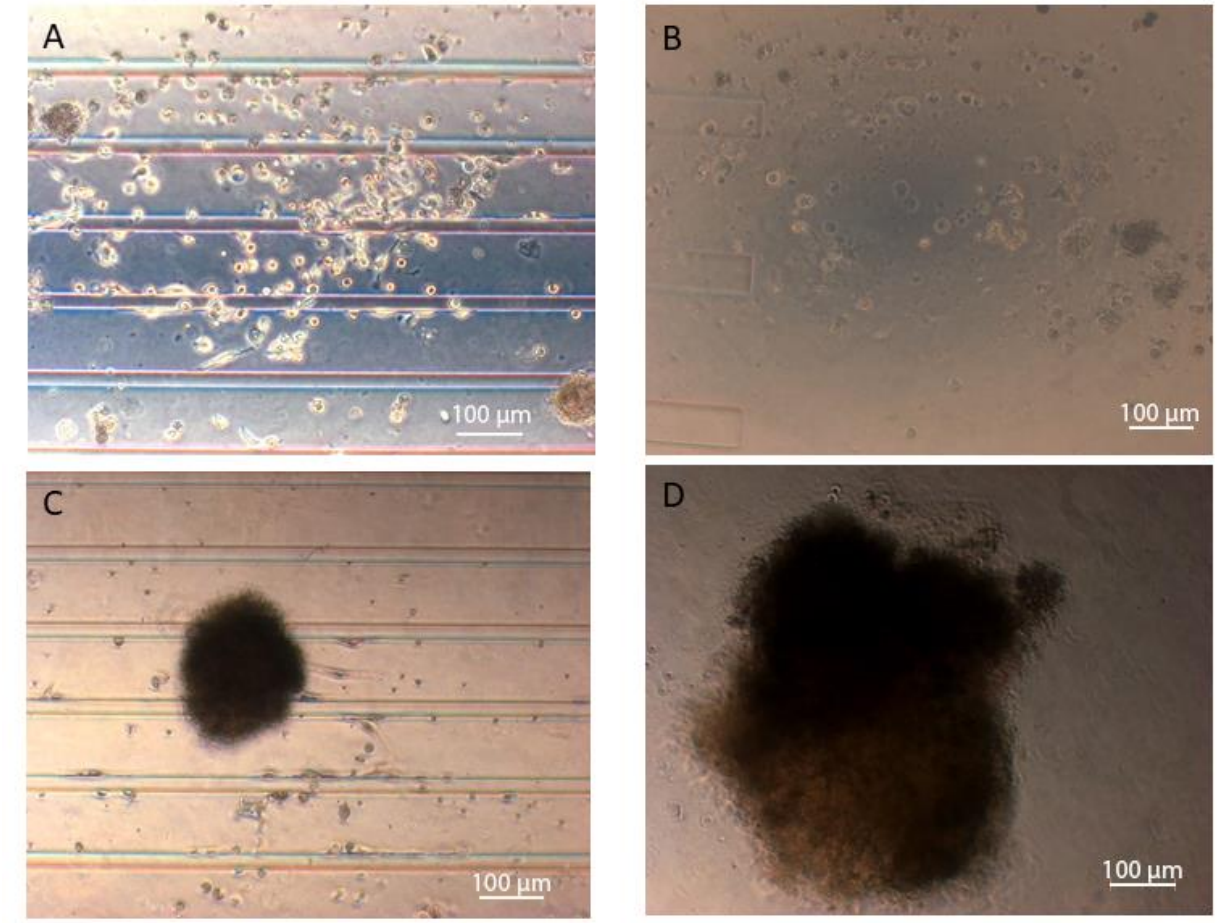

Figure 7.6: Axonal outgrowth from DRG explants. A: cellular growth along microchannels from cells deposited by an explant which is no longer attached to the PDMS substrate. B: Cells left on the PDMS by an explant which is no longer attached to the substrate. No outgrowth is observed from the cells. C: Direct cell outgrowth from a small explant. D: No cell outgrowth noticed from a complete DRG explant.

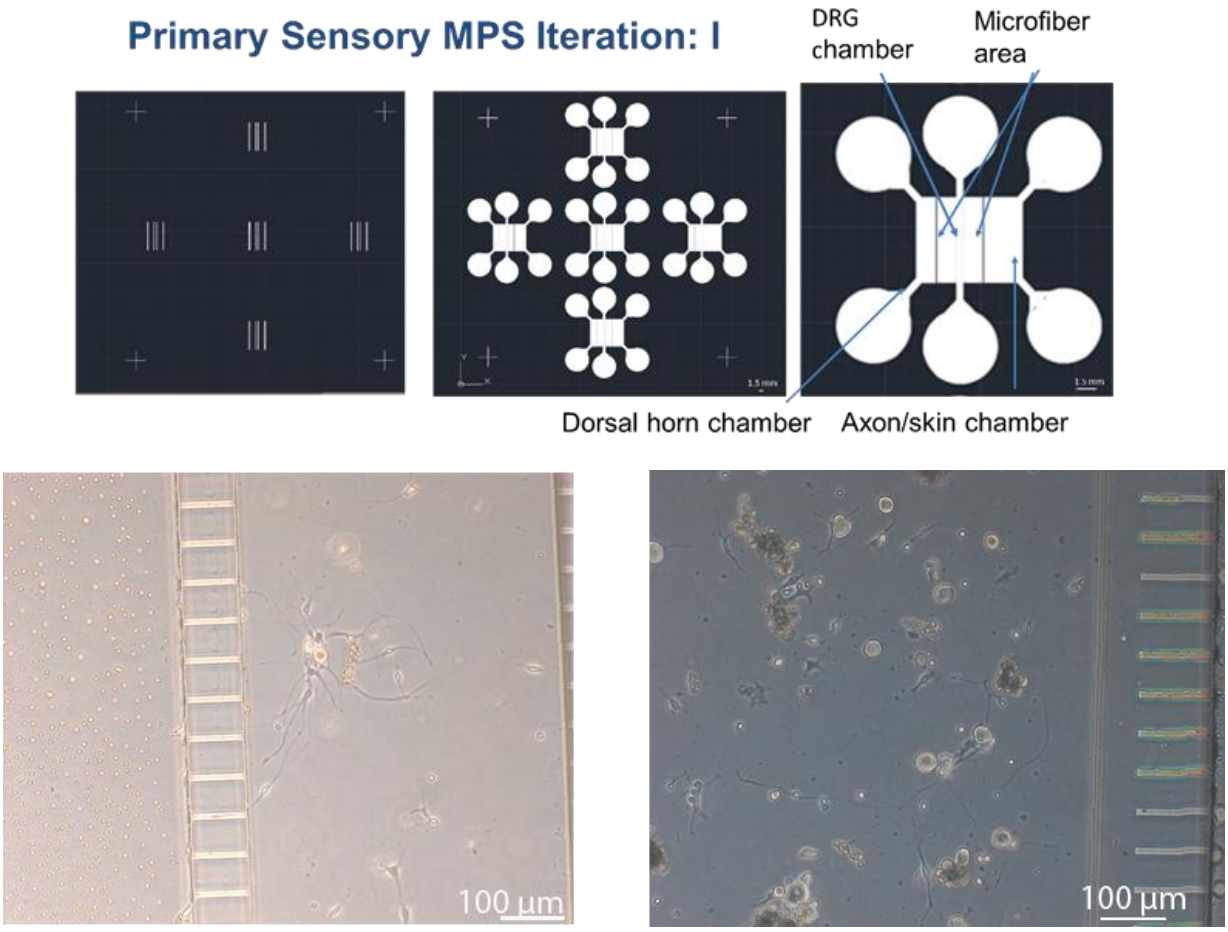

Figure 7.7: The first iteration of the primary sensory microphysiological system. Top: design of the microfluidic system. Left: microchannel layer (length 200 µm for outer channels, 100 µm for inner channels, height 3 µm for all); middle: cell culture chambers (height 100 µm), and input and output wells; right: zoomed in image of one device design. Bottom: DRG cells cultured and growing in the cell culture chambers of the microfluidic device.

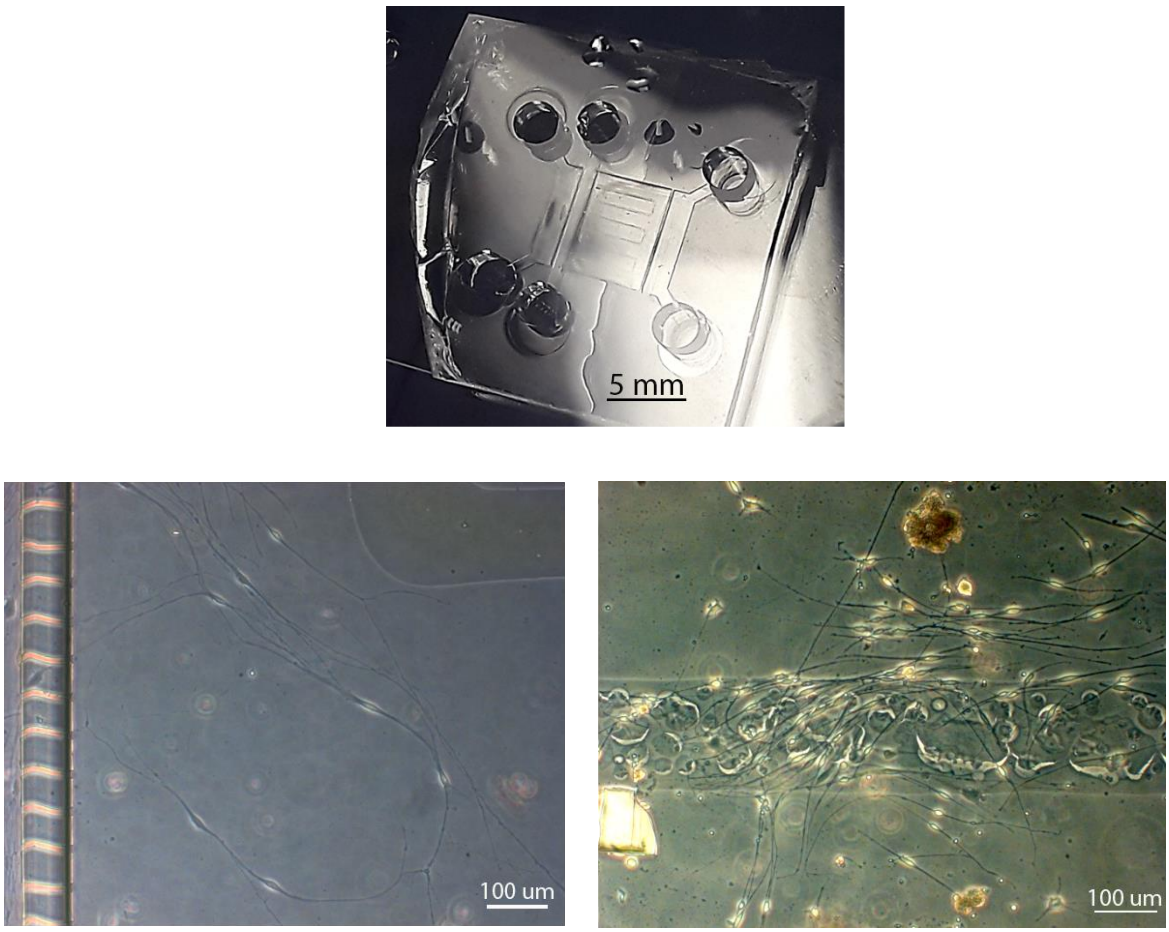

Figure 7.8: Top: Complete microphysiological system iteration 2. Bottom: DRG cells cultured within the microphysiological system iteration 2 and interacting with the scaffold (top right corner of left image, across center of right image).

7.7 Work Cited

1. Devor, M., *Unexplained peculiarities of the dorsal root ganglion.* Pain, 1999. **Suppl 6**: p. S27-35.
2. Hogan, Q., *Labat Lecture: The Primary Sensory Neuron: Where it is, What it Does, and Why it Matters.* Regional anesthesia and pain medicine, 2010. **35**(3): p. 306-311.
3. Tucker, B.A. and K.M. Mearow, *Peripheral sensory axon growth: from receptor binding to cellular signaling.* Can J Neurol Sci, 2008. **35**(5): p. 551-66.
4. Priestly, J., *Neuropeptides: Sensory Systems*, in *Encyclopedia of Neuroscience*, L.R. Squire, Editor. 2009, Academic Press: Oxford. p. 935-943.
5. Tsantoulas, C., et al., *Probing Functional Properties of Nociceptive Axons Using a Microfluidic Culture System.* PLoS ONE, 2013. **8**(11): p. e80722.
6. Taylor, A.M., et al., *A microfluidic culture platform for CNS axonal injury, regeneration and transport.* Nat Meth, 2005. **2**(8): p. 599-605.
7. Hosmane, S., et al., *Circular compartmentalized microfluidic platform: Study of axon-glia interactions.* Lab on a Chip, 2010. **10**(6): p. 741-747.
8. Yang, I.H., et al., *Compartmentalized microfluidic culture platform to study mechanism of paclitaxel-induced axonal degeneration.* Experimental Neurology, 2009. **218**(1): p. 124-128.
9. Ai, X., et al., *Microfluidic Coculture Device for Monitoring of Inflammation-Induced Myocardial Injury Dynamics.* Analytical Chemistry, 2018. **90**(7): p. 4485-4494.
10. Park, J., et al., *Microfluidic compartmentalized co-culture platform for CNS axon myelination research.* Biomedical Microdevices, 2009. **11**(6): p. 1145.
11. Park, J., et al., *Three-dimensional brain-on-a-chip with an interstitial level of flow and its application as an in vitro model of Alzheimer's disease.* Lab on a Chip, 2015. **15**(1): p. 141-150.
12. Roggenkamp, D., et al., *Atopic Keratinocytes Induce Increased Neurite Outgrowth in a Coculture Model of Porcine Dorsal Root Ganglia Neurons and Human Skin Cells.* Journal of Investigative Dermatology, 2012. **132**(7): p. 1892-1900.
13. Tsutsumi, M., et al., *In vitro formation of organized structure between keratinocytes and dorsal-root-ganglion cells.* Experimental Dermatology, 2012. **21**(11): p. 886-888.
14. Klusch, A., et al., *Coculture Model of Sensory Neurites and Keratinocytes to Investigate Functional Interaction: Chemical Stimulation and Atomic Force Microscope–Transmitted Mechanical Stimulation Combined with Live-Cell Imaging.* Journal of Investigative Dermatology, 2013. **133**(5): p. 1387-1390.

15. Roggenkamp, D., et al., *Epidermal Nerve Fibers Modulate Keratinocyte Growth via Neuropeptide Signaling in an Innervated Skin Model.* Journal of Investigative Dermatology, 2013. **133**(6): p. 1620-1628.
16. Bird, M.M., *Establishment of synaptic connections between explants of embryonic neural tissue in culture: experimental ultrastructural studies.* Experimental Brain Research, 1985. **57**(2): p. 337-347.
17. Vikman, K.S., et al., *A two-compartment in vitro model for studies of modulation of nociceptive transmission.* Journal of Neuroscience Methods, 2001. **105**(2): p. 175-184.
18. Ohshiro, H., S. Ogawa, and K. Shinjo, *Visualizing sensory transmission between dorsal root ganglion and dorsal horn neurons in co-culture with calcium imaging.* Journal of Neuroscience Methods, 2007. **165**(1): p. 49-54.
19. Shipshina, M.S., S.A. Fedulova, and N.S. Veselovskii, *Induction of Long-Term Depression of Synaptic Transmission in a Co-Culture of DRG and Spinal Dorsal Horn Neurons of Rats.* Neurophysiology, 2011. **43**(4): p. 261-270.
20. Shypshyna , M.S., et al., *Modulating Effect of Peptide Semax on the Level of Synaptic Activity and Short-Term Plasticity in Glutamatergic Synapses of Co-Cultured Dorsal Root Ganglion and Dorsal Horn Neurons of Rats.* 2016. **7**(3): p. 263-272.
21. Pfister, B.J., et al., *An in vitro uniaxial stretch model for axonal injury.* Ann Biomed Eng, 2003. **31**(5): p. 589-98.
22. Daud, M.F.B., et al., *An aligned 3D neuronal-glial co-culture model for peripheral nerve studies.* Biomaterials, 2012. **33**(25): p. 5901-5913.
23. Lichti, U., J. Anders, and S.H. Yuspa, *Isolation and short-term culture of primary keratinocytes, hair follicle populations and dermal cells from newborn mice and keratinocytes from adult mice for in vitro analysis and for grafting to immunodeficient mice.* Nat. Protocols, 2008. **3**(5): p. 799-810.
24. Siriphorn, A., S. Chompoopong, and K. Tilokskulchai, *The Neurite Outgrowth Measurement of Dorsal Root Ganglia Explants Cultured on Estrogen and Schwann Cell-Conditioned Medium by Using Image Analysis*. Vol. 61. 2009. 130-134.
25. Badea, A., et al., *3D-Printed pHEMA Materials for Topographical and Biochemical Modulation of Dorsal Root Ganglion Cell Response.* ACS Applied Materials & Interfaces, 2017. **9**(36): p. 30318-30328.
26. Badea, A., *Design and Evaluation of Neuroregenerative Properties of 4D Hydrogel Scaffolds*, in *Chemistr*. 2017, University of Illinois at Urbana-Champaign: Urbana, IL.

Chapter 8

Conclusions and Future Outlook

8.1 Conclusion

Within this dissertation, I have explored the neurochemical contents of the dorsal root ganglia, their cells, and their interfacing tissues, as well as the ability to measure neuropeptide release from such systems. Along the way, I became interested in the creation of a structurally relevant cell culture system for the primary sensory neurons as well as validated our cell culture and stimulation/release paradigms. While much work remains to be done in these categories, I have created a solid platform from which future projects can move.

8.2 Future Outlook

8.2.1 Itch Peptide Studies

The validation set of itch peptidomics experiments is underway. If we find specific peptides that are reliably changing in the itch model treatment versus control, we should both follow up with validating the itch-related function of these peptides as well as look into the dynamics of those peptide within the system. For example, it is not enough to just know that a particular peptide changes in amount, instead it would be better to track that peptide over time to understand dynamically when that peptide is involved in the cellular response to the treatment. These types of experiments are much more involved, but could be extremely useful in understanding the pathogenesis of such diseases.

Additionally, it would be useful to develop an improved method for neuropeptide extraction from skin. So far, we have not been able to successfully extract neuropeptide signal from skin samples, as the peptides derived from skin proteins are so much more

prevalent they saturate the system. The nerve endings in the skin are important sensory and release sites for perturbations, so it would be particularly useful to understand what neuropeptides are responding at the site of damage and which neuropeptides might be implicated in continuing the sensitization and disease response cycle.

Finally, I could see the integration of different aspects of my project by using the microphysiological system described in Chapter 7 to better study the release mechanisms of the peptides that are identified as important to the pathogenesis of itch.

8.2.2 Cellular Release Measurements

The ability to detect neuropeptides released from cells in an untargeted way is an area of possible growth for this project. My results have shown that it is possible to culture small amounts of cells within restricted spaces and detect release of a neuropeptide, Substance P, from those cells using enzyme-linked immunosorbent assay (ELISA). However, we have been unable to detect similar levels of peptide release using current mass spectrometric techniques that are amenable to untargeted studies. Of course, there are many options for targeted studies of such release. However, when studying a system as complex as the neuropeptide system, it is important to detect the multiple peptide players that might be involved in a single response to a perturbation rather than just target one or two. Therefore, I could see the integration of the cell culture and ELISA techniques outlined in Chapter 6 to guide improvements in sample preparation and analyte detection methods for untargeted mass spectrometry of cellular release.

8.2.3 Microphysiological System

The microphysiological system project has a variety of directions for potential growth. First, the integration of the hydrogel scaffold within the microfluidic device is a novel idea

for which we have overcome some logistical challenges. By having the successful integration of such a scaffold within our device, we open the possibility of testing a variety of scaffold designs within that designated space, particularly to determine the best design for generating a nerve-like structure within the device. Once this type of structure is developed within the device, we can then use the device to study other aspects of nerve growth, such as regeneration or myelination, within a controlled, but more structurally relevant growth system than others available.

Second, it is the ultimate goal to grow spinal cord neurons, DRG neurons, and skin cells within the same device to create a biologically relevant stimulation and release model. The device was designed with that goal in mind and, therefore, it would be an obvious next step to incorporate other cells into the device. Once incorporated, we would study how the cells interact, what type of innervation may occur, and how the presence of certain cell types within the system may influence stimulation, release, and possibly the progression of injury response.

8.2.4 Single Cell Peptide Profiling

Although I didn't discuss it within this dissertation, I would like to address the potential importance of and use for single cell peptide profiling within the sensory system. Primary sensory neurons are divided into subtypes based on morphology and protein expression, and these subtypes can be related to functionality [1-6]. Within the DRG are various types of sensory neurons, classified by size, myelination state, immunohistochemical staining, and physiological response to stimulants. There are multiple studies characterizing subpopulations of DRG sensory neurons, which has become increasingly complex [1-7]. Historical characterizations loosely conform to basic categories: 1) large and medium

diameter low-threshold mechanoreceptors, which express heavy-chain neurofilament (NF)200 and the neurotrophin receptors trkA, trkC, and p75NTR; 2) small diameter unmyelinated polymodal nociceptors or thermoreceptors that constitutively synthesize CGRP and express trkA; and 3) small diameter unmyelinated polymodal nociceptors which bind lectin *Griffonia simplicifolia* isoelectin B4 (IB4), with some overlap between CGRP positive neurons and both NF200 and IB4 populations [1-7].

However, recent efforts have used single cell transcriptomics to distinguish between DRG neuronal subtypes with unprecedented detail [7]. While it is encouraging that further information and classifications have been discovered about sensory neuron subtypes, the influx of transcriptomic data lead us to wonder what the actual peptide content of these cells might be, and if we could differentiate between cellular subtypes using mass spectrometry. Theoretically, we should be able to distinguish between cell subtypes using peptide profiles with the same, if not increased, detail as the transcriptomic studies.

There are many approaches to single cell peptidomics [8]. Single-cell peptide studies require a highly sensitive approach that can characterize analytes on a subcellular level, such as matrix-assisted laser desorption/ionization-mass spectrometry imaging (MALDI-MSI). The Sweedler lab has already used MALDI-MSI to probe the chemical heterogeneity of DRG slices and to compare the chemical profile of these slices to surrounding structures [9] as well as used single cell MALDI-MS profiling to characterize cellular subpopulations [10]. These initial proof of concept studies utilized cells and cellular subpopulations that contained a relatively high abundance of peptides which were easily distinguished from each other, such as *Aplysia californica* and pancreatic islet cells.

Throughout my graduate career, the idea of using single cell peptide profiling to differentiate between sensory neuronal subtypes was compelling. I performed various studies but found it difficult to detect expected neuropeptides within the DRG cells. During this time, a post-doctoral researcher in our lab, Dr. Thanh Do, took up the project and was able to use peptide profiling to differentiate subtypes of sensory neurons [11]. This work is extremely promising. However, we did not compare the mass spectrometric subtypes that were obtained in our study to the current biological/morphological subtypes in use today. Therefore, it is a logical next step for our lab to use immunofluorescent and morphological measurements to complement mass spectrometry peptide profiling results so we can determine how well the two methods of subtype characterization overlap.

8.3 Work Cited

1. McMahon, S.B., et al., *Expression and coexpression of Trk receptors in subpopulations of adult primary sensory neurons projecting to identified peripheral targets.* Neuron, 1994. **12**(5): p. 1161-1171.
2. Bangaru, M.L., et al., *Sigma-1 receptor expression in sensory neurons and the effect of painful peripheral nerve injury.* Molecular Pain, 2013. **9**: p. 47.
3. Torsney, C., et al., *Characterization of sensory neuron subpopulations selectively expressing green fluorescent protein in phosphodiesterase 1C BAC transgenic mice.* Molecular Pain, 2006. **2**(1): p. 1-8.
4. Inoue, K.-i., et al., *Runx3 controls the axonal projection of proprioceptive dorsal root ganglion neurons.* Nat Neurosci, 2002. **5**(10): p. 946-954.
5. Tucker, B.A. and K.M. Mearow, *Peripheral sensory axon growth: from receptor binding to cellular signaling.* Can J Neurol Sci, 2008. **35**(5): p. 551-66.
6. Priestly, J., *Neuropeptides: Sensory Systems*, in *Encyclopedia of Neuroscience*, L.R. Squire, Editor. 2009, Academic Press: Oxford. p. 935-943.
7. Usoskin, D., et al., *Unbiased classification of sensory neuron types by large-scale single-cell RNA sequencing.* Nat Neurosci, 2015. **18**(1): p. 145-153.
8. Rubakhin, S.S., et al., *Profiling metabolites and peptides in single cells.* Nat Meth, 2011. **8**(4s): p. S20-S29.
9. Rubakhin, S.S., A. Ulanov, and J.V. Sweedler, *Mass Spectrometry Imaging and GC-MS Profiling of the Mammalian Peripheral Sensory-Motor Circuit.* Journal of the American Society for Mass Spectrometry, 2015. **In Press**.
10. Ong, T.-H., et al., *Classification of Large Cellular Populations and Discovery of Rare Cells Using Single Cell Matrix-Assisted Laser Desorption/Ionization Time-of-Flight Mass Spectrometry.* Analytical Chemistry, 2015. **87**(14): p. 7036-7042.
11. Do, T.D., et al., *Optically Guided Single Cell Mass Spectrometry of Rat Dorsal Root Ganglia to Profile Lipids, Peptides and Proteins.* ChemPhysChem, 2018. **19**(10): p. 1180-1191.